Structural aspects of the ice-water system

N H FLETCHER

Department of Physics, University of New England, Armidale, NSW, Australia

Contents

Rep. Prog. Phys. 1971 **34** 913–994

Abstract. A review is given of the present state of structural knowledge about the water molecule, small molecular clusters, the various stable and metastable polymorphs of ice and liquid water. Mention is also made of 'polywater' and of surface and interfacial structures. The discussion is restricted primarily to structural matters and the emphasis is upon work done since 1965.

This review was completed in October 1971.

1. Introduction

Water is such an important substance to mankind that an immense amount of work has been done on its properties in the solid, liquid and vapour states. The prime interests in various studies may be chemical, biological or geophysical but underlying them all are the basic structural problems which are generally the concern of the physicist. It is entirely with these structural aspects of the subject that this present review is concerned; many quite closely related topics have been given little if any mention.

For those who would pursue other aspects of the water–ice system in any detail, there are now several general references available. Dorsey (1940) made a classic compilation of the literature prior to 1938 while two recent books (Eisenberg and Kauzmann 1969, Fletcher 1970) give connected accounts, from rather different viewpoints, of the present state of our knowledge. Finally, the proceedings of the continuing series of International Symposia on the Physics of Ice held in Erlenbach in 1962 (unpublished), in Sapporo in 1966 (Ôura 1967) and in Munich in 1968 (Riehl *et al* 1969) provide interesting individual views from major contributors to our understanding of the subject.

The object of the present article, then, is to provide a connected account of structural aspects of the water–ice system, ranging from the water molecule itself through the many crystalline polymorphs of ice to the structure of liquid water and to some aspects of the surface structures of these phases. Although earlier work is not completely neglected, the emphasis is upon advances made during the past few years.

2. The water molecule

The water molecule is small and, relatively speaking, simple. It contains only three nuclei and ten electrons so that, whilst an exact solution of the Schrödinger equation to determine its structure is out of the question, we may hope that approximate methods may lead to a very close approach to reality. This is, of course, the approach of a theoretician; an experimental physicist might stress rather the structural information which can be obtained from judiciously chosen measurements. In practice we combine both these ways of attacking the problem and we

shall see that, whilst some aspects of the structure of the water molecule are not finally resolved, the picture which we have is sufficient for most of our present purposes.

2.1. *Experimental information*

Several pieces of experimental information tell us immediately that the water molecule is triangular rather than linear. The molar heat capacity C_p for water vapour at constant pressure near 100 °C is 20·6 J mol^{-1} K^{-1} which is equivalent to a C_v value of about $3{\cdot}3k$ per molecule. Since vibrational modes should not be appreciably excited at this temperature, this value implies a finite moment of inertia about each of three orthogonal axes so that the molecule cannot be linear.

A measurement of the dielectric constant of water vapour leads to the same conclusion, for it is found to have the form

$$\epsilon/\epsilon_0 = 1 + A + B/T. \tag{2.1}$$

The temperature-independent term A represents the contribution of electronic and distortional polarization of the molecule while the B/T term implies a permanent dipole moment. Indeed an elementary statistical treatment of the orientation of dipoles in an electric field gives the explicit form

$$B = n\mu^2/3k \tag{2.2}$$

where μ is the molecular dipole moment and n the number of molecules per unit volume. The derived dipole moment for the water molecule (Nelson *et al* 1967) is 0·728 au† or $1{\cdot}85 \pm 0{\cdot}02$ D (1 D = 10^{-18} esu cm). This is a large, though not extreme, molecular moment and indicates a considerable deviation from linearity. It is natural to assume the moment to be directed so that the hydrogen regions of the molecule are positive and the oxygen negative, though experiment gives us no information on this point.

Table 1. Geometry of the H_2O molecule†

Moments of inertia	$I_x = 2{\cdot}9376 \times 10^{-40}$ g cm^2 = $1{\cdot}1517 \times 10^4$ au
	$I_y = 1{\cdot}0220 \times 10^{-40}$ g cm^2 = $0{\cdot}4007 \times 10^4$ au
	$I_z = 1{\cdot}9187 \times 10^{-40}$ g cm^2 = $0{\cdot}7522 \times 10^4$ au
Bond length O—H	r_0 = 0·9572 Å = 1·8089 au
Bond angle H—O—H	α = 104·52°

† From Benedict *et al* (1956).

Finally, and most precisely, a study of the absorption spectrum of water vapour in the far infrared shows, not the regular series of lines to be expected from the rotational transitions of a linear molecule, but rather an apparently irregular jumble, indicating the presence of three unrelated principal moments of inertia. Detailed analysis of these lines yields precise values for the geometry of the water molecule as shown in table 1. The principal axes are chosen so that the z axis bisects the H—O—H angle in the plane of the molecule, the x axis is perpendicular to the plane of the molecule and the y axis is perpendicular to the x and z axes. The origin is the centre of mass of the molecule. The values given are those for ordinary hydrogen and the oxygen isotope ^{16}O and refer to a hypothetical equilibrium

† $e = \hbar = m = 1$. See appendix for numerical values.

situation. The bond lengths and bond angle are very little different for HDO or D_2O. The anharmonicity of interatomic vibrations alters the average experimental values at finite temperature in a way which need not concern us here (Eisenberg and Kauzmann 1969 pp5–6).

Experimental values are available for several other quantities related to the distribution of electrons in the molecule (Verhoeven and Dymanus 1970, Arrighini and Guidotti 1970) but these are more useful as a check on the accuracy of theoretical calculations than for building a direct experimental model for the molecule. For this reason we shall defer consideration of them until later.

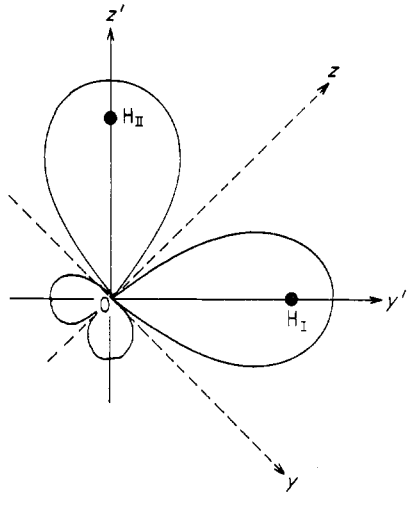

Figure 1. Schematic diagram of the first-order approximation to the valence electron structure of the water molecule.

2.2. *Simple theoretical models*

A reasonably satisfactory first-order model for the electronic structure of the water molecule can be built up from very simple considerations of bond formation (Pauling 1960, Coulson 1961). The ground state of an oxygen atom is the ^3P configuration $(1s)^2(2s)^2(2p)^4$ and that of hydrogen the ^2S configuration (1s). To prepare the oxygen for bonding it is necessary to form directed orbitals which effectively place it in a ^3S configuration $(1s)^2(2s)^2(2p_x)^2(2p_{y'})(2p_{z'})$ where primes have been placed on the y' and z' axis directions since, as we shall see, they differ from those used before. Since ^3P and ^3S states for oxygen differ little in energy, there is little penalty paid for this rearrangement and we now have two unpaired electrons in p orbitals directed along the y' and z' axes which can be used for bonding.

The simplest criterion for a strong chemical bond is that the overlap between the unpaired electron orbitals on the two atoms concerned should be as large as possible. This is achieved if the two hydrogen atoms are placed on y' and z' axes respectively, with the O—H distances determined by the balance between the attraction caused by bonding overlap and the electrostatic repulsion of the nuclei. In this approximation the water molecule appears as in figure 1 with an H—O—H angle of 90°. The relation between y, z and y', z' axes is apparent and the bonding orbitals have been shown schematically. We shall return to consider the electron

distribution in these bonds in more detail later. For the present we note that their wavefunctions can be written as two doubly occupied spin-paired orbitals

$$\left.\begin{aligned}\psi_{\mathrm{I}} &= \lambda \mathrm{O}(2\mathrm{p}_{y'}) + \mu \mathrm{H}_{\mathrm{I}}(1\mathrm{s}) \\ \psi_{\mathrm{II}} &= \lambda \mathrm{O}(2\mathrm{p}_{z'}) + \mu \mathrm{H}_{\mathrm{II}}(1\mathrm{s})\end{aligned}\right\} \tag{2.3}$$

where the ratio λ/μ determines the polarity of the bonds and their absolute values are chosen to achieve normalization.

Leaving aside the O(1s) electrons, which will always be relatively unaffected by bonding, the remaining outer shell electrons lie in pairs in the orbitals

$$\psi_{\mathrm{III,IV}} = 2^{-1/2}(\mathrm{O}(2\mathrm{s}) \pm \mathrm{O}(2\mathrm{p}_x)) \tag{2.4}$$

which can be described as lone pairs.

This simple picture is remarkably close to the real situation, though, as we have seen, the experimental value of the H—O—H angle is about 104·5° rather than the predicted 90°. This can be accounted for in simple terms by the repulsion between the two protons and their accompanying electron bond clouds which, however they are distributed, will not be electrically neutral.

To improve the model we must introduce the concept of bond hybridization, recognizing that, because the O(2s) and O(2p) electrons are all of roughly the same energy, their wavefunctions may mix together in a bonding situation to give greater overlap with the other atomic orbital involved in the bond. The nature of sp^3 (tetrahedral), sp^2 (trigonal) and sp (diagonal) hybrids for the carbon atom is well set out in standard texts (eg Pauling 1960, Coulson 1961). For the water molecule bonding orbitals given by (2.3), the simple $\mathrm{O}(2\mathrm{p}_{y'})$ and $\mathrm{O}(2\mathrm{p}_{z'})$ functions are replaced by hybrids to give

$$b_{\mathrm{I,II}} = \lambda 2^{-1/2}\{(1+\gamma^2)^{-1/2}(\gamma \mathrm{O}(2\mathrm{s}) + \mathrm{O}(2\mathrm{p}_z)) \pm \mathrm{O}(2\mathrm{p}_y)\} + \mu \mathrm{H}_{\mathrm{I,II}}(1\mathrm{s}) \tag{2.5}$$

which, for convenience, now use O(2p) orbitals referred to y, z rather than y', z' axes. If $\gamma = 0$ we have the simple situation of (2.3), while if $\gamma > 0$ the angle between the hybrids b_{I} and b_{II} is greater than 90° and approaches 180° as $\gamma \to \infty$. This angle α is given by

$$\alpha = 2\cos^{-1}\{(2+\gamma^2)^{-1/2}\} \tag{2.6}$$

and, if maximum overlap with the H(1s) wavefunctions is taken as a bonding criterion, should be chosen equal to the H—O—H bond angle. If this is done, then the O—H bonds are 'straight' while otherwise they may be termed 'bent'.

Hybridization of the bonding orbitals necessarily implies a related hybridization of the lone-pair orbitals so that the forms (2.4) are replaced by

$$l_{\mathrm{III,IV}} = 2^{-1/2}\{(1+\gamma^2)^{-1/2}(\mathrm{O}(2\mathrm{s}) - \gamma \mathrm{O}(2\mathrm{p}_z)) \pm \mathrm{O}(2\mathrm{p}_x)\}. \tag{2.7}$$

If $\gamma = 0$ so that there is no hybridization, l_{III} and l_{IV} reduce simply to ψ_{III} and ψ_{IV}, while if $\gamma > 0$ they represent lobes of electron density directed out from the side of the oxygen atom remote from the O—H bonds.

In one of the first more modern treatments of the water molecule, Duncan and Pople (1953), following earlier work by Pople (1950), discussed its structure on the basis of the hybrid bond formulation set out above but with the restrictive assumption that the bonds are straight and the oxygen hybrids directed exactly at their respective hydrogen atoms to ensure maximum bonding overlap, thus determining the parameter γ. They used the O—H bond length and H—O—H angle given by

experiment so that the geometry of the nuclei was fixed, and simple analytic approximations (Slater functions (Slater 1930)) of the form

$$S_{nlm}(r, \theta, \phi) = [(2\zeta)^{n+1/2}\{(2n)!\}^{-1/2}]\, r^{n-1} e^{-\zeta r} Y_{lm}(\theta, \phi) \qquad (2.8)$$

with ζ determined from atomic data. The core functions O(1s) were left out of the calculation as we have done.

With these assumptions, the only undetermined parameter was the ratio λ/μ giving the polarity of the O—H bonds. This was fixed by the requirement that the computed electric dipole moment for the molecule should equal the experimental one, giving $\lambda/\mu = 1{\cdot}06$. The angle between the bond hybrids was, of course, fixed at 104·5° by assumption, and the angle between the lone-pair hybrids l_{III} and l_{IV} became 120·2°. The total hybridization pattern, as given by the parameter γ, was thus quite close to the tetrahedral sp^3 form in which both these angles would be 109·5°.

The main conclusions of importance to our present purpose concern the general electrical shape of the molecule, as indicated by the contributions of the nuclei, the bonds and the lone pairs, to the total dipole moment of 0·724 au. These were

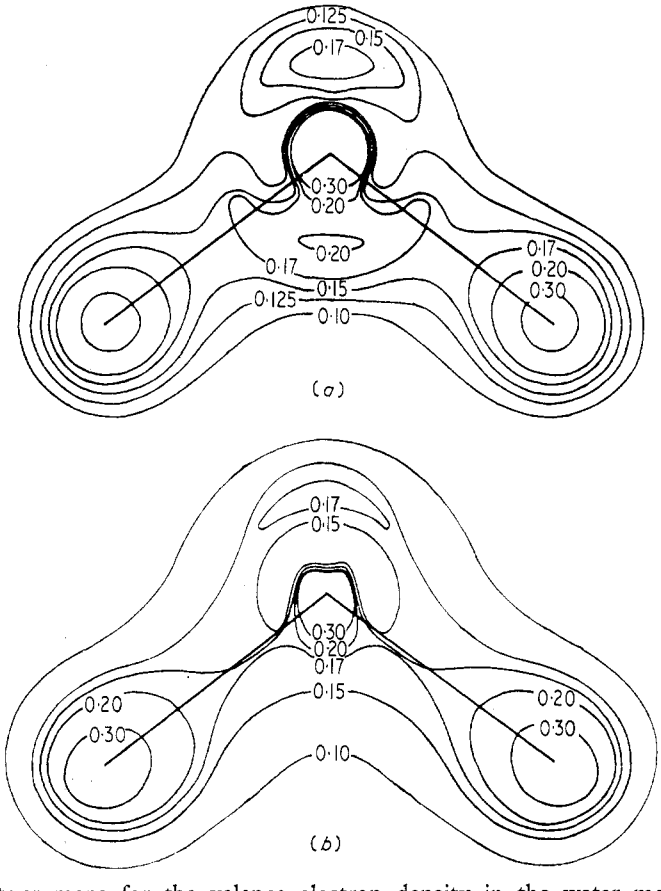

Figure 2. Contour maps for the valence electron density in the water molecule (in au): (*a*) with hybridization parameter chosen to minimize the resultant forces on the nuclei and (*b*) with hybridization parameter chosen to give straight bonds (Bader and Jones 1963).

respectively $+2{\cdot}215$, $-2{\cdot}683$ and $+1{\cdot}192$ au which indicates that the bonding electrons actually contribute a greater negative value to the moment than the positive contribution of the nuclei and most of the resulting moment arises from the lone pairs. We shall see, however, that this conclusion has been brought into question by more recent work. The actual distribution of electronic density in the bonding orbitals b_1 and b_2 for the Duncan–Pople model is shown in figure 2(*b*), where it is contrasted with the distribution suggested by a more recent calculation.

2.3. *More sophisticated calculations*

Modern calculations on the structure of the water molecule do not represent any great change in principle over what was possible twenty years ago but the large computational problems involved have only become capable of solution with the recent development of large fast computers. The method used is basically that of Hartree–Fock self-consistent field (SCF) theory, the detailed application of which to molecular calculations is set out in a classic paper by Roothaan (1951).

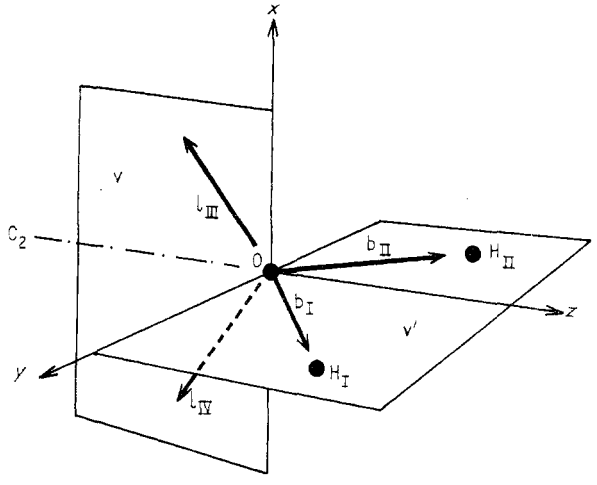

Figure 3. Symmetry elements and bond orbitals for the water molecule.

The first basic approximation is that of Born and Oppenheimer which shows that, to sufficient accuracy for our purposes, the motion of electrons and nuclei can be treated separately. The electronic problem is solved for a fixed nuclear configuration and this electronic energy, together with nuclear repulsion, provides a total effective potential for the nuclear motion. This nuclear motion will concern us only briefly in the present discussion and we shall concentrate on the electronic problem. The corrections to electronic properties due to neglect of zero-point nuclear motion can be shown to be very small, though not completely negligible in some cases, for the water molecule (Kern and Matcha 1968).

The first requirement is to enumerate the possible one-electron states for the problem and for this purpose orbitals related to the symmetry of the molecule as a whole ('molecular orbitals' or MOs) are used. Their symmetry classification depends upon that of the molecule itself, which is illustrated in figure 3. The point group of the molecule is C_{2v} which implies a twofold rotation axis C_2, which is the z axis, and two orthogonal mirror planes v and v′ passing through this axis and constituting

the xz and yz planes respectively. The possible molecular orbitals can be classified into four symmetry types depending upon their behaviour under the symmetry operations of this point group. This is illustrated in table 2, which is the character table for the point group C_{2v}. An entry of $+1$ in a column indicates that the orbital concerned is invariant under the symmetry operation at the head of that column while an entry of -1 indicates a change of sign under that operation. The symbol I represents the identity operator. Orbitals of different symmetry type are automatically orthogonal and the matrix elements of the hamiltonian between them also vanish, thus greatly simplifying the whole problem.

Table 2. Character table for the point group C_{2v}

C_{2v}	I	C_2	v	v′
A_1	+1	+1	+1	+1
A_2	+1	+1	−1	−1
B_1	+1	−1	+1	−1
B_2	+1	−1	−1	+1

Since there are ten electrons in the water molecule, the Pauli exclusion principle states that in the ground state they will generally be found two-by-two with opposite spins in the five different MOs of lowest energy. A few molecules do not have this closed-shell structure but water is not one of them. The ten-electron ground state wavefunction Ψ is then a 10×10 Slater determinant of the one-electron functions ψ_i.

The hamiltonian for the system can be written, if we agree to neglect relativistic effects, as

$$H = \sum_{i=1}^{10} H_i + \sum_{i<j} \frac{e^2}{r_{ij}} \tag{2.9}$$

where H_i represents the hamiltonian for the ith electron in its interaction with the nuclei and the final summation represents the interaction between pairs of electrons. To solve the problem we must then vary the form of all the ψ_i so that the energy is a minimum. Having achieved such a true minimum, E is the ground state energy of the system and Ψ the ground state wavefunction.

Such a programme cannot, however, be physically realized because the unrestricted variation of all the ψ_i cannot be achieved. Instead it is usual to vary the form of the ψ_i over only a limited range of possibilities and so to obtain an approximation to the wavefunction, and an upper bound to the energy. There are several possible ways of doing this but all involve an expansion of each ψ_i as a linear combination of a set of judiciously chosen basis functions. The linear coefficients in this expansion, plus sometimes a small number of nonlinear parameters within the basis functions themselves, then serve as variational parameters for the molecular problem.

The obvious set of functions over which to expand the molecular orbitals is the set of atomic orbitals characteristic of the individual atoms—the LCAO approach. The explicit forms of the various MOs are then as follows

$$\left.\begin{aligned} \psi(A_1) &= a_1\,O(1s) + a_2\,O(2s) + a_3\,O(2p_z) + a_4(H_I(1s) + H_{II}(1s)) \\ \psi(B_1) &= O(2p_x) \\ \psi(B_2) &= b_1\,O(2p_y) + b_2(H_I(1s) - H_{II}(1s)). \end{aligned}\right\} \tag{2.10}$$

There are no MOs of type A_2 unless we include atomic orbitals of higher angular

momentum. There are actually four different A_1 orbitals and two B_2 orbitals because of the possible number of independent choices of coefficients a_i and b_i. Ideally the atomic orbitals should themselves be SCF AOs for the atoms concerned, but in practice some form of analytic approximate wavefunction, like the Slater functions (2.8), is usually used.

With an expansion like (2.10) in terms of a small set of basis functions (actually in this case a minimal basis because no smaller set of AOs could be used) the problem is now tractable. The number of integrals to be evaluated is, however, very large and many of them involve functions expanded about two or three different centres. Single-centre integrals represent intra-atom terms and are fairly simple to evaluate; two-centre integrals are most important to the energy of the molecule and require accurate evaluation; three-centre integrals are generally numerically small and, because of the immense difficulty in their computation, are sometimes only approximated.

The first well known study of the water molecule founded upon this method is that of Ellison and Shull (1953, 1955). Later McWeeny and Ohno (1960) corrected some of the integrals used in this work, as well as introducing new features which we shall discuss presently, and several other more recent calculations have started from a similar basis (eg Andriessen 1969, Pitzer and Merrifield 1970). Some workers have introduced configuration interaction, which means that instead of a single Slater determinant a linear combination of them was used, representing contributions from distributions of electrons other than the pure ground state (McWeeny and Ohno 1960, Klessinger 1965 and most later workers). Another way in which the final result can be improved is to include a greater number of atomic orbitals in the expansions (2.10) so that we have more than a minimal basis. This has been done by Aung *et al* (1968) and Arrighini *et al* (1970) with good results. The wavefunctions can similarly be generalized to include spin (Guberman and Goddard 1970).

All MO calculations agree on the ordering of the orbitals in energy so that the ground state configuration of the water molecule can be written

$$(A_1^{(1)})^2(A_1^{(2)})^2(B_2^{(1)})^2(A_1^{(3)})^2(B_1^{(1)})^2 \qquad (2.11)$$

with the orbital energy increasing from left to right as usual. The two remaining calculated orbitals from the minimal basis set, which are unoccupied, lie with $A_1^{(4)}$ below $B_2^{(2)}$.

Table 3 shows the values of the LCAO expansion coefficients of (2.11) for the five occupied orbitals as calculated by Ellison and Shull (1955) and, for a similar minimal basis, by Aung *et al* (1968). The orbital exponents ζ assumed for the calculation, which were not regarded as variational parameters, were slightly different for the two cases, and these are given in parentheses below each AO. It can be seen that there is a good measure of agreement between these two calculations, though some obvious differences as well.

It is also instructive to transform the orbitals to a new linear combination which shows up the LCAO composition of the equivalent bond and lone-pair combinations. This has been done in table 4 for the calculation of Ellison and Shull (1955) and is there compared with the results of Duncan and Pople (1953) and with those of a calculation by Bader and Jones (1963) which seeks to minimize the resultant force on each nucleus. While the column entries are similar, there are significant differences in the relative contributions of $O(2p_z)$ to bonds and lone pairs between the

Duncan–Pople and the other two cases. The lone pairs are considerably less prominent in the Ellison–Shull and Bader–Jones calculations so that their contribution to the molecular dipole is smaller than was concluded by Duncan and Pople. The more recent calculation of Aung *et al* (1968) gives results similar to those of Ellison and Shull, as indeed do most of the more accurate treatments.

Table 3. Molecular orbital LCAO coefficients

	$H_I(1s)$	$H_{II}(1s)$	O(1s)	O(2s)	$O(2p_z)$	$O(2p_x)$	$O(2p_y)$
Ellison and Shull (1955)							
ζ	(1·0)	(1·0)	(7·7)	(2·275)	(2·275)	(2·275)	(2·275)
$A_1^{(1)}$	0·0023	0·0023	−1·0002	−0·0163	−0·0024	0	0
$A_1^{(2)}$	0·1215	0·1215	−0·0286	0·8450	0·1328	0	0
$A_1^{(3)}$	0·2362	0·2362	−0·0258	−0·4601	0·8277	0	0
$B_2^{(1)}$	0·5486	−0·5486	0	0	0	0·5428	0
$B_1^{(1)}$	0	0	0	0	0	0	1·0000
Aung *et al* (1968)							
ζ	(1·27)	(1·27)	(7·66)	(2·25)	(2·21)	(2·21)	(2·21)
$A_1^{(1)}$	0·0036	0·0036	−0·9968	−0·0152	−0·0031	0	0
$A_1^{(2)}$	0·1517	0·1517	−0·2219	0·8425	0·1320	0	0
$A_1^{(3)}$	0·2644	0·2644	0·0934	−0·5159	0·7872	0	0
$B_2^{(1)}$	0·4235	−0·4235	0	0	0	0·6240	0
$B_1^{(1)}$	0	0	0	0	0	0	1·0000

Aung *et al*, as we remarked before, have also carried out much more detailed calculations using an extended basis set of 1s, 2s and 2p functions on each hydrogen atom and 1s, two sets of 2s, three sets of 2p (with different ζ values) and a set of 3d functions on the oxygen. Arrighini *et al* (1970) similarly used an extended basis of 29 atomic orbitals including all 1s, 2s, 2p, 3s, 3p and 3d orbitals on oxygen, 1s and 2p on hydrogen and an additional set of functions for each of H(1s), O(1s), O(2s) and O(2p). The improvement of agreement between calculated and experimental quantities is generally quite significant, largely through the effects of the d functions.

Table 4. Equivalent bond and lone-pair orbitals

		Ellison and Shull (1955)	Bader and Jones (1963)	Duncan and Pople (1953)
Bonds	$H_I(1s)$	0·577	0·487	0·58
	$H_{II}(1s)$	−0·199	−0·243	0
	O(1s)	−0·026	0	0
	O(2s)	−0·006	−0·109	0·06
	$O(2p_z)$	0·561	0·634	0·37
	$O(2p_y)$	±0·384	±0·359	±0·49
Lone pairs	O(1s)	−0·009	0	0
	O(2s)	0·680	0·707	0·58
	$O(2p_z)$	−0·192	−0·002	−0·41
	$O(2p_x)$	±0·707	±0·707	±0·71

Another method basically similar to this seeks to expand the molecular orbitals, not in terms of functions like those of Slater which have a reasonable resemblance to the true AOs, but rather in terms of simple gaussian distributions $\exp\{-a(\boldsymbol{r}-\boldsymbol{r}_0)^2\}$ together with an appropriate angular factor. From three to five of these gaussians centred at a single point are needed to represent a single AO as well as would a

Slater function, which involves $\exp(-a|\boldsymbol{r}-\boldsymbol{r}_0|)$ but this added complexity is compensated for by the fact that a two-centre gaussian integral can be readily reduced to a single-centre one. Examples of this approach are the work of Moskowitz and Harrison (1965), Harrison (1967) and Neumann and Moskowitz (1968), while Moccia (1964) and Bishop and Randić (1966) have further simplified the calculation by collecting all the gaussian basis functions onto a single centre. Despite its computational simplification this latter approach suffers the clear disadvantage that it is almost impossible to represent the electron density cusps which must occur at the proton positions by any number of angularly varying gaussians centred on the oxygen nucleus. The results of these calculations do not differ greatly from those using Slater bases.

The agreement between the orbital energies given by these calculations is quite good and the calculated total molecular energy is within 0·8% of the experimental value. The binding energy, which is calculated as the difference between the large total molecular energy and that of the separated atoms, is, however, less reliable.

This last comment brings us to the crux of the problem. How good an approximation to the true wavefunction, and hence to the true electron density, is the result of the calculation obtained by minimizing the energy with respect to a limited set of basis functions ? We recall that to obtain an energy which is correct to second order in a perturbation only requires a wavefunction which is corrected to first order. Simply choosing the treatment giving the lowest total energy may not therefore give us the best picture of the electron density distribution.

Several tests of the calculations can be devised. One might simply compare the calculated values of as many molecular properties as possible with the measured quantities (Neumann and Moskowitz 1968, Aung *et al* 1968, Arrighini *et al* 1970, Guberman and Goddard 1970). This is a good, though somewhat specific test. One might check how well the virial theorem, which states that the total potential energy should be minus twice the total kinetic energy, is satisfied. The agreement is in fact better than 0·5% for the calculation of Aung *et al* and better than 0·03% for that of Neumann and Moskowitz.

Finally, and most important, since in most cases the positions of the nuclei were assumed to be those given by experiment, one might look at how closely the forces acting on these nuclei balance. Here we can invoke the Hellmann–Feynman theorem, which states that the electron density distribution given by the electron wavefunction can simply be evaluated and treated as a classical charge distribution in order to calculate the forces on the nuclei. This force balance for the case of the water molecule has been investigated in detail by Bader and Jones (1963) and also by Bader (1964).

If the electron distribution in the molecule is achieved simply by superposing the electron densities of the component atoms then, because the electron clouds overlap adjacent nuclei, the total force on these will not balance. The electron distribution must then be adjusted to move electronic density into the regions shown shaded in figure 4. These regions, which subtend an angle of 76° in the plane of the molecule and nearly 180° in the perpendicular plane, may be called binding regions (Bader 1964). The physical reasonableness of computed electron distributions can then be checked by examining the charge density differentials relative to the component atoms. Bader and Jones (1963) showed that the bonding orbitals proposed by Duncan and Pople (1963) and shown in figure 2(*b*) do not satisfy the force-balance criterion and so are unacceptable. The distribution of bonding electrons

shown in figure 2(*a*), which was derived from a minimal LCAO basis by minimizing the forces on all nuclei rather than the energy, is satisfactory from this point of view and differs little from the computed results of Ellison and Shull (1955) and of later workers. Direct calculation indeed shows that these later calculations do give acceptably small resultant nuclear forces (Neumann and Moskowitz 1968).

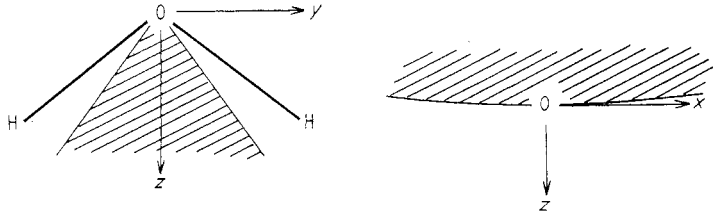

Figure 4. Binding regions for the electronic charge density of the water molecule.

The conclusion to which we are drawn is therefore that the O—H bonds in the water molecule are 'bent' with a hybrid angle substantially less than the 104·5° bond angle, as shown in figure 2(*b*). This means that the bond hybridization is very far from sp^3 and the bonds are more nearly pure p functions than originally thought. This is borne out by the coefficients shown in table 4 and also by an examination of this particular point by Petke and Whitten (1969). Consequently the lone pairs are close to simple sp hybrids with an included angle approaching 180°. The total electron density distribution in the molecule is illustrated in figure 5.

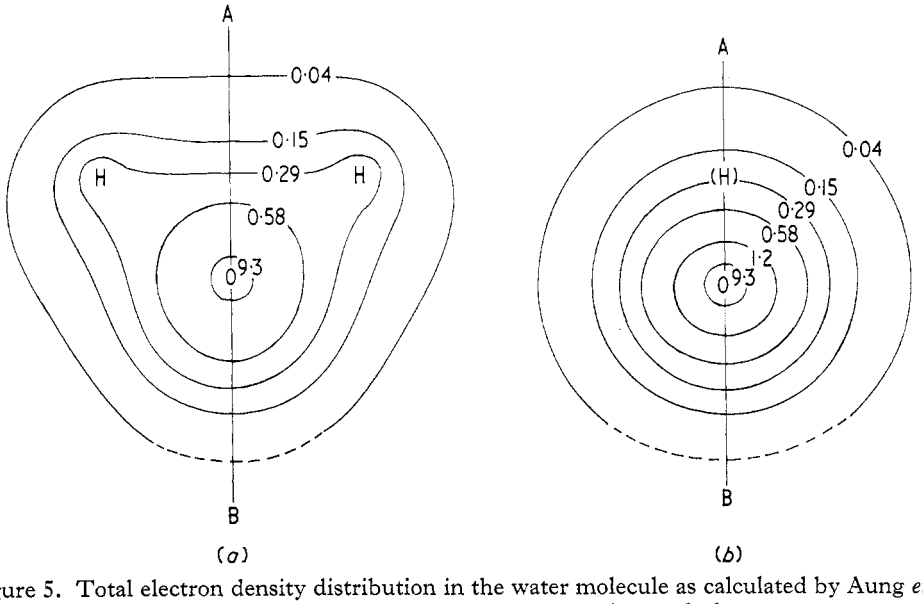

Figure 5. Total electron density distribution in the water molecule as calculated by Aung *et al* (1968). The contours are shown in two orthogonal planes.

Many of the properties of the water molecule have been calculated by various authors and compared with experimental values, where these are available. Quite extensive tabulations and comparisons have been given by Neumann and Moskowitz (1968), Aung *et al* (1968), Eisenberg and Kauzmann (1969 table 1.7), Arrighini *et al* (1970) and by Guberman and Goddard (1970). Most of these properties will not

concern us here, but it is useful to have estimates of the dipole and quadrupole moments, since these are important for the geometry of interaction between molecules.

The dipole moment of a molecule is defined by

$$\mu = \int \boldsymbol{r}\rho(\boldsymbol{r})\,\mathrm{d}\boldsymbol{r} \tag{2.12}$$

where ρ is the charge density function, including both electronic and nuclear contributions. The quadrupole moments are similarly defined by

$$Q_{\alpha\beta} = \int r_\alpha r_\beta \rho(\boldsymbol{r})\,\mathrm{d}\boldsymbol{r}. \tag{2.13}$$

Unlike the dipole moment they are not independent of the choice of origin, which is usually taken as the centre of mass of the molecule. Since the contributions of the spherically symmetric electron distribution to the quadrupole moments is large and negative ($Q \simeq -4{\cdot}3$ au), it is often more useful to compute the deviations of the quadrupole tensor components from this mean, using the definition due to Buckingham (1958)

$$\theta_{\alpha\beta} = \tfrac{1}{2}(3Q_{\alpha\beta} - \delta_{\alpha\beta}\sum_\alpha Q_{\alpha\alpha}). \tag{2.14}$$

The moments calculated by several workers, together with experimental values derived by Verhoeven and Dymanus (1970), are given in table 5. A representative

Table 5. Electric moments of the water molecule relative to the centre of mass

	Theoretical				Experimental
	Aung *et al* (1968)	Neumann and Moskowitz (1968)	Guberman and Goddard (1970)	Arrighini and Guidotti (1970)	Verhoeven and Dymanus (1970)
μ (au)	0·756	0·784	0·870	—	0·727 ± 0·01
θ_{xx} (au)	−1·104	−1·801	−1·787	−2·019	−1·859 ± 0·02
θ_{yy} (au)	+1·110	+1·881	+1·833	+2·062	+1·956 ± 0·02
θ_{zz} (au)	−0·006	−0·080	−0·046	−0·043	−0·097 ± 0·02

calculation of the contribution of the nuclei and various electron orbitals to these total moments is set out in table 6. Most other reasonably reliable computations should give fairly similar values.

Table 6. Contributions to electric moments of the water molecule†

	μ (au)	Q_{xx} (au)	Q_{yy} (au)	Q_{zz} (au)
$A_1^{(1)}$	−0·0008	−0·0354	−0·0354	−0·0654
$A_1^{(2)}$	−0·6426	−0·9858	−1·4548	−1·2082
$A_1^{(3)}$	0·1716	−0·9402	−1·2732	−2·9246
$B_1^{(1)}$	−0·1456	−2·7518	−0·9910	−0·9608
$B_2^{(1)}$	−0·7898	−0·8498	−3·4318	−1·2724
Total electronic	−1·407	−5·563	−7·186	−6·431
Nuclear	2·192	0·000	4·078	2·015
Total	0·785	−5·563	−3·108	−4·416

† From Neumann and Moskowitz (1968).

2.4. *Summary of the electrical structure of the water molecule*

Lest the detailed description we have given above should obscure the general picture, let us restate our present view of the electrical structure of the water molecule. The contours given in figure 5 show a total electron distribution which is not too far from being spherical, with two small 'ears' around the two proton positions. The dipole moment of the molecule is quite large, 0·7 au, where 1 au represents an electronic charge displaced by one Bohr radius or about 0·5 Å. This dipole is contributed partly by the protons in the O—H bonds and partly by the lone-pair electrons which protrude on the opposite side of the molecule, the lone pairs making a rather smaller contribution to the moment than that of the O—H bonds and their associated nuclei.

The shape of the bonding orbital electron density is something like that shown in figure 2(*a*), with the bonds being slightly bent, rather than straight as in figure 2(*b*). The lone-pair electrons protrude from the molecule as a general ridge of negative charge density rather than being localized as two tetrahedrally directed lobes.

Despite this final qualification, it is a reasonable first approximation to consider the water molecule to be roughly tetrahedral in shape, with two positive and two negative vertices. We must beware of taking this simplification too far but, as we shall see, it is remarkably successful in accounting for many of the complex structures into which water molecules may arrange themselves.

2.5. *Nuclear positions and molecular distortions*

In all the calculations discussed above, the results have been quoted for a geometry in which the nuclei were held fixed at their experimentally determined positions. In some cases the calculations were also performed for a range of O—H distances and H—O—H angles and an attempt made to predict equilibrium values for these quantities by minimizing the energy. The results, while yielding bond lengths not differing greatly from those determined experimentally, give values ranging from 90° to 120° for the H—O—H angle. Clearly the energies involved in slight distortions of the molecule are very small compared with the total molecular energy and the calculations are not all of sufficient accuracy to allow reliable prediction of optimum values, although some calculations with extended basis sets have predicted H—O—H angles within about 1° of the experimental value (eg Diercksen 1969).

It is possible, however, to derive force constants for the distortion of the model directly from infrared spectral data and, since these distortions are important from a structural viewpoint, we deal with them briefly here. Most theoretical treatments based on calculations of total molecular energy as a function of geometry yield force constants of about the correct magnitude but we shall not discuss these in detail here.

If we denote by r_0 the equilibrium O—H distance and by α the equilibrium H—O—H angle and then let δr_1 and δr_2 be the deviations of the two actual O—H distances and $\delta\alpha$ the deviation of the H—O—H angle from these equilibrium values, the change in molecular energy δU can be written approximately

$$2\delta U = f_r(\delta r_1{}^2 + \delta r_2{}^2) + f_\alpha(r_0\,\delta\alpha)^2 + 2f_{rr}\,\delta r_1\,\delta r_2 + 2f_{r\alpha}\,r_0\,\delta\alpha(\delta r_1 + \delta r_2). \qquad (2.15)$$

There are higher-order terms which may be included in the expression to allow for anharmonic effects but these need not concern us at present.

The force constants derived by Mills (1963) and by Kuchitsu and Morino (1965) are shown in table 7. The more general anharmonic expression and its associated force constants are given by Eisenberg and Kauzmann (1969 p11). From the small magnitude of f_{rr} it is clear that the stretching vibrations of the two O—H bonds are very little coupled, while the larger value for $f_{r\alpha}$ shows a stronger interaction between bond length and bond angle. Since f_α is an order of magnitude smaller

Table 7. Distortion force constants for the water molecule†

	Mills (1963)	Kuchitsu and Morino (1965)
f_r (au)	5·43	5·430
f_α (au)	0·49	0·489
f_{rr} (au)	−0·06	−0·071
$f_{r\alpha}$ (au)	0·17	0·146

† Calculated with all angles in radians.

than f_r, it is apparent that angular distortion of the molecule is relatively easy, compared with bond stretching, and this in itself explains why it is difficult to calculate the equilibrium value of the H—O—H angle *ab initio*.

3. Clusters of water molecules

Before we come to discuss water molecules in condensed phases it will be useful to consider the structures of very small clusters of water molecules and the interactions between the molecules which comprise them. The properties of such clusters are, of course, of prime importance in understanding the behaviour of the vapour phase and the phenomenon of condensation but this is outside the scope of the present discussion, apart from the remark that information about the interactions between molecular pairs, triplets, etc can be derived from the numerical values of the second, third, etc virial coefficients for the gas concerned (Eisenberg and Kauzmann 1969 chap 2).

3.1. *Simple molecular interactions*

The simplest treatments of the interaction between water molecules are classical approximations in which the true molecule is replaced by a hard sphere of appropriate radius in which is embedded a set of point charges of appropriate signs and magnitudes to simulate the molecular charge distribution. Bernal and Fowler (1933), for example, used a model with three point charges, Bjerrum (1951) used a regular tetrahedral four-charge model and Rowlinson (1951) used both a three-charge and a four-charge model with parameters chosen to give agreement with the second virial coefficient of water vapour. Some of these calculations were supplemented by allowance for the polarizability of the molecules and for dispersion forces. Instructive though these models were at the time, they have now been replaced by much more sophisticated calculations although, as we shall see later, they have recently been used in preliminary models for the structure of liquid water.

With the advent of reliable calculations of the electric multipole moments for the water molecule, as discussed in the previous section, it becomes possible to evaluate

explicitly the electric potential of an isolated molecule from an expression like

$$V(r,\theta,\phi) = r^{-2}(\mu\cos\theta) + \tfrac{1}{2}r^{-3}\{(Q_{zz}-Q_{xx})(1-3\sin^2\theta\cos^2\phi) + (Q_{zz}-Q_{yy})(1-3\sin^2\theta\sin^2\phi)\} + \ldots \quad (3.1)$$

and then deduce the energy of interaction of the permanent multipole moments of a second molecule with the appropriate derivatives of this potential. The leading term is the dipole–dipole interaction which, for molecules with orientations (θ,ϕ), (θ',ϕ') and separation r, has the form

$$U_{11}(\theta,\phi;\,\theta',\phi') = -\mu^2 r^{-3}\{\cos\theta'(3\cos^2\theta-1) + \sin\theta'\sin\theta\cos(\phi-\phi')\}. \quad (3.2)$$

This energy has equal ranges of positive and negative sign but, for freely rotating molecules at temperature T such that $\mu^2 r^{-3} \ll kT$, there is an average attractive interaction

$$\bar{U}_{11} = -\frac{2\mu^4}{3kTr^6} = -a_1 r^{-6}. \quad (3.3)$$

The dipole–quadrupole and quadrupole–quadrupole interactions can be similarly treated and decrease even more rapidly with distance.

The other major contributions to the interaction energy are those due to polarization or induction, to dispersion forces and to overlap repulsion. The first is simple to treat. To first order, and denoting the angular factor by $F(\theta)$, the field derived from (3.1) is

$$E = -\mu r^{-3} F(\theta) \quad (3.4)$$

and in this field a molecule of polarizability α develops an induced dipole $\mu' = \alpha E$ parallel to E. The total interaction energy is then, for freely rotating dipoles,

$$\bar{U}' = -\overline{\mu' E} = -\alpha\mu^2 r^{-6}\overline{(F(\theta))^2} = -a_2 r^{-6} \quad (3.5)$$

where an extra factor of 2 has been included to allow for the reciprocal induction effect of the first molecule upon the second.

The dispersion forces arise from the fact that, though the instantaneous dipole moment of a charge distribution may be zero, there will be quantum mechanical fluctuations about this state and the instantaneous dipole can induce a parallel dipole in a neighbouring molecule by a mechanism like that discussed above. The original fluctuation is proportional to the polarizability α, and the total interaction energy has the approximate value

$$U'' \simeq -\tfrac{3}{4} I\alpha^2 r^{-6} = -a_3 r^{-6} \quad (3.6)$$

where I is the ionization energy of the molecule. Notice that all three interaction energies are negative so that the forces are attractive. For two water molecules at room temperature the values of the coefficients a_i are roughly

$$\left.\begin{aligned} a_1 &\simeq 200\times10^{-60}\ \text{erg cm}^6 \\ a_2 &\simeq\ 10\times10^{-60}\ \text{erg cm}^6 \\ a_3 &\simeq\ 50\times10^{-60}\ \text{erg cm}^6. \end{aligned}\right\} \quad (3.7)$$

Finally there is a repulsive interaction at close range due to overlap of closed electron shells. A form

$$U''' = +a_4 r^{-n} \quad (3.8)$$

with n in the range 9 to 12 is usually assumed but the details need not concern us here.

An interaction function composed of terms of this type is quite adequate for molecules which are rather widely separated, as in the vapour phase, but it is by no means clear that it is a good approximation in the condensed state or even for small molecular clusters. For one thing the multipole expansion (3.2) converges very slowly at small separations and may fail completely if the charge distributions interpenetrate appreciably. For another, the approximation of treating the two molecules as separate units precludes any partial charge transfer which is a feature of many types of chemical bonds or quantum mechanical associations.

Before turning to such calculations, which have only become practicable in the past five years, we should mention one other completely different approach which is best described as semi-empirical. In this treatment, as exemplified by the work of Lippincott and Schroeder (1955), a multiparameter potential of appropriate form is assumed for the interactions between each pair of atoms in the two molecules and the parameters are determined by comparison with experimental data in a variety of similar chemical systems. Such an approach, though telling us nothing fundamental about the molecular interaction, may often lead to a model which allows the prediction of numerical values for several other related experimental quantities.

3.2. *The hydrogen bond*

The general electron density contours for the water molecule, as shown in figure 5, show that the hydrogen atom is relatively bare and its added electron density does not cause any great deviation of the electron cloud from sphericity. This phenomenon, which is unique to hydrogen, means that another atom can approach quite closely to the oxygen atom, even along the line of the O—H bond, and the general electronic overlap and molecular interaction may be quite large. Such an association, written O—H···O in the present case, is called a hydrogen bond. The only really satisfactory way to treat it is by a thoroughgoing solution of the Hartree–Fock equation for all the electrons involved.

Most of the earlier approaches to this problem, like those of Tsubomura (1954), Coulson and Danielson (1954), Coulson (1959), Weissmann and Cohan (1965) and Hasegawa *et al* (1969) limited the complexity of the calculation by considering, not the whole of the two molecules involved, but only the three atoms and four electrons actually involved in the O—H···O bond. To simulate the effect of the remaining parts of the two molecules, the orbitals centred on the oxygen atoms were taken to be tetrahedral sp^3 or sometimes trigonal sp^2 hybrids and the dimer geometry was assumed to be such that the O—H bond of the proton-donor molecule was directed exactly at one of the lone-pair hybrids of the other molecule. Some of these calculations were by an SCF MO approach while others used a valence bond method and included bonding possibilities like O—H O, O^- H^+ O, O^- H—O^+ and O^+ H^- O. We shall remark further on some of these calculations later in connection with the position of the proton on the O—H···O bond but it is clear that any calculation of this sort has severe limitations when compared with a full treatment of the 20 electrons (or 16 if we neglect O(1s) electrons) involved in the whole water dimer.

3.3. *Quantum theory of the water dimer*

A proper quantum mechanical solution for the structure of the water dimer includes, of course, all the different interactions which we mentioned in § 3.1 and

some workers have attempted to separate and identify these (eg Weissmann *et al* 1967). The separation depends to some extent, however, upon the definitions adopted and, though it is instructive, we shall not pursue it here.

The calculation methods used for the $(H_2O)_2$ dimer are essentially the same as those discussed in the preceding section for the monomer. Usually LCAO SCF molecular orbitals are used with the individual AOs represented by Slater functions or by combinations of gaussians. The complications arise mainly from the number of different orbitals involved and from the geometrical variables needed to specify the relative positions of the two molecules, even if each is treated as mechanically rigid. In addition one must beware of spurious effects when a limited basis set is used, since the added basis functions from the second molecule may modify the effective monomer energy of the first by extending its basis set. For this reason an extended basis is desirable for the monomer, although this adds to the complexity of the calculation.

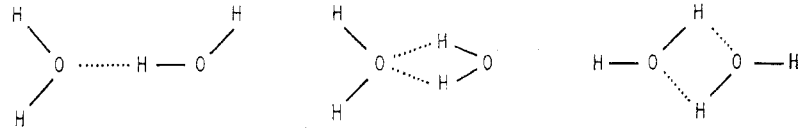

Figure 6. Possible equilibrium configurations for the water dimer: (*a*) linear, (*b*) bifurcated and (*c*) cyclic.

The water dimer system has been studied recently in detail by Morokuma and Pedersen (1968), Kollman and Allen (1969), Morokuma and Winick (1970) and Del Bene and Pople (1970) using basis sets consisting of s and p type AOs on the oxygen and a single s type AO on the hydrogen. Similar calculations by Diercksen (1969) and by Hankins *et al* (1970) supplemented this rather minimal basis with functions of d symmetry on the oxygen and p symmetry on the hydrogen, this extended basis giving an improved treatment of the monomer and minimizing the effects of basis augmentation introduced by the second molecule.

The earlier calculations investigated three plausible configurations for the water dimer: linear, bifurcated and cyclic, as shown in figure 6. From arguments of symmetry the minimum-energy arrangement might be expected to be one of these, or at most a slightly distorted version of it. All studies agree that the configuration of lowest energy is the linear one, with the bifurcated and cyclic lying above it in energy in that order. The studies do not show whether the latter two configurations represent metastable states, but this is unimportant. Experimental studies have shown that hydrogen bonds are generally nearly straight and it is interesting that this is also true in the simple unconstrained case of the water dimer.

Figure 7(*a*) shows the geometry of the linear configuration in greater detail. The proton H_1 is taken to lie on the line joining O_1 and O_2 and the plane of molecule 1 is perpendicular to that of molecule 2, since calculations show this to be close to the minimum-energy situation. The configuration is then specified by the O_1O_2 distance R and the two angles θ and ϕ. We choose the zero of ϕ to be the *trans* configuration shown, with the line O_1H_1' lying in the symmetry plane v of molecule 2. The equilibrium parameters calculated by the studies cited above are shown in table 8, together with the computed dimer binding energy ΔU. The experimental value of this latter quantity is about 0·008 au so that it provides some

guide to the accuracy of the calculation. Those calculations having much too large values of ΔU also have small values for R (there is no experimental value available with which to compare this) and there is a suspicion that these two effects may be due to the basis-augmentation effect for the monomer referred to above. This casts some doubt on the θ value calculated by Morokuma and Pedersen (1968), since their binding energy shows greatest error. There is also a query about the $\theta = 0$ value given by Diercksen (1969), since this is an isolated minimum and his tabulated results show a much broader and only slightly less deep minimum near $\theta = 40°$.

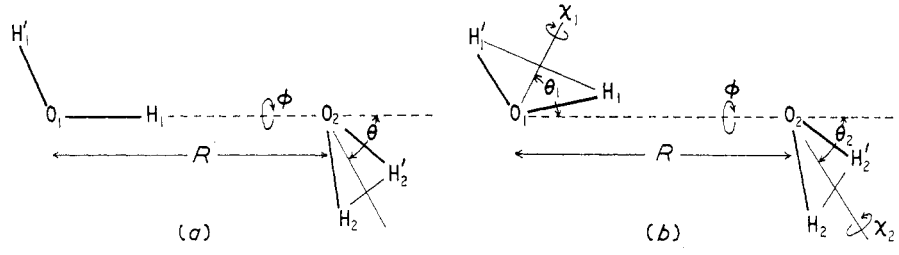

Figure 7. Coordinate systems for discussion of the water dimer.

We are thus led to the conclusion that the water dimer configuration is very close to that drawn in figure 7(*a*), with the most likely value of $\theta = 40 \pm 10°$ and the separation $R \simeq 5{\cdot}7$ au (3·0 Å) or a little less. This θ value is less than the 54·73° which would be expected for exact tetrahedral bonding, but is sufficiently close for the tetrahedral picture to be a useful guide.

Table 8. Equilibrium water dimer configuration from various calculations. In all cases $\phi = 0$

	R (au)	θ (deg)	ΔU (au)
Morokuma and Pedersen (1968)	5·0	0	−0·0200
Kollman and Allen (1969)	5·7	25	−0·0084
Del Bene and Pople (1970)	5·2	58	−0·0097
Diercksen (1969)	5·6	0?	−0·0078
		40	−0·0075
Morokuma and Winick (1970)	5·3	54	−0·0104
Hankins *et al* (1970)	5·7	40	−0·0075

Whilst most of the calculations did not investigate in detail the possible distortions of nuclear geometry of the molecules due to their interaction, there is some data on the effect of varying the position of the proton H_1 along the bond. This suggests that the equilibrium monomer O_1—H_1 length suffers little if any change during the bond formation, calculated changes ranging from zero to an increase of 0·02 au or about 10% of the normal O—H distance.

The force constants for distortion of the hydrogen bond in the dimer can be evaluated from the numerical results of some of the calculations discussed above. With the slightly extended coordinate scheme shown in figure 7(*b*) and assuming a quadratic variation of energy with coordinate, we find the values shown in table 9, with the definition

$$f_{\alpha\beta} = \frac{\partial^2 U}{\partial\alpha\,\partial\beta} \simeq \frac{\delta^2 U}{\delta\alpha\,\delta\beta}. \tag{3.9}$$

Because of the limited number of calculated configurations, these quantities are, however, little better than first-order estimates. The agreement between different calculations is generally only within about a factor of three overall, but some useful conclusions can be drawn. The small value of $f_{\phi\phi}$ shows that the dimer can distort most easily by torsional motion about the O—H···O bond as axis. All other angular distortions are about an order of magnitude stiffer, $f_{\theta_1\theta_1}$ which measures the tendency of the hydrogen bond to remain linear being the largest of these. The force constant f_{RR} is measured in different units from the other $f_{\alpha\beta}$ and, because the equilibrium

Table 9. Estimated force constants for distortion of the water dimer†

	Del Bene and Pople (1970)	Morokuma and Pedersen (1968)	Hankins *et al* (1970)	Kollman and Allen (1969)	Diercksen (1969) (for $\theta_2 = 40°$)
f_{RR} (au)	0·023	0·03	0·012	0·009	0·008
$f_{\theta_1\theta_1}$ (au)	0·041				
$f_{\chi_1\chi_1}$ (au)	0·030				
$f_{\theta_2\theta_2}$ (au)	0·012	0·01	0·004	0·012	0·003
$f_{\chi_2\chi_2}$ (au)	0·017				
$f_{\phi\phi}$ (au)	0·0014		0·0005		

† Calculated with all angles in radians.

distance R is about 5·7 au, the stiffness for a given fractional change of this coordinate is considerably greater than for a corresponding angular distortion (if we may speak loosely). Since the value of kT at room temperature is about 0·001 au, the rms distortions of the dimer are quite appreciable, amounting to about 10° for angles θ_i and χ_i and 0·2 au for R. The parameter $f_{\phi\phi}$ is of the same magnitude as kT so that axial distortions about the bond axis are almost of the nature of hindered rotations rather than oscillations.

It is also important to note that, in those cases where the energy curves have been extended to large distortions in either angular or separation coordinates (Morokuma and Pedersen 1968, Diercksen 1969, Hankins *et al* 1970), there is no break in the curves but just a smooth increase in energy. This will be important for our later consideration of structures with distorted hydrogen bonds.

Finally let us consider the change in electron distribution brought about by dimer formation. This is important, as we shall see in the next section, when the formation of larger clusters and of condensed phases is examined. The simplest way to evaluate this effect is to compare the computed total dipole moment of the dimer with the vector sum of the computed moments for two monomers arranged in the same geometry. This has been done by Kollman and Allen (1969), Diercksen (1969) and Hankins *et al* (1970) and their calculations all indicate that the dipole moment of the dimer exceeds the vector sum of monomer moments by about 10%. This increased polarity should mean an enhanced tendency to bond another molecule to form a trimer, so that there is a measure of cooperative quality about the bonds.

The situation can be examined in more detail, short of actually plotting out electron density contours for the dimer, by giving the Mulliken atomic orbital populations, which simply sum the total occupancy of AOs on a given atomic centre. These are shown for the typical calculations of Del Bene and Pople (1970) and Hankins *et al* (1970) in figure 8. Although the details vary because of differences in the calculations, the conclusions are the same and may be summarized as follows.

(i) During hydrogen bond formation there is a small transfer of electronic charge (estimated at 0·045 and 0·011 au respectively in these cases) from the proton acceptor molecule 2 to the proton donor molecule 1.

(ii) The protruding hydrogen H_1' on the donor molecule has more associated electron charge in the dimer than in the monomer and so bonding reduces its polarity.

(iii) The hydrogens H_2 and H_2' of the acceptor molecule have less electronic charge associated with them in the dimer than in the monomer, so that their polarity is enhanced.

(iv) The oxygen atoms, particularly that of the donor molecule, have an enhanced electron density in the dimer.

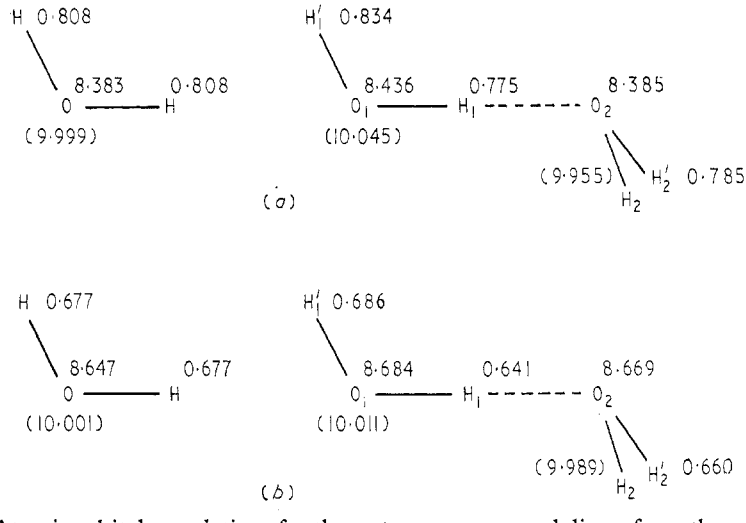

Figure 8. Atomic orbital populations for the water monomer and dimer from the calculations of (*a*) Del Bene and Pople (1970) and (*b*) Hankins *et al* (1970).

From a very simple assessment of this situation, it is clear that dimer formation has enhanced the polarity, and hence the bonding capacity, of both the protons of the acceptor molecule and of the lone pairs of the donor molecule. In the next section we shall examine the implications of this effect for the formation of larger molecular clusters.

3.4. *The water trimer*

Quantum mechanical calculations for trimers and higher polymers of water are limited to those of Del Bene and Pople (1970), who used a minimal basis set to investigate a variety of polymers, and of Hankins *et al* (1970) who studied trimers bonded in tetrahedral configuration. The discussion derives, therefore, largely from these two papers.

It is clear that we can distinguish three major types of trimer, as shown schematically in figure 9: that in which the central molecule is a double donor, that in which it is a double acceptor, and the donor–acceptor or sequential type. In their calculation Del Bene and Pople assumed that the bonding geometry was such that each pair of molecules formed a minimum energy dimer and concluded that the sequential trimer was most stable, followed by the double donor and then the

double acceptor configurations as shown in the first line of table 10. For the slightly different geometry which they assumed, Hankins *et al* also found the sequential trimer to be the most stable, the other two having nearly equal energy. Successive rows of the table show the energy attributable to two dimer-like bonds and the interaction energy between the two unbonded molecules at the ends of the trimer. The final row gives the difference between the first row and the sum of the second and third rows and thus represents the extent to which the bond formation is non-additive. A negative sign implies a cooperative effect in molecular bonding.

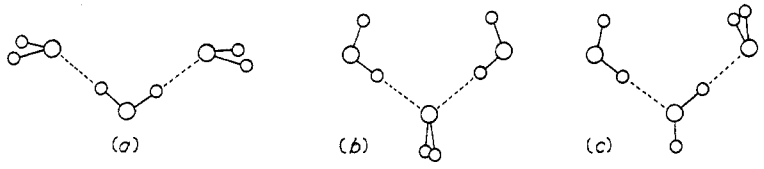

Figure 9. Possible equilibrium configurations for the water trimer: (*a*) double donor, (*b*) double acceptor and (*c*) sequential.

For each of the two geometries studied, the sequential trimer exhibits a cooperative bonding effect and this is of such a magnitude that the formation of the second bond stabilizes each of the bonds of the trimer by about 15%. Both the relative stability of the sequential trimer and the extent of the cooperative effect are essentially what we would expect from the discussion of the dimer leading to figure 8.

Table 10. Interaction energies for I double-donor, II double-acceptor and III sequential trimers

Reference	Del Bene and Pople (1970)			Hankins *et al* (1970)		
Species	I	II	III	I	II	III
Trimer binding energy (au)	−0·0149	−0·0162	−0·0234	−0·0098	−0·0097	−0·0156
2 × dimer binding (au)	−0·0194	−0·0194	−0·0194	−0·0107	−0·0107	−0·0128
Unbonded interaction (au)	+0·0016	+0·0017	−0·0007	+0·0010	+0·0013	−0·0011
Nonadditivity (au)	+0·0030	+0·0016	−0·0032	−0·0001	−0·0003	−0·0017

The two calculations differ upon the question of cooperative bonding in the other trimers and it is not clear whether this is simply due to the different geometry or whether it represents an actual disagreement. Hankins *et al*, whose calculation suggests cooperative effects for all tetrahedral trimers, have shown that the non-additivity is not simply due to electrostatic effects but has a deeper quantum origin. The whole question of cooperative bonding is not, in fact, a new one but was discussed long ago in a qualitative way by Frank (Frank and Wen 1957, Frank 1958). We shall return to this important effect when considering the structure of water and ice.

3.5. *Larger molecular clusters*

In addition to the dimer and trimer, Del Bene and Pople (1970) have investigated the structure and energy of several larger water polymers, both of the chain and cyclic type. As expected, the optimum configuration is always the sequential one. As the chain length of the polymer increases, the polarity of the terminal protons increases and so does the bond strength. At the same time the geometrical

flexibility of the molecule becomes greater and it can, with increasing ease, be bent to a cyclic structure, thus forming an extra bond between its two ends. For a trimer, such a cyclic structure involves considerable bond bending but, rather surprisingly, the cyclic structure proves more stable than the chain despite this. The cyclic pentamer fits together to a nearly plane structure with minimum strain energy because the bond angles involved are all 108°. On the calculations of Del Bene and Pople the energy of thirty molecules grouped into six cyclic pentamers is slightly lower than that of the same thirty molecules arranged as five cyclic hexamers. A plane cyclic hexamer is apparently just as stable as a puckered hexamer with a tetrahedral bonding arrangement. The calculated binding energies, including a set in which the proton positions on the bond are varied, are shown in table 11.

Table 11. Calculated polymer binding energies and the bond energy in the cyclic configuration†

Species	Chain (au)	Cyclic (au)	Cyclic (optimized) (au)	Bond energy (au)
$(H_2O)_3$	−0·0234	−0·0268	−0·0271	0·0090
$(H_2O)_4$	−0·0392	−0·0605	−0·0633	0·0158
$(H_2O)_5$	−0·0660	−0·0848	−0·0900	0·0180
$(H_2O)_6$		−0·1029		0·0171

† From Del Bene and Pople (1970).

The intramolecular O—H bond length at the energy minimum was found to increase about 0·08 au from the monomer value 1·81 au in the case of the cyclic pentamer. Shifts for smaller polymers were correspondingly less.

The extent of cooperative bonding in the cyclic polymers can be judged from an examination of the gross atomic orbital populations as shown in table 12. The

Table 12. Gross atomic populations for cyclic polymers†

Species	O	H	H′
H_2O	8·383	0·808	0·808
$(H_2O)_3$	8·444	0·736	0·819
$(H_2O)_4$	9·467	0·711	0·823
$(H_2O)_5$	8·475	0·701	0·824
$(H_2O)_6$	8·476	0·698	0·826

† From Del Bene and Pople (1970).

hydrogen on the bond is denoted by H and the unbonded hydrogen by H′. The bonding hydrogen loses a good fraction of its electron cloud to the neighbouring oxygen, thus increasing the bond polarity. The polarity of the protruding hydrogen, on the other hand, is not greatly reduced, so that it can still form bonds of reasonably high strength.

When the discussion is extended to more complex branched or three-dimensional clusters of water molecules, the possible variety of structures is immense and the only ones we shall consider here are those of simple geometry which are known to have reasonable stability. The most important of these are those occurring in the clathrate hydrate structures, a review of which has recently been given by Jeffrey

and McMullan (1967). Briefly these are hydrates in which a simple molecule like Ar, Kr, Xe, C_2H_2, N_2O, Cl_2 or a host of others becomes surrounded by a cage of water molecules giving a formula like $8X.46H_2O$ or several other variations. These hydrates, which are solid, form under conditions of reasonably high pressure and low temperature (one to several atmospheres at 0 °C) and have been fairly extensively studied.

We shall be concerned only with the cage of water molecules surrounding the hydrated molecule because, as we shall see later, one can envisage a situation in which the clathrate cage encloses not an inert gas molecule but simply an unbonded water molecule. The simplest clathrate cages are the pentagonal dodecahedron (12-hedron) of 20 molecules and the tetrakaidecahedron (14-hedron) of 24 molecules, which are illustrated in figure 10. The first of these has 12 regular pentagonal faces

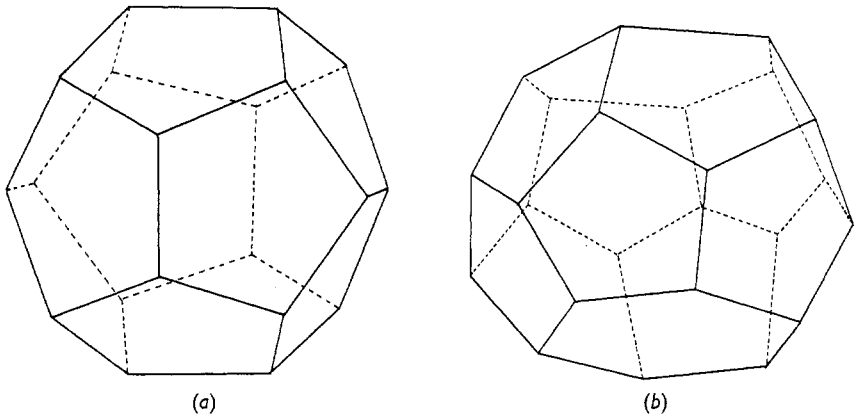

Figure 10. Geometrical bases of common clathrate structures: (*a*) the pentagonal dodecahedron, (*b*) the tetrakaidecahedron.

while the second has 12 pentagonal and 2 hexagonal faces. Other clathrates made from pentagonal and hexagonal faces also exist (the 15-hedron and 16-hedron of 26 and 28 molecules respectively) but these have too large a cavity for our present concern. The clathrate hydrates themselves generally involve two or more cage types in combination.

Since we have established the relatively great stability of nearly plane pentagonal and hexagonal rings of water molecules, the stability of these particular structures is not surprising, though it is clearly not possible to make all the rings with a sequential bond pattern. The numbers of faces F, vertices (molecules) V and edges (bonds) E of a convex polyhedron are related by Euler's theorem

$$F+V=E+2 \tag{3.10}$$

from which we see that the 20 molecules of the 12-hedron make 30 bonds and the 24 molecules of the 14-hedron make 36 bonds. Since a water molecule can only realistically make 4 bonds to its neighbours, or an average of 2 per molecule, in any conceivable structure, the figure of 1·5 bonds per molecule in the clathrates, coupled with the fact that the bond angles are close to their equilibrium values (108° in the 12-hedron, 108° and 120° in the 14-hedron), explains the stability of these structures. No detailed calculations appear yet to have been published.

4. Structure of ordinary ice

As we shall see later, the phase diagram of ice is quite complex and there are eight distinct stable crystalline polymorphs as well as two metastable crystalline forms and an amorphous state. For the present we discuss only ordinary ice, which is the phase crystallizing from water at atmospheric pressure. The hexagonal habit of natural ice crystals, particularly those growing directly by sublimation from the vapour as snow flakes (Nakaya 1954), makes it extremely likely that the crystal structure is hexagonal, and indeed this is found to be true. There are appreciable anisotropies in optical, mechanical and other properties but, with the exception of crystal habit (Fletcher 1970 pp111–29), these are minor, so that an isotropic approximation is often useful.

4.1. *Density of ice*

The density of ice is less than that of water—a circumstance of immense importance for its geophysical and even biological implications—and many careful measurements have been made. Dorsey (1940 pp462–9) summarizes the best published measurements prior to that date, the generally accepted value given in the International Critical Tables of 1928 being $0{\cdot}9168 \pm 0{\cdot}0005$ g cm^{-3} at 0 °C. Individual measurements have, however, often given results outside this range. In some cases this could be due to impurities but both Nichols in 1899 and Barnes in 1901 (quoted by Dorsey 1940) observed a decrease in the density of natural ice crystals with time, Nichols giving 0·91792 g cm^{-3} for new crystals and 0·91629 g cm^{-3} for those one year old, while Barnes' values were 0·91659 for new crystals, 0·91645 for those one year old and 0·91634 g cm^{-3} for those two years old.

More recently Butkovich (1955) has reported measurements on glacier ice ranging from 0·91670 to $0{\cdot}91676 \pm 0{\cdot}00002$ g cm^{-3} while Dantl and Gregora (1968), using laboratory-grown single crystals, found $0{\cdot}91999 \pm 0{\cdot}00006$ g cm^{-3} for freshly grown crystals falling to $0{\cdot}91680 \pm 0{\cdot}00004$ g cm^{-3} for aged crystals. In all cases the measurements were made at temperatures below 0 °C and then corrected to 0 °C using measured thermal expansion coefficients (eg Fletcher 1970 p131). Dantl and Gregora attribute their observed density change to the slow annealing out of electric fields built into the growing ice crystals by differential inclusion of impurity ions—the Costa Ribeiro or Workman–Reynolds effect (Workman and Reynolds 1950). This seems a reasonable explanation, though annealing out of interstitial molecules would produce the same result. Many of the other discordant observations are probably attributable to bubbles or to dissolved impurities. The ICT density value can therefore reasonably be accepted in the form

$$\rho_0 = 0{\cdot}9168 \pm 0{\cdot}0001 \text{ g cm}^{-3} \tag{4.1}$$

for aged ice of normal isotopic composition at 0 °C. This rather low value implies a large volume per molecule in the crystal and hence a structure very different from close packing. The corresponding figure for D_2O ice is 1·0172 g cm^{-3}.

4.2. *Crystal structure of Ice I_h*

X ray diffraction studies of the crystal structure of ice go back to those of Rinn in 1917 and of Dennison (1921), an excellent account of this early work being given by Barnes (1929) and a more complete bibliography by Dorsey (1940 pp424–7).

Many of these earlier ideas were erroneous, and credit for correct determination of the molecular arrangement in the crystal (without reference to proton positions) is usually given to Barnes (1929), whose careful single-crystal data confirmed the conclusions drawn from theoretical speculation by Bragg (1922).

The structure of Ice I_h is the hexagonal analogue of the diamond cubic and belongs to the space group $P6_3/mmc$ (or D^4_{6h} in the Schönflies notation). It is illustrated in figure 11 and in plate 1(*a*). The significance of the space group notation is set

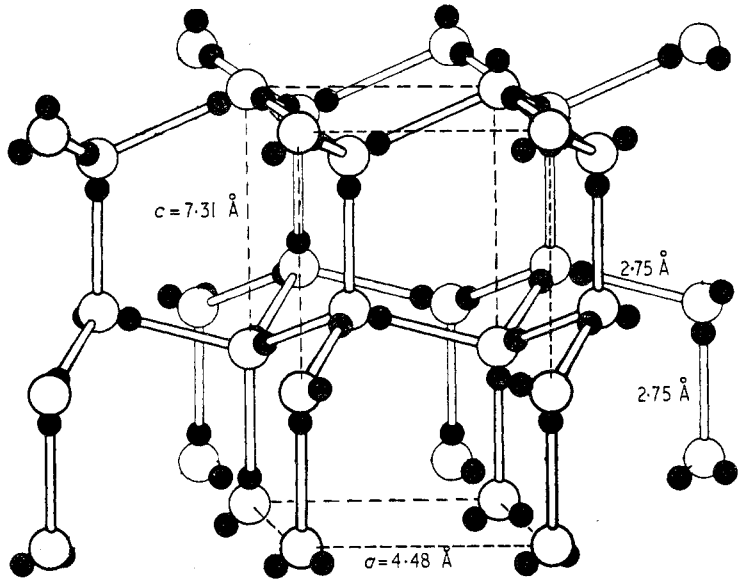

Figure 11. The crystal structure and unit cell of Ice I_h with one of the possible proton configurations shown.

out in standard texts on crystallography and in the International Tables (International Union of Crystallography 1952). It is worthwhile noting the topological similarity between Ice I_h and the silica mineral tridymite, the Si atoms playing the role of O in the ice structure and the Si—O—Si bridges corresponding to the O—H···O bonds. Similar analogies are found in several other ice structures as we shall point out later.

Putting aside for the moment the positions of the protons, it is clear that each water molecule is tetrahedrally coordinated, forming a very open structure as required, and that the puckered hexagon is an important structural unit. Alternatively the structure might be described in terms of puckered sheets of water molecules lying perpendicular to the hexagonal *c* axis. The unit cell for this structure is a prism set on a rhombic base with included angle $\frac{2}{3}\pi$. In this cell there are four molecules, the oxygen atoms (which are essentially all that is seen in x ray diffraction) being centred at the points $\pm(\frac{1}{3}, \frac{2}{3}, z_0)$, $\pm(\frac{2}{3}, \frac{1}{3}, \frac{1}{2}+z_0)$, where z_0 is very nearly equal to $\frac{1}{16}$. If $z_0 = \frac{1}{16}$ exactly and the lattice parameter ratio $c/a = (8/3)^{1/2} = 1{\cdot}633\ldots$, then the environment of each molecule is exactly tetrahedral. We shall examine deviations from this ideal geometry presently.

A critical review of the best diffraction data on lattice constants prior to 1958 has been given by Lonsdale (1958). Since that time some more extensive data sets

have been obtained by La Placa and Post (1960) and Brill and Tippe (1967). Both of these latter sets claim better accuracy and consistency than the earlier measurements and agree acceptably well with each other, as shown in table 13. The uncertainty for the a and c parameters in the case of the results of Brill and Tippe is only a few parts in 10^4 and the ratio c/a is reliable to about 1 in 10^4. Their results do not show any evidence of the bump in a near -140 °C found by La Placa and Post.

Table 13. Lattice parameters of Ice I_h

Temperature (°C)	La Placa and Post (1960)			Brill and Tippe (1967)		
	a (Å)	c (Å)	c/a	a (Å)	c (Å)	c/a
−10	4·5190	7·3616	1·6291			
−20	4·5169	7·3570	1·6288			
−40	4·5128	7·3500	1·6287			
−60	4·5088	7·3440	1·6289			
−80	4·5052	7·3388	1·6290	4·5108	7·3438	1·6280
−100	4·5021	7·3344	1·6291	4·5062	7·3360	1·6280
−120	4·5001	7·3304	1·6289	4·5025	7·3298	1·6279
−140	4·4990	7·3267	1·6285	4·5000	7·3261	1·6280
−160	4·4961	7·3233	1·6288	4·4987	7·3240	1·6280
−180	4·4948	7·3201	1·6286	4·4979	7·3225	1·6280
−200				4·4974	7·3215	1·6279
−220				4·4971	7·3208	1·6279
−240				4·4969	7·3202	1·6278
−260				4·4968	7·3198	1·6278

The density predicted by these lattice parameter measurements is in satisfactory agreement with the results of macroscopic determinations, discussed before. The same is less true of the thermal expansion coefficients α_a and α_c which are shown, in comparison with macroscopic measurements by Jakob and Erk (1928) on single crystals and by Hamblin (Powell 1958) and Dantl (1962) on single crystals, in figure 12. It seems likely that the expansion coefficients are actually negative for a small range of temperatures above 0 K, as is the case for other tetrahedrally bonded materials, though this is not shown by the x ray results. The detailed explanation of the effect need not concern us here, apart from the observation that it is associated with a negative Gruneisen $\gamma_i = -(\partial \ln \nu_i / \partial \ln V)_T$ for the modes ν_i of the transverse acoustic branch of the lattice vibration spectrum which are dominant in this temperature range. This point has been discussed in more detail elsewhere (Fletcher 1970 pp130–43). Whilst there do not seem to have been any recent measurements on D_2O ice, it is worth remarking that the lattice constants and thermal expansion coefficients appear to be almost identical with those of H_2O ice (Lonsdale 1958).

Two points are worthy of further note. Firstly, the expansion coefficients α_a and α_c are very little different so that expansion is nearly isotropic; secondly, the c/a ratio 1·628 is slightly but significantly less than the ideal value 1·633. The earlier work discussed by Lonsdale (1958) suggested that this ratio might approach the ideal value at sufficiently low temperatures but this does not now appear to be so. Thus either the O—O bonds parallel to the c axis are slightly shorter than the oblique bonds, or else the parameter z_0 is slightly less than $\frac{1}{16}$ so that the bond angles are not exactly tetrahedral or, of course, we may find these two effects in combination.

To elucidate these points it is necessary to perform a single crystal diffraction study, as distinct from the powder analyses appropriate to lattice parameter determination. For various reasons which will become apparent shortly, the studies which have been made have both been with neutrons, one by Peterson and Levy (1957) on D_2O ice at 223 and 123 K and a very recent work by Chamberlain *et al* (1972) (see also Chamberlain 1971) on H_2O ice at 77 K. The neutron diffraction data include information on deuteron or proton positions, which necessarily adds further variables to the structure, and we shall return to these later. For our

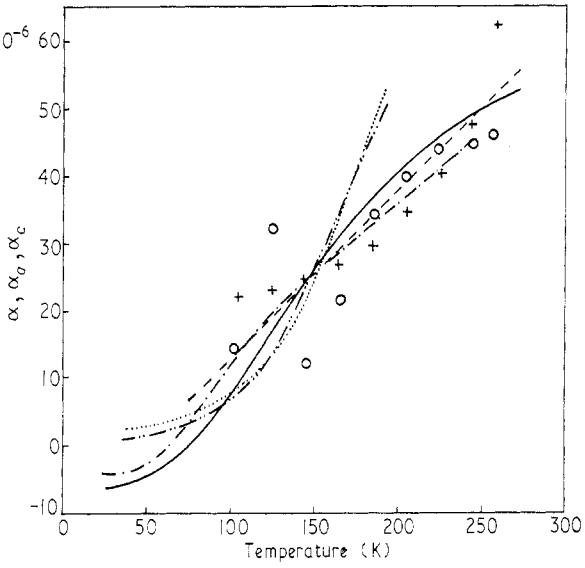

Figure 12. The thermal expansion coefficient α for ice as determined from macroscopic measurements (—— Jakob and Erk (1928), – – – – Hamblin (Powell 1958), —·—· Dantl (1962)) and the expansion coefficients α_a and α_c as determined from x ray measurements (○ α_a, + α_c La Placa and Post (1960) and —··—·· α_a, ····· α_c Brill and Tippe (1967)).

present purposes we note that the results, after computer refinement and corrections for extinction, achieved R values (indicating residual intensity disagreements) of 0·036 for the data of Peterson and Levy and 0·047 for those of Chamberlain. These values are quite acceptable.

The conclusions drawn from the two studies are summarized in figure 13 and table 14, which indicate the near-tetrahedral environment of a representative water molecule in the structure. Clearly the deviation from an ideal tetrahedral environment is small in the case of D_2O ice and is entirely lost in the experimental uncertainties for the case of H_2O ice.

4.3. *Proton positions in Ice I_h*

Since the electron concentration around the protons on a water molecule is small, it is almost impossible to determine proton positions in the ice structure by x ray diffraction and it is only comparatively recently that neutron diffraction techniques have been available to solve this problem. Early discussions of proton positions in ice are therefore based on indirect evidence.

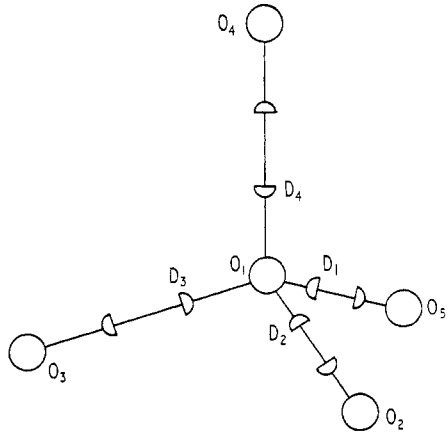

Figure 13. The nearest-neighbour environment of a molecule in D_2O ice showing the half-deuteron positions.

In his analysis of the ice structure, Barnes (1929) proposed that the most likely position for the hydrogens was at the midpoint of each of the O—O bonds, basing his preference for this arrangement on grounds of maximum symmetry and an estimate of the size of a hydrogen atom. There are several arguments against this structure. It implies that ice should be an ionic crystal with a dielectric constant of order 10, whereas it is found to have a value near 100. It also suggests that water should be a highly conducting ionic liquid, which is certainly not the case.

Table 14. Crystallographic data for the ice structure from neutron diffraction studies

	D_2O (223 K)†	D_2O (123 K)†	H_2O (77 K)‡
z_0	0·0629 ± 0·0006	0·0620 ± 0·0004	0·0625 ± 0·0003
Length O_1O_4	2·752 ± 0·008 Å	2·755 ± 0·006 Å	2·74 ± 0·02 Å
Length O_1O_2	2·765 ± 0·0002 Å	2·746 ± 0·0002 Å	2·74 ± 0·02 Å
Length $O_1D_4(H_4)$	1·011 ± 0·009 Å	1·008 ± 0·007 Å	1·013 ± 0·01 Å
Length $O_1D_3(H_3)$	1·015 ± 0·005 Å	1·009 ± 0·007	1·008 ± 0·01 Å
Angle $O_4O_1O_3$	109°33′ ± 9′	109°18′ ± 7′	109·5° ± 1°
Angle $O_3O_1O_2$	109°24′ ± 1′	109°38′ ± 1′	109·5° ± 1°
Angle $D_2O_1D_3$	109°52′ ± 16′	109°54′ ± 15′	109·5° ± 1°
Angle $D_3O_1D_4$	109°6′ ± 18′	109°11′ ± 13′	109·5° ± 1°

Deuteron and proton positions are corrected for thermal motion.
† From Peterson and Levy (1957).
‡ From Chamberlain (1971).

Both these difficulties can be avoided in a structure which maintains water molecules intact in its framework. There is now ample evidence to support this contention but we simply mention the fact that the infrared spectrum of ice shows bands which can be identified with the corresponding vibrations of water molecules in the vapour and which show relatively little frequency shift (Ockman 1958). Thus the O—H stretching modes of the water molecule in the vapour are at 3652 and 3756 cm^{-1} and these can be identified with an absorption band in the range 3150–3380 cm^{-1} in ice, while the H—O—H bending mode in the free molecule is at 1595 cm^{-1} and in ice it is at 1650 cm^{-1}. These small frequency shifts imply that

intermolecular bonding causes a relatively small perturbation of the normal molecular structure.

If we accept this evidence, as we must, then the fact that the O—O distance in ice is 2·76 Å while the O—H distance in the water molecule is about 0·96 Å means that the protons must be placed very asymmetrically on the bonds. The question is how this is to be accomplished. The obvious solution is to recall that it is a first approximation to regard the water molecule as a regular tetrahedron with two positive and two negative vertices, as we discussed in §2.4. The ordinary Ice I_h structure, since it is stable at low pressures and low temperatures, is presumably the structure of minimum energy, and this will be achieved by arranging the molecular tetrahedra vertex to vertex in a + − sense. The question to be answered is exactly how is this achieved in the actual structure.

The earliest approach to this problem seems to have been that of Bernal and Fowler (1933). They observed that it is not possible to produce a molecular arrangement within the four-molecule unit cell we have discussed which achieves a + − arrangement for all the molecular vertices involved. They were thus led to examine larger unit cells on the basis that, though these larger cells would actually lead to superlattice lines in the diffraction pattern, the x ray scattering power of the nearly bare protons is so small that the intensity of any such lines would be well below the background.

The smallest acceptable unit cell which they found was three times as large as that proposed by Barnes and thus contained 12 molecules. All the + − vertex joins were properly made but the structure itself was polar, belonging to the space group *C6mc* or C_{6v}^3. Given the undetectability of the protons using x rays, this would be indistinguishable by those means from the $P6_3/mmc$ or D_{6h}^4 space group of Barnes. This Bernal–Fowler structure is, however, polar in an electrical sense and should exhibit piezoelectric or pyroelectric effects. The experimental evidence on this point is still not entirely clear, because of a variety of other electrical effects in ice, but the weight of opinion is against the existence of such effects.

Bernal and Fowler went on to consider other structures not exhibiting electrical polarity, the simplest of these involving a unit cell of 96 molecules belonging to the space group C3 or C_3^2. They pointed out that such a large unit cell was rather unlikely on physical grounds and went on to say: 'It is quite conceivable and even likely that at temperatures just below the melting point the molecular arrangement is still partially or even largely irregular, though preserving at every point tetrahedral coordination and balanced dipoles. In that case ice would be crystalline only in the position of its molecules but glass-like in their orientation. Such a hypothesis may be still necessary to explain the dielectric constant and the absence of pyroelectricity.'

We now know that this conjecture of Bernal and Fowler is correct and that ice has a statistical structure, as far as proton positions are concerned, determined only by the two rules: (i) the molecular tetrahedra are all arranged with the positive vertices of one near the negative vertices of others; (ii) water molecules are preserved as structural entities. Alternatively, these rules might be expressed in a more formal sense: (i) there is one proton placed asymmetrically upon each O—O bond; (ii) the protons are arranged so that about each oxygen there are two 'near' and two 'far' protons. We shall discuss some interesting thermodynamic evidence in support of this statistical structure, which is usually associated with Pauling (1935), in the next section. For the moment we shall pursue further the diffraction studies.

Despite the fact that the Pauling model is now quite generally accepted as representing the actual structure of ice, there is another model, proposed by Rundle (1953, 1955), which deserves some attention since it constitutes an intermediate state between the completely disordered statistical structure and completely ordered structures like those of Bernal and Fowler. Rundle recognized that the bonds parallel to the *c* axis are crystallographically distinct from the oblique bonds forming the puckered basal sheets and proposed therefore that the protons on these *c* axis bonds should be ordered, in the sense that all would be at, say, the lower end of their bond, while protons on oblique bonds are all disordered. The Bernal–Fowler polar structure made the same assumption about *c* axis bonds but also imposed the smallest possible unit-cell ordering upon the oblique bonds.

Table 15. Scattering cross sections (b) for thermal neutrons

Atom	Oxygen	Hydrogen	Deuterium
Coherent (*a*)	$4{\cdot}23 \pm 0{\cdot}07$	$1{\cdot}78 \pm 0{\cdot}02$	$5{\cdot}76 \pm 0{\cdot}14$
Coherent (*b*)	4·16	1·74	5·61
Incoherent (*a*)	$< 0{\cdot}07$	$79{\cdot}6 \pm 0{\cdot}4$	$2{\cdot}0 \pm 0{\cdot}2$

(*a*) Hughes and Schwartz (1958)
(*b*) from scattering lengths compiled by C G Shull (private communication)

On quite general grounds we should expect an ordered equilibrium structure at low enough temperatures and a transition through a Rundle-type structure to one like that of Bernal and Fowler is possible, even though the equilibrium may never be attained because of the long relaxation time required. Both of these structures are polar but we have noted that Bernal and Fowler also proposed a nonpolar structure of much larger unit cell as a remote possibility. A modification of the Rundle model to produce a nonpolar structure can be made by choosing a unit cell of twice the Barnes size and placing protons on alternate ends of the two *c* axis bonds. This structure does not seem to have been considered but this is of no importance.

Although x ray diffraction is unable to help us locate the proton positions, since the x ray scattering cross section varies as the square of the atomic number, the same is not true of neutron diffraction. The coherent neutron scattering cross sections of oxygen, hydrogen and deuterium are in fact all comparable, as shown in table 15. The great problem about performing neutron diffraction experiments on ice arises from the large value for the incoherent scattering cross section of the proton. For this reason most studies have used D_2O ice so that the diffraction peaks can be more readily measured against the background.

The first such neutron diffraction study was made by Wollan *et al* (1949) using the powder technique on D_2O ice at 163 K. They compared the observed diffraction intensities for six prominent lines with those calculated from the Barnes symmetrical proton arrangement, the Bernal–Fowler polar structure, the Pauling statistical structure and another structure in which the water molecules were assumed to rotate freely. The agreement was very much better for the statistical structure than for any of the other models and the deviations for these others were sufficiently great to rule them out.

The first single crystal neutron diffraction work was done, again on D_2O ice, by Peterson and Levy (1957). At 223 K they first confirmed the characteristic extinctions for the space group $D^4_{6h}(P6_3/mmc)$ and searched unsuccessfully for any

superlattice lines, thus eliminating any structures with an enlarged unit cell. A comparison of the observed structure factors for 11 reflections, of the form (*h*0*l*) which are sensitive to proton order, with the predictions of the Rundle and Pauling models effectively eliminated further consideration of the former. The same was true of data taken at 123 K. Subsequently a set of 56 reflections was measured at both 223 and 123 K and the structure was refined by a least-squares method at each temperature assuming the proton distribution of the Pauling statistical model. The resulting proton positions and bond angles are shown in figure 13 and the first two columns of table 14. In the figure the two hydrogen positions shown on each bond behave in the statistical model as though each is occupied by a halfdeuteron, for diffraction purposes. This represents a spatial average over the positions of all the deuterons in the crystal.

The reason why data were taken at both 223 and 123 K is that we should expect an ordered arrangement of deuterons to represent the equilibrium configuration at absolute zero and it is important to determine whether this ordering actually occurs or whether the disorder characteristic of the structure at higher temperatures becomes 'frozen in' so that a metastable residual disorder is preserved. The data on D_2O show this to be so at least down to 123 K. Because, however, the substitution of deuterons for protons changes substantially the Curie temperature of many hydrogen-bonded ferroelectrics, it is important to repeat the structure determination with normal H_2O ice, in spite of the experimental difficulties. The crucial transition temperature which has been suggested by observed experimental anomalies in the attainment of thermal equilibrium (Giauque and Stout 1936), in specific heat (Van den Beukel 1968, Pick 1969) in dielectric behaviour (Dengel *et al* 1964) and in elastic constants (Helmreich and Bullemer 1969) is at about 100 K. With this in mind Chamberlain and Moore (Chamberlain 1971) undertook a single crystal neutron diffraction study of H_2O ice at 77 K, taking advantage of the advances in experimental technique which have occurred since the time of Peterson and Levy to overcome the problems introduced by proton incoherent scattering. For various incidental reasons only 83 individual reflections were measured, though more than this number could be resolved. A least-squares refinement of the data with anisotropic extinction correction gave an R value of 0·047 for the Pauling model, which represents a quite acceptable agreement, while the Rundle polar model failed to refine properly and led to nonphysical values for some of the parameters involved. The proton position data as determined are shown in figure 13 and the third column of table 14. The geometry is not significantly different from that found for D_2O ice and we conclude that the Pauling statistical model is valid down to at least 77 K. It is most unlikely that the proton system can attain an ordered state at a temperature lower than this in any reasonable time.

4.4. *Proton positions and thermal motion*

Whilst we have discussed the proton positions in ice on the tacit assumption that they lie upon the O—O bonds, it is by no means clearly necessary that this be so. On the one hand such a structure will give the lowest bond energy, as indicated by our discussion in § 3, but on the other hand it involves a change in the molecular H—O—H angle from the value 104·5° characteristic of the molecular geometry in the vapour to the tetrahedral angle 109·5°.

Some authors have argued that the force necessary to deform the H—O—H angle of a molecule is so much greater than the force required to shift a proton

slightly off the O—O bond direction that the molecule should maintain its normal 104·5° angle (Rundle 1953, Chidambaram 1961). Indeed the effective force constant for the intramolecular distortion is $r_0^2 f_\alpha$ which, from table 7, has the value 1·6 au, while the appropriate intermolecular force constant is, from table 9, $f_{\theta_1\theta_1} = 0{\cdot}04$ au. These authors therefore proposed models in which the protons have a number of possible symmetry-related positions closely distributed about the linear bond positions in such a way as to preserve the normal H—O—H angle. Chidambaram (1961) showed that such a modification, when applied to the linear Pauling model, could give equally good agreement with the neutron diffraction data of Peterson and Levy, the spread in proton positions being covered by the thermal vibration ellipsoids of the deuterons. Rundle (1953) made the existence of these proton site clusters (with the restriction that the *c* axis bonds are linear and have only one proton site) an essential feature of his model, required in order to explain the residual entropy data which we shall discuss in the next section.

These arguments, however, overlook completely the fact that the electronic structure of a fourfold hydrogen-bonded water molecule is very different from that of an isolated molecule. In § 3.3 we saw that even for a singly bonded molecule the dipole moment is enhanced by some 10%. Coulson and Eisenberg (1966a) calculate that, in the Ice I_h structure, the electric field of surrounding molecules is sufficient to increase the effective molecular dipole moment by 40% on a purely classical basis, while Onsager and Dupuis (1962) from experimental data estimate the increase to be 100%. It is quite clear that these figures imply a very substantial distortion of the electron cloud of the molecule, a distortion which, from the symmetry of the crystal environment, will tend to reinforce tetrahedral hybridization of the atomic orbitals. We should expect, therefore, that the equilibrium H—O—H angle in the Ice I_h structure will be very nearly tetrahedral, so that the O—H···O bonds should be linear to a very close approximation.

This contention is borne out by the neutron diffraction data of Peterson and Levy (1957) and Chamberlain (1971). At 123 K the former investigators found the ellipsoids representing the motion of the deuterons relative to the oxygen nucleus to be approximately oblate spheroids symmetrical about the bond directions. The behaviour of deuterons D_1 and D_3 (see figure 13) is not identical. The rms longitudinal amplitude for D_1 is $0{\cdot}0655 \pm 0{\cdot}016$ Å while for D_2 it is 0·0597 Å. The transverse amplitudes are essentially identical at 0·15 Å. These displacements are essentially due to the zero-point motion of the deuterons at this low temperature and, from their magnitudes, the appropriate vibration frequencies can be calculated. Peterson and Levy deduce frequencies of 2200 ± 538 and 2660 cm^{-1} for the longitudinal motion of D_1 and D_2 corresponding to O—D bond stretching. This is in satisfactory agreement with the position of the O—D stretching band in D_2O ice at 2330–2420 cm^{-1}. A similar analysis applied to the transverse vibrations gives a frequency of 420 cm^{-1}. This is not to be identified with the D—O—D bending modes but rather with the libration or rocking modes of the molecule as a whole. Again the calculation is in satisfactory agreement with the position of the librational absorption band in D_2O ice, which extends from 350 to 750 cm^{-1}. (The observed spectral features of H_2O and D_2O ice are discussed by Fletcher 1970 pp134–43). It is not possible to include the off-bond shifts of 0·15 Å required to maintain the 104·5° H—O—H angle within these data without seriously impairing this agreement.

Similar analysis by Chamberlain (1971) of his neutron diffraction data on H_2O ice also shows differences between motions of the protons H_1 and H_2. The thermal

ellipsoids were again oblate spheroids, the rms longitudinal amplitudes being 0·075 and 0·067 Å respectively for H_1 and H_2, while the transverse amplitudes were both 0·16 Å. The asymmetries are thus in just the same directions as observed by Peterson and Levy. The calculated O—H stretching frequencies of 3020 and 3544 cm^{-1} are in good agreement with the observed stretching band 3150–3380 cm^{-1} in H_2O ice and the transverse frequency of 670 cm^{-1} with the observed libration band 500–1050 cm^{-1}.

The quite impressive agreement between these two studies and their separate agreement with independent experimental data gives confidence to the assertion that the Pauling statistical model for ice with essentially linear O—H···O bonds describes the actual structure of ice, be it stable or only metastable, down to 77 K, and probably at all lower temperatures.

4.5. *Proton disorder and residual entropy*

As is well known from classical statistical mechanics, entropy is associated with disorder and, if a system can be found with equal probability in any one of a set of W states, the configurational entropy associated with this uncertainty is

$$S_0 = k \ln W. \tag{4.2}$$

If any of the statistical models of ice represents the correct metastable state at very low temperatures, then this disorder should become frozen in and there should be a residual entropy S_0 at 0 K.

Experimental determination of this residual entropy is straightforward in principle, for if $C_p(T)$ is the heat capacity per mole of water molecules, including any delta-function singularities due to latent heat at phase changes, then the entropy S of this mole of material at temperature T is given by

$$S = S_0 + \int_0^T \frac{C_p}{T} \mathrm{d}T \tag{4.3}$$

From experimental measurements C_p can be determined over the range from ice near 0 K to a dilute vapour above room temperature where molecular clustering is negligible. The entropy of such a vapour can be determined independently to high accuracy by knowledge of the molecular partition function, so that comparison of this value with that given by equation (4.3) determines S_0.

This approach was taken by Giauque and Stout (1936), who measured the specific heat of ice down to 15 K and then extrapolated to lower temperatures to evaluate the integral as closely as possible. The extrapolation has since been confirmed by Flubacher *et al* (1960) and the final result is

$$S_0(\text{expt}) = 3{\cdot}4 \pm 0{\cdot}2 \text{ J mol}^{-1} \text{K}^{-1} = (0{\cdot}41 \pm 0{\cdot}03) Nk \tag{4.4}$$

where N is Avogadro's number. For D_2O ice Long and Kemp (1936) found the similar value $0{\cdot}39Nk$. It is these entropies which must be explained in terms of proton disorder.

The number W of possible proton configurations in ice was first calculated by Pauling (1935) who, for his model which we have discussed, used a very simple analysis as follows. Consider an ice crystal of N molecules, where N is sufficiently large that surface effects can be neglected. This crystal contains $2N$ O—H···O bonds on each of which the proton has two possible positions, leading to 2^{2N}

configurations. Consider, however, the four bonds made to an individual molecule. These have sixteen possible configurations, but only six of these satisfy the requirement that the molecule should exist as H_2O, with two near and two far protons. This consideration reduces the possible number of configurations by a factor $(\frac{6}{16})^N$, giving a final value $W = (\frac{3}{2})^N$ and an entropy

$$S_0(\text{calc}) = Nk \ln (\tfrac{3}{2}) = 0{\cdot}4055Nk \tag{4.5}$$

in excellent agreement with the experimental value in equation (4.4).

Several other methods of calculation, by considering the allowed orientations of a molecule in ice subject to the restriction that it makes its four nearest-neighbour bonds correctly (Pauling 1935) or by considering the number of possible orientations available to a molecule which is being added to the growing face of a crystal with which it is required to make two proper bonds (Bjerrum 1951), lead to the same result.

Recent re-examinations of those calculations, to which we shall return in a moment, show that the result is not exact but requires modification by about 1%, which preserves the agreement with experiment. On the other hand the model of Rundle (1953), when an initial error is corrected (Lipscomb 1954), gives either much too low a value $\frac{1}{6}Nk \ln 2 = 0{\cdot}16Nk$ if the protons lie directly upon the bonds, or rather too high a value $0{\cdot}47Nk$ if proton configurations lying close to but not exactly on the O—O bond lines are considered as distinct. This thermodynamic evidence thus confirms the conclusions drawn from diffraction studies.

Returning now to the Pauling calculation, we find that the essential defect is best seen in Pauling's second approach which goes as follows. Consider a molecule in ice. Since the two protons are indistinguishable, there are six distinct possible orientations of the molecule, giving 6^N configurations, if proper bond formation is neglected. The probability that a given bond is made correctly from a proton and a lone pair is, however, $\frac{1}{2}$ and there are $2N$ bonds, so the possible number of configurations must be reduced by $(\frac{1}{2})^{2N}$, giving $W = (\frac{3}{2})^N$ as before. As Hollins (1964) has pointed out, this procedure would be correct for an open or dendritic structure, but fails to take proper account of the closed rings of molecules which occur in ice.

As can be seen from figure 11 and plate 1(*a*), there are many six-membered rings in ice but none of smaller size. If we consider the polarity of water molecule 'vertices' around such a ring, then they must have a pattern such as $+\ -,\ +\ -,\ +\ +,\ -\ +,\ -\ -,\ +\ -$, where the commas represent the positions of the bonds and must therefore separate a pair of opposite signs. Since, however, the sequence represents a ring, its first and last signs must be opposite if the final closing bond is to be correctly made. This will be the case if the number of similar pairs, $+\ +$ or $-\ -$, in the ring is even. Once the sign of the first vertex has been chosen for a given molecule, the probability that the second has the same sign is $\frac{1}{3}$, so the probability of finding an even number of similar pairs in the series, and hence of making the final bond correctly, is equal to the sum of the coefficients of even powers of x in the expansion of $(\frac{2}{3} + \frac{1}{3}x)^6$. This sum amounts to 365/729, while the probability of finding an odd number of pairs, and hence of not making the bond correctly, is 364/729. Consideration of the existence of the ring has thus increased the probability of forming the final bond correctly from the value $\frac{1}{2}$, characteristic of a dendritic structure, to $365/729 = 0{\cdot}500686\ldots$. Since, as can be seen from plate 1(*a*), each molecule participates in twelve six-membered rings, the total number of such rings in a crystal with N molecules is $2N$, so a revised estimate for

the number of configurations is

$$W \simeq (\tfrac{3}{2})^N (1 + \tfrac{1}{729})^{2N}. \tag{4.6}$$

This result is not exact because of interference between rings and the existence of rings of larger size but it does suggest that the Pauling value is slightly low. DiMarzio and Stillinger (1964) and later Nagle (1966) have extended this work and Nagle's final result is

$$S_0(\text{calc}) = (0{\cdot}4100 \pm 0{\cdot}0001)\, Nk = 3{\cdot}409 \text{ J mol}^{-1} \text{K}^{-1} \tag{4.7}$$

which is about 1% higher than Pauling's value and still in excellent agreement with experiment.

4.6. *Proton configurations and lattice energy*

Since this article is restricted to a discussion of structural aspects of the water–ice system, we will not have occasion to consider lattice energy in any detail. There are, however, two aspects of the energy problem which bear on our present concern and these will be taken up in this and the following subsections.

We have seen that the proton configurations in ice are apparently disordered down to absolute zero. We cannot imagine, however, that the energies of these states are all identical and it must be simply that the energy differences are so small that, by the time the temperature has been lowered so that kT is comparable with the energy differences involved, the mechanism of configuration change for the protons has become so slow that the random arrangements are unable to become ordered in the time of the experiment.

The mechanism of proton rearrangement involves the motion of point defects through the crystal. The defects concerned are ion states (H_3O^+ and OH^-) and the orientational or Bjerrum defects which consist of doubly occupied (D) or empty (L) bonds. Thus each defect involves a violation of one or other of the Bernal–Fowler rules governing the structure of the perfect crystal. The concentration of these defects is small (about 10^{11} cm^{-3} for ions and 10^{16} cm^{-3} for orientational defects at -10 °C) and decreases rapidly at lower temperatures. A detailed discussion of these point defects and their influence on the properties of ice is given by Fletcher (1970 chap 7–9).

Dielectric relaxation measurements on both pure and impure ice crystals (Engelhardt and Riehl 1966, Bishop and Glen 1969, Mascarenhas 1969, Glockmann 1969, Chamberlain and Fletcher 1971) suggest that the relaxation time becomes long compared with the duration of a typical experiment at temperatures below about 100 K, but that above this temperature relaxation occurs increasingly rapidly. The nonoccurrence of an ordered configuration therefore implies that the energy difference ΔU between ordered and disordered states is less than TS_0 which is about 340 J mol^{-1} at 100 K.

There have been several fairly detailed attempts to evaluate the lattice energy of ice, ranging from those using a simplified electrostatic model for the water molecule (Rowlinson 1951) to more sophisticated calculations with better molecular models (Coulson and Eisenberg 1966b, Campbell *et al* 1967). The calculations of Coulson and Eisenberg show the importance of non-nearest neighbours, which contribute 20% of the total lattice energy, and of interactions higher than dipole–dipole, which contribute nearly 40% of the total energy. They also show the importance of mutual polarization effects which increase the individual molecular dipole

moments by a factor 1·4. These authors, however, used an ensemble average for the configurations of distant molecules and were not, therefore, able to determine ΔU.

Campbell *et al*, using only the permanent molecular moments, made extensive energy evaluations for many different molecular configurations and found energy differences of the order of 1000 J mol^{-1}. This is sufficiently high that we might have expected proton ordering, and hence a transition to a ferroelectric or antiferroelectric state, at about 200 K. The fact that this is not observed suggests either that the mechanism for cooperative ordering is different from that for dielectric relaxation (which is improbable) or that the calculation omits certain features of physical importance. It seems likely that these effects may arise in the mutual polarization of molecules in the crystal together with the nonelectrostatic cooperative bond reinforcements upon which we commented in § 3.4.

4.7. *Cooperative bonding in the ice structure*

When discussing the quantum mechanical treatment of the water molecule trimer in § 3.4, we remarked that there was a cooperative bonding interaction which stabilized each bond by about 15% and that, while some of this stabilization could be accounted for by simple electric polarization effects, part of it appeared to have a deeper quantum origin.

In principle the extent of cooperative bonding could be worked out by comparing the experimental lattice energy, $(56 \pm 1) \times 10^3$ J mol^{-1}, (Whalley 1957, Eisenberg and Kauzmann 1969 p101) with the value derived from a semiclassical calculation. (Note that the lattice energy differs from the cohesive energy at 0 K because of a correction for zero-point vibrations of molecules in the vapour and solid states.) Unfortunately calculations of sufficient accuracy are not available and we must fall back on indirect estimates.

In § 3.3 we saw that the dipole moment of a dimer was calculated quantum mechanically to be about 10% greater than the vector sum of the vacuum moments of the two constituent molecules. At the other end of the scale, the semiclassical calculation of Coulson and Eisenberg (1966a) suggests that the moment of a tetrahedrally bonded water molecule in an ice crystal is enhanced by about 40%. We might thus reasonably interpolate an enhancement of 10% per bond. Alternatively, in § 3.4 we saw that the formation of a trimer increased the bonding energy for each bond by about 15% over the dimer value, while Coulson and Eisenberg (1966b) calculate a 35% enhancement of bond energy for a tetrahedrally bonded molecule. We might reasonably approximate this progression by saying that each bond formed by a molecule (after the first) strengthens each of the bonds which it makes by about 12%. The strength of the bond involves, of course, interactions higher than dipole–dipole and, in addition, effects of quantum origin. These figures are only rough estimates and not to be taken too seriously, but we will find them of assistance in our later discussions of other ice and water structures.

In a compact three-dimensional structure such as ice, however, it is not possible to make all the six-membered rings with sequential configurations and, indeed, a given molecule will be in the 'wrong' sequence for half of the rings in which it participates. The average H bond energy in ice, 0·0106 au, is therefore considerably less than the value of 0·017 au shown in table 11 for the cyclic hexamer. This reduction does not negate the idea of cooperative bonding, since table 10 shows that the bonding energy of a nonsequential trimer is only about 0·6 times that of a sequential trimer.

Finally it is useful to examine the force constants for bond distortion in ice and to compare them with those set out in table 9 for the water dimer. An average value for the bond bending force constant $f_{\theta\theta}$, which is approximately the average of $f_{\theta_1\theta_1}$ and $f_{\theta_2\theta_2}$, can be derived from the known moments of inertia of the water molecule and the observed librational infrared band at 500–1050 cm^{-1}. The derived value based on the centre frequency of 700 cm^{-1} is

$$f_{\theta\theta} \simeq \tfrac{1}{2}(f_{\theta_1\theta_1}+f_{\theta_2\theta_2}) \simeq 0{\cdot}024 \text{ au} \tag{4.8}$$

where angles are measured in radians. This is comfortably within the range of values for $f_{\theta_1\theta_1}$ and $f_{\theta_2\theta_2}$ shown in table 9. Similarly far-infrared spectral data (Bertie and Whalley 1967) yield the O—O stretching constant f_{RR} as

$$f_{RR} \simeq 0{\cdot}012 \text{ au} \tag{4.9}$$

which again lies within the range for f_{RR} in table 9. The same data gives a bond-bending force constant $f'_{\theta\theta}$ which refers to distortions of the O—O—O bond angles and which has the value

$$f'_{\theta\theta} \simeq 0{\cdot}008 \text{ au} \tag{4.10}$$

with angles in radians. Since for the dimer $f_{\theta_2\theta_2} \ll f_{\theta_1\theta_1}$, geometrical considerations suggest that these distortions will emphasize the angles θ_2 so that $f'_{\theta\theta} \simeq f_{\theta_2\theta_2}$ and again the ice value is not very different from the dimer values shown in table 9.

5. Cubic ice and vitreous ice

Most of the ice structures we shall study are equilibrium phases under particular conditions of temperature and pressure. There are, however, three recognized metastable states with sufficiently well characterized properties that they merit individual study. One of these, Ice IV, exists only under high pressure and we shall discuss it later. The other two form at low pressure and low temperature and were first observed in sublimation deposits formed in an electron microscope. We give these brief consideration here.

5.1. *Cubic Ice I_c*

The first report of a cubic phase of ice seems to have been made by König (1944), who found that ice formed slowly from the vapour at temperatures between -80 and -150 °C showed a cubic electron diffraction pattern. Below -150 °C the pattern was diffuse, indicating an amorphous or at least microcrystalline structure, while above -80 °C the normal hexagonal pattern was observed. Several other studies failed to repeat the observation but the existence of a cubic phase was confirmed by Honjo *et al* (1956), Lisgarten and Blackman (1956) and Dvoryankin (1960) by electron diffraction and by Shallcross and Carpenter (1957) and Dowell and Rinfret (1960) by x ray diffraction. There was, however, some diagreement about the range of occurrence of the cubic form, faster deposition from the vapour narrowing the range to -100 to -120 °C. In many cases the cubic form could not be prepared free from hexagonal contamination.

Analysis of the diffraction pattern showed the oxygen atoms to be arranged in a diamond cubic structure as shown in figure 14 and plate 1(*b*) which belongs to the space group $F\bar{4}3m$ or T_d^2. It is immediately clear that the tetrahedral bonding of nearest neighbours is the same as in the Ice I_h structure and it is useful to examine the relation between this and the cubic structure which is referred to as Ice I_c.

The Ice I_h structure consists of two interpenetrating HCP structures based on the points (0, 0, 0) and (0, 0, $\frac{3}{8}$) respectively in the rhombic unit cell, the packing of these double layers following the sequence ABABAB.... The Ice I_c structure consists of the same sort of double layer stacked in an ABCABC... sequence but is more usually described in terms of cubic axes, in which case it can be regarded as two interpenetrating FCC structures based on (0, 0, 0) and ($\frac{1}{4}$, $\frac{1}{4}$, $\frac{1}{4}$) respectively in the cubic unit cell.

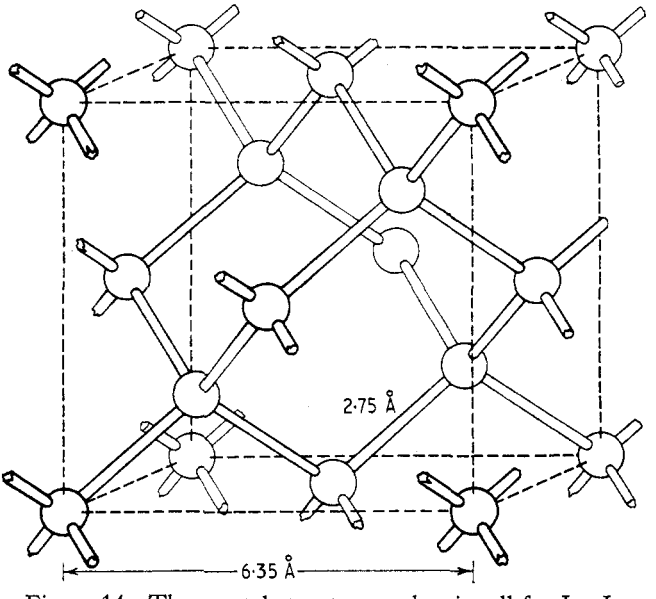

Figure 14. The crystal structure and unit cell for Ice I_c.

An analogous situation exists in the ZnS system in which the hexagonal mineral wurtzite consists of interpenetrating HCP arrangements of Zn and S respectively while the cubic mineral sphalerite consists of interpenetrating FCC lattices of Zn and S. The fact that both forms of ZnS exist stably under reasonable conditions emphasizes the energetic similarity of the structures. It is also worth noting that diamond, silicon and germanium have the same structure as Ice I_c. No hexagonal polymorphs are known for silicon or germanium but there has been a report of hexagonal diamond. We have already noted the similarity between Ice I_h and the silica mineral tridymite. In the same way Ice I_c is analogous to cristobalite.

The vapour growth methods noted above produce Ice I_c in a form convenient for diffraction study but for little else. Recently Bertie *et al* (1963, 1964) were able to produce larger samples by first preparing one of the high-pressure ice polymorphs, cooling to liquid nitrogen temperature, releasing the pressure and warming the sample to about -120 °C.

All the available evidence suggests that Ice I_c is probably not really stable with respect to Ice I_h but only metastable, at least in the region around -120 °C. At temperatures above this there is a slow transformation of Ice I_c to Ice I_h, the rate becoming fast above -70 °C, while no tendency for a transformation in the opposite direction has ever been observed (Dowell and Rinfret 1960). It may be that, well below -100 °C, Ice I_c is the stable form, but that the transformation rate is then unobservably slow. Bjerrum (1951) attempted to show by calculation that hexagonal

ice is more stable than cubic ice from consideration of the relative weights of different nearest-neighbour molecular configurations in the two structures. Although he arrived at the desired conclusion, his calculation was based upon a simple four-charge model for the water molecule which is so far from adequate, on our present knowledge, that the calculation now has little value.

Direct measurement of the heat released during transition from Ice I_c to Ice I_h has been attempted by several workers but their results are subject to disagreement on interpretation. The most recent and careful measurements are those of Sugisaki *et al* (1968) and Ghormley (1968). The former attribute an energy release of about 160 J mol^{-1} between 160 and 210 K to the diffuse $I_c \rightarrow I_h$ transition while Ghormley attributes a rather similar heat evolution of about 220 J mol^{-1} between 193 and 223 K to recrystallization of the cubic phase and places an upper limit of about 20 J mol^{-1} on the $I_c \rightarrow I_h$ transition, which he assumes to occur above 220 K. The former interpretation seems to be preferable but, in the absence of x ray data on the phases involved, the question is not completely settled. These figures suggest that the lattice energy of Ice I_h is lower than that of Ice I_c, indicating that the cubic phase is only metastable at all temperatures, but that the difference in lattice energies is only about 0·5%.

The lattice constant for Ice I_c has been measured by most of the workers mentioned. Blackman and Lisgarten (1958) give a lattice parameter $a_0 = 6{\cdot}350 \pm 0{\cdot}008$ Å at 140 K. This gives an O—O bond distance of 2·75 Å which is equal, within experimental error, to the bond distance in Ice I_h. The densities are similarly equal within experimental error. A neutron diffraction study of D_2O Ice I_c made by Arnold *et al* (1968) gave the very similar result $a_0 = 6{\cdot}353 \pm 0{\cdot}001$ Å at 80 K.

Few properties of Ice I_c have been studied in detail, but those that have, including infrared absorption over the range 350–4000 cm^{-1} (Bertie and Whalley 1964a) and dielectric behaviour (Gough and Davidson 1970) show almost complete identity with the properties of Ice I_h. Ghormley (1968) reported that the specific heat of Ice I_c exceeds that of Ice I_h by 10 to 30% over the range 100–200 K but this rather surprising finding is contradicted by the work of Sugisaki *et al* (1968) who found virtual identity of C_v for the two phases over the temperature range 30–200 K.

5.2. *Proton positions in Ice I_c*

The similarities in dielectric constant and infrared absorption between Ices I_h and I_c lead us to suspect that protons in Ice I_c should also be disordered, and diffraction studies show that this is so. In the case of Ice I_c these studies have mostly been by electron diffraction which, though not as sensitive for the determination of proton positions as neutron diffraction, is considerably better than x ray methods.

The determination of proton positions by electron diffraction was carried out by Honjo and Shimaoka (1957, also Shimaoka 1960). Because of the fine grain size of the ice deposit, the diffraction study was of the powder type, 28 reflections being measured. Comparison of observed intensities with those calculated for the Pauling statistical model, for a Barnes model, and for the simplest type of polar model favoured the Pauling structure unambiguously. The R factor had a value 0·08, which is not particularly good, but the anisotropic thermal motion of the hydrogens was not corrected for. Measurements of intensities at 77, 113 and 153 K allowed a Debye temperature for the molecules, treated as rigid units, to be estimated as

200 ± 12 K (see Fletcher 1970 p143 for discussion of this value) and correction for the associated thermal motion made possible the calculation of potential Fourier maps to make the proton positions visible. As in the case of Ice I_h, the proton potential distributions were found to be equivalent to two half-hydrogens symmetrically placed on the bond. The O—H distance was found to be $0{\cdot}96 \pm 0{\cdot}03$ Å, which is slightly shorter than the O—H distance 1·01 Å found in Ice I_h. It is, however, unlikely that this difference is significant, since the electron diffraction results appear not to have been corrected for relative motion of O and H atoms.

As with Ice I_h, the hydrogens are distributed as oblate spheroids symmetrical about the O—H···O bond. This thermal ellipsoid is not analysed in detail by Honjo and Shimaoka except for a suggestion that it may imply a statistical distribution of H positions not exactly on the O—O line and hence a not ideally tetrahedral H—O—H angle. From the Ice I_h data, however, these ellipsoids may simply represent the expected anisotropic zero-point motion of the protons.

No really careful determination of proton positions by neutron diffraction has been made but Arnold *et al* (1968) show that their powder data on D_2O Ice I_c at 80 K lead to an R value of 0·095 for a Pauling model with linear O—D···O bonds and an O—D distance of 1·01 Å, while a polar model has a very large error residual R. Again, this less than ideal residual for the Pauling model is probably largely due to the lack of proper correction for the thermal motions involved.

We conclude, therefore, with reasonable certainty that the Pauling model is applicable to Ice I_c down to temperatures below 77 K. Cubiotti and Geracitano (1967) have produced thermostimulated current curves to suggest a ferroelectric transition near 190 K but the suggestion that this might be evidence for proton ordering is belied by the direct diffraction evidence, as well as by the fact that the observed behaviour can be explained without the necessity of invoking a ferroelectric transition (Chamberlain and Fletcher 1971). Again, of course, an ordered structure must be the true ground state at 0 K, but it seems certain that the disordered proton configurations are effectively frozen in well above the temperature at which ordering should occur. The residual entropy of Ice I_c has not been calculated in detail but should differ from that of Ice I_h by less than 1 in 10^3.

5.3. *Vitreous ice*

The existence of an amorphous or glassy form of ice at low temperatures seems to have been first reported by Burton and Oliver (1935), the material being formed by slow deposition from the vapour at temperatures below about 140 K. It is interesting to note that both silicon and germanium, upon whose similarity in structure to Ice I_c we have already commented, can also be prepared in an amorphous state by condensation onto a substrate at room temperature or rather above. In fact the formation range of these amorphous deposits is roughly similar, as a fraction of the absolute melting temperature, to the formation range for amorphous ice.

Studies, by thermal or diffraction means, of the transformation of vitreous ice to Ice I_c as the temperature is raised have been made by several workers (Pryde and Jones 1952, Ghormley 1956, 1968, de Nordwall and Staveley 1956, Blackman and Lisgarten 1957, Dowell and Rinfret 1960, Beaumont *et al* 1961, McMillan and Los 1965, Sugisaki *et al* 1968). They agree, in general terms, that an irreversible transition from the amorphous state to Ice I_c takes place on heating in the range 110

to 140 K. At the lower temperature the transition takes about 10^8 s while at about 140 K the time is around 10^2 s so that for practical purposes there is a fairly sharp transition near 140 K (Dowell and Rinfret 1960). Measurements of the enthalpy released by the transition are in the range 1640 to 1800 J mol^{-1} (Ghormley 1968, Sugisaki *et al* 1968).

Of the physical properties of amorphous ice only the heat capacity seems to have been given any detailed attention. We shall return to this to some extent in the next section when we discuss the possible existence of a glass transition in

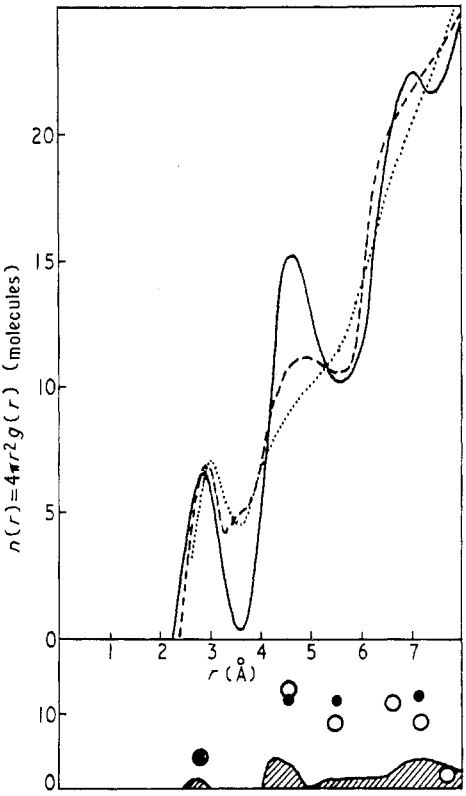

Figure 15. The radial distribution $n(r)$ for molecules in vitreous ice at 83 K as determined by Bondot (1967). The broken and dotted curves show $n(r)$ for liquid water as determined by Morgan and Warren at 1·5 °C and at 83 °C respectively. The lower part of the figure shows the radial distribution of molecules in Ice I_h ○, in Ice I_c ● and, as an approximation, in Ice III.

liquid water at low temperatures. Ghormley (1968) reported that the measured heat capacity of the amorphous ice which he prepared was some 27% greater than that of Ice I_h over the temperature range 100–150 K while Sugisaki *et al* (1968), in what appears to be a rather more careful experiment, found an excess of only about 5% over the range 20 to 130 K.

From our present point of view it is the structure of this amorphous state which is of most interest. Many of the earlier workers made some diffraction measurements by x ray or electron beams, but the most detailed work is that of Bondot (1967, 1969). In the first of these papers, x ray methods were used to determine the radial distribution function for vitreous ice at 83 K as shown in figure 15. Shown

also for comparison are the radial distribution functions for ordinary liquid water at 1·5 °C and 83 °C, as determined by Morgan and Warren (1938) and the discrete molecular distributions in the cubic and hexagonal Ice I_c and I_h structures, adjusted to a nearest-neighbour separation of 2·82 Å.

It is clear from this figure that the structure of vitreous ice is very similar to what we should expect from an extrapolation of the liquid water distribution to lower temperatures. The peaks are very much sharper and are detectable to much larger distances than in the normal liquid, indicating a much better defined bonding network and less thermal motion. In his second paper, Bondot (1969) analysed the radial distribution function into a sequence of gaussian functions representing successive coordination shells. The numerical weighting N, centre distance R and halfwidth Δ of each gaussian were used as adjustable parameters in a least-squares refinement of the diffraction data. Optimum values for the first two shells were found to be

$$\left.\begin{array}{lll} N_1 = 4{\cdot}23 & R_1 = 2{\cdot}77 \text{ Å} & \Delta_1 = 0{\cdot}50 \text{ Å} \\ N_2 = 15{\cdot}57 & R_2 = 4{\cdot}52 \text{ Å} & \Delta_2 = 0{\cdot}97 \text{ Å}. \end{array}\right\} \tag{5.1}$$

The coordination is thus very close to fourfold and the second-neighbour distribution does not differ greatly from that in Ice I_c or Ice I_h. When the analysis is continued, the third-neighbour distribution is also found to be similar to that in the ices but significant differences appear with the fourth- and fifth-neighbour gaussians near 7 Å separation. From figure 15 it can be seen that Ice I_h has 22 molecules in the range 6·5 to 7·5 Å while Ice I_c has only 12. The vitreous ice distribution shows about 35 molecules in the two gaussians covering this range, so that if one wishes to make an analogy between its structure and that of a distorted ice framework, the analogy is much better for Ice I_h as a starting point than for Ice I_c.

Following a suggestion by Bernal (1964), however, Bondot also compared his radial distribution function with that for the synthetic silica mineral keatite which has a structure analogous to Ice III. The complex radial distribution function for Ice III, adjusted to give an average nearest-neighbour distance of 2·82 Å as with the Ice I_h and I_c structures, is also shown in figure 15. The Ice III structure agrees slightly better with the calculated gaussians for first, second and third neighbours than do the Ice I structures, and significantly better near 7 Å, where its distribution contains 29 molecules. Bondot concludes, therefore, that the short-range order in vitreous ice is best described by analogy with the Ice III structure, and almost equally well by analogy with a distorted Ice I_h structure. This conclusion is, of course, of pictorial rather than fundamental significance but may be useful in some of our later discussions.

5.4. *The glass transition in water*

Since amorphous ice can be produced by condensing water vapour on a cold substrate, it is natural to ask whether the same vitreous state could be attained by rapid cooling of ordinary liquid water to a temperature below 160 K. The simplest approach is experimental. It is known from a variety of studies related to cloud physics (see eg Fletcher 1962a chap 8) that even very pure water droplets of micrometre size, cooled at a rate of a few degrees per minute, freeze spontaneously at around −40 °C. Larger droplets or those containing suspended solids can be supercooled only to a lesser extent before nucleation of the ice phase occurs. The

water sample to be used must therefore be very finely divided and the cooling rate extremely rapid. For this purpose Pryde and Jones (1952) used a block of porous copper containing water which they quenched in liquid oxygen. On two occasions subsequent thermal measurements showed a sharp increase in heat capacity near 126 K which they attributed to a glass transition, indicating that a true vitreous state had been achieved. Unfortunately these results could not be repeated in subsequent experiments so that the conclusion remains in doubt. It is perhaps relevant to note that Bridgman (1935) found similar difficulties with the preparation of the metastable Ice IV once the stable polymorph, Ice V, had been formed in his apparatus.

An estimate of the cooling rate necessary to achieve the vitreous state by this means can be made from the theory of the homogeneous nucleation of freezing (see, for example, Fletcher 1970 pp85–97). The nucleation rate J can be written as

$$J \sim \frac{n_L kT}{h} \exp\left(-\frac{\Delta g}{kT}\right) \exp\left(-\frac{\Delta F^*}{kT}\right) \tag{5.2}$$

where n_L is the number of molecules per unit volume of liquid, Δg is the activation free energy for self diffusion and ΔF^* is the free energy barrier to homogeneous nucleation, given by

$$\Delta F^* = \frac{16\pi\sigma^3}{3\{\Delta S_v(T_0 - T)\}^2} \tag{5.3}$$

where σ is the free energy per unit area of the ice/water interface, ΔS_v is approximately the entropy of fusion and T_0 is the melting temperature of ice. Inserting appropriate numerical values derived from experiment in the range 230–270 K as a first approximation, we find

$$\lg J \simeq 35 - \frac{2000}{T} - \frac{4 \times 10^6}{T(273 - T)^2} \tag{5.4}$$

where J is in nucleation events per cm^3 per second. This expression shows that J has a maximum value of about 10^{21} $cm^{-3}s^{-1}$ at about 180 K and that the rate exceeds 10^{20} $cm^{-3}s^{-1}$ between 150 and 200 K. If the postulated glass region at low temperatures is to be reached, then the cooling rate for a droplet of volume V cm^3 must exceed about $10^{22} V$ $K s^{-1}$. For a micrometre-sized droplet, $V \sim 10^{-12}$ cm^3 so that the rate must exceed 10^{10} $K s^{-1}$. It seems unlikely that such a cooling rate could ever be achieved in practice and the uncertainties inherent in the calculation above are unlikely to be sufficient to reduce the predicted rate by more than a few orders of magnitude.

There are several semiempirical methods by which a glass transition temperature for water can be predicted, on the assumption that a metastable vitreous state could somehow be achieved. Pryde and Jones (1952) remarked that the viscosity of most glasses at their transition temperature is around 10^{13} poise and a hopeful extrapolation of the data available between 570 and 260 K suggests a glass transition near 120 K. This is, however, a very long extrapolation, since the total variation of viscosity over the measured temperature range is only about a factor of 10, while the extrapolation involves a viscosity change by a factor of 10^{14}. A calculation using a similar criterion but based upon a different extrapolation rule for viscosity by Miller (1969) gave the higher predicted transition temperature 162 ± 1 K.

Perhaps better is extrapolation from the behaviour of aqueous solutions which are known experimentally to show glass transitions. A rather long extrapolation of this type by Yannas (1968) from glycerol–water mixtures suggests a glass transition in pure water at 127 ± 4 K. A much more extensive study by Angell and Sare (1970), using a variety of ionic solutions forming glasses with as little as 3% of the salt in aqueous solution, suggests a glass transition temperature for pure water of 138 ± 10 K.

Finally we should note that the glass transition might be approached from the low-temperature side when amorphous ice, assumed to be the vitreous state, might undergo a structural modification to a state characteristic of a supercooled liquid. The diffraction studies suggest that there is no great structural difference between amorphous ice and liquid water, but there might be some characteristic change in heat capacity as with other glass transitions. McMillan and Los (1965) were the first to report such an observed transition at about 139 K and Sugisaki *et al* (1968) found a similar transition in their experiments at about 135 K. This is very close to the temperature at which crystallization to Ice I_c takes place and this may explain the fact that no such transition was observed by Ghormley (1968), who used the rather rapid heating rate of 20 K min^{-1}.

These experiments all seem to suggest the reality of a glass transition in water at about 130–140 K but Angell and Sare (1970) have pointed out that this interpretation is not without its difficulties on thermodynamic grounds for, if the heat capacity of normal water is extrapolated smoothly into the supercooled region, then thermodynamic considerations and the observation that vitreous ice and ordinary ice have nearly the same heat capacity require that the glass transition take place at a temperature not below 170 K. The apparent contradiction may arise from the extrapolation of the specific heat of supercooled water to 170 K, for at this temperature its viscosity would be very large so that many thermal modes associated with molecular rotations would be inactive. The question is, however, not yet completely settled and we should suspend our judgement.

6. High-pressure polymorphs of ice

The existence of a number of high-pressure phases of ice is a natural consequence of the very open structure of normal Ice I_h. Such a four-coordinated arrangement of nearly spherical molecules could never be expected to remain stable in the limit of high pressures and must ultimately collapse to a much more nearly close packed configuration. One of the most interesting things about ice is the fact that this collapse takes place through a series of structures each with a considerable stability range. There are, in fact, no less than ten crystalline phases of ice which have received study and it is by no means certain that the list is completely exhausted (Whalley 1969). In addition, the clathrate compounds which we mentioned in §3.5 are water frameworks containing foreign molecules whose only role is to occupy the large cavities in the structure and so prevent its collapse. It is possible that these frameworks might form stable phases at negative pressures.

6.1. *The phase diagram of water*

The phase diagram of water, as far as it is known at present, is shown in figure 16. The study of this diagram began with the work of Tammann (1900) who explored it out to about 3 kbar and discovered the phases now known as II and III. Bridgman

(1912) extended the pressure range to 18 kbar and discovered Ices V and VI, and much later (Bridgman 1937), achieved pressures up to about 45 kbar and discovered Ice VII. He also investigated the phase diagram of D_2O (Bridgman 1935) and substantiated the existence of the metastable form Ice IV of which there had been some indication in his studies of H_2O. The most recent discoveries have been those of Ice VIII and Ice IX by Whalley *et al* (1966, 1968). The melting line of Ice VII has been followed by Pistorius *et al* (1963) out to a nominal pressure of 200 kbar, without finding any further phase changes. Whalley *et al* (1966) questioned the

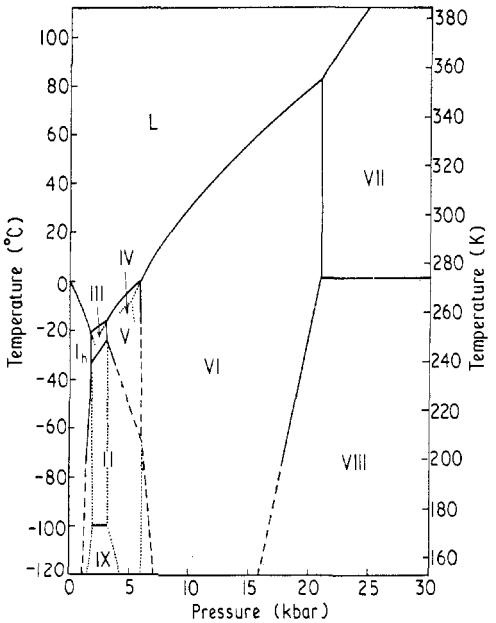

Figure 16. The phase diagram for ice. Broken lines represent presumed continuations of phase boundaries which have not yet been fully investigated; dotted lines represent metastable continuations of one phase into the region of stability of another.

accuracy of the pressure determination at this extreme limit and a later reassessment by Pistorius *et al* (1968) set the highest pressure reached at about 170 kbar, at which pressure the melting point of Ice VII was 442 °C. The melting curve of Ice VII over the measured range can then be approximated by the Simon equation in the form

$$p - 22 \simeq 6{\cdot}429\left\{\left(\frac{T}{354{\cdot}8}\right)^{4{\cdot}543} - 1\right\} \tag{6.1}$$

where p is in kbar and T in K.

The volume changes at the various phase transitions can be measured directly in the course of experiment but, because of the difficulties of calorimetry under high-pressure conditions, the latent heats and entropy changes must be determined indirectly. This is accomplished from the Clausius–Clapeyron equation

$$\frac{\mathrm{d}p}{\mathrm{d}T} = \frac{S_2 - S_1}{V_2 - V_1} \tag{6.2}$$

which relates the entropies and volumes of two adjacent phases to the slope of the

phase boundary which separates them. These quantities are shown for H_2O in table 16.

Table 16. Triple-point relations for the phase diagram of water, H_2O

Phases	Pressure (bar)	Temperature (°C)	Volume change ($cm^3\ mol^{-1}$)	Latent heat ($J\ mol^{-1}$)	Entropy change (Nk)
			L–I–Vap (reference 1)		
I → L			−1·63	5985	2·6
I → Vap	0·006	+0·01	–	50 900	22·4
L → Vap			–	44 910	19·8
			L–I–III (reference 2)		
I → L			−2·43	4230	2·03
III → L	2070	−22·0	0·84	3830	1·84
I → III			3·27	393	0·19
			L–III–V (reference 2)		
III → L			0·43	4617	2·17
V → L	3460	−17·0	1·42	4688	2·20
III → V			−0·98	−71	−0·03
			L–V–VI (reference 2)		
V → L			0·95	5274	2·32
VI → L	6250	+0·16	1·65	5290	2·33
V → VI			0·70	−17	−0·01
			L–VI–VII (reference 3)		
VI → L			0·59	6362	2·16
VII → L	21 500	+81·6	1·64	6362	2·16
VI → VII			−1·05	0	0·00
			I–II–III (reference 2)		
I → II			−3·92	−753	−0·38
I → III	2130	−34·7	−3·53	167	0·08
II → III			0·39	921	0·46
			II–III–V (reference 2)		
II → III			0·26	1272	0·61
II → V	3440	−24·3	−0·72	1205	0·58
III → V			−0·98	−67	−0·03
			VI–VII–VIII (reference 4)		
VI → VII			−1·0 (3)	−92	−0·04
VI → VIII	21 200	+5	−1·0 (3)	−1197	−0·51
VII → VIII			0·00	−1105	−0·47

References: 1, International Critical Tables;
2, Bridgman (1935);
3, Bridgman (1937), with corrected pressure (Pistorius *et al* 1963, Brown and Whalley 1966);
4, Brown and Whalley (1966), Whalley *et al* (1966).

Similar tabulations for D_2O are given by Bridgman (1935) up to the V–VI transition, and Pistorius *et al* (1968) have studied the region to 40 kbar. Generally speaking the results for D_2O and H_2O are very similar. The triple point temperatures for D_2O are about 3 K higher than those for H_2O and the pressures higher by 1 to 5%. There are, however, irregularities which suggest minor structural differences between the two materials which have not been investigated in detail.

6.2. *Metastability*

The phenomenon of metastability is well known to all those who study phase transitions. The earliest theoretical discussion seems to be that of Gibbs in the last

century (see Gibbs 1928) and his ideas were later developed into a theory of the nucleation of phase changes by Volmer, with subsequent refinements being made by Becker and Döring and by Zeldovich and Frenkel. General accounts of the theory have been given by Volmer (1939), Frenkel (1946) and Hirth and Pound (1963) while particular application to the freezing of water is discussed by Fletcher (1970 pp85–103). Briefly, in order that a new phase form, it must commence as a tiny embryo with a large surface-to-volume ratio and hence an appreciable free energy of formation ΔF, because of the interfacial free energy involved. The maximum value ΔF^* of this free energy of embryo formation is the free energy barrier to nucleation, and the nucleation rate J has the form given in equations (5.2) and (5.3). The presence of foreign particles of appropriate size, shape and surface structure may reduce the value of ΔF^* very considerably and hence promote the phase change (Fletcher 1963b).

In the phase diagram of figure 16 the metastable prolongations of some of the phase boundaries are shown. The phase Ice IV is entirely metastable in the region of stability of Ice V and Bridgman remarked that once Ice V had been produced in a pressure cell it was then impossible to produce Ice IV in it, presumably because of a residual nucleation effect. Similarly, Ice III can be supercooled metastably into the stability region of Ice II and actually undergoes a phase change to another metastable form, Ice IX, at about -100 °C. Most of the other phase regions can be extended metastably in this way and, in particular, liquid water can be supercooled (by as much as 40 °C for small pure droplets) over much of the range. Evans (1967) has investigated the properties as selective nucleators of all the high-pressure ices and has found insoluble organic materials which selectively nucleate each of the ices except II and VII from liquid water.

A rather different sort of metastability, first noted by Tammann (1909), has since been used by many workers to study the properties of the high-pressure ices. Tammann found that, if these polymorphs are cooled to liquid nitrogen temperature, they can then be brought to ordinary atmospheric pressure without undergoing a phase change. When the temperature is allowed to rise above about 150 K all the polymorphs then transform to cubic Ice I_c and finally, at a higher temperature, to Ice I_h (Bertie *et al* 1963, 1964).

6.3. *Proton order in the high-pressure ices*

Before we consider any crystallographic data on the ice phases, it is possible to make some general deductions about them on the basis of relatively simple observations. Thus Bertie and Whalley (1964a,b) have examined the infrared spectra and Taylor and Whalley (1964) and Marckmann and Whalley (1964) the Raman spectra of nearly all the ice polymorphs in the region covering the intramolecular vibration frequencies. (These measurements are conveniently summarized by Eisenberg and Kauzmann (1969) in their table 3.16, though for Ices III and VII we should read IX and VIII as discussed below.) While there are some significant differences between these spectra, they all have bands in fairly clear relation to the distortional vibrations of an isolated water molecule, so that we may reasonably conclude that molecules remain intact in all the ices. Indeed the shifts from the free-molecule spectra are all sufficiently similar to those for Ice I_h that it is very likely that all the protons are fully bonded as in that structure.

The existence of intact water molecules in all the ice structures immediately recalls one of the Bernal–Fowler rules governing the structure of Ice I. If the

second rule is also obeyed, then it is logical to ask whether the structures of the high-pressure polymorphs are statistical, as with Ice I, or whether their protons are ordered. Before turning to the diffraction evidence, we shall see that this question can be answered quite unambiguously from other experimental results.

Examination of the intramolecular vibrations of the ice polymorphs is made easier by using a dilute solution of HDO in H_2O, for the deuteron vibration frequency is sufficiently different from that of the protons that deuterons are essentially uncoupled and act as a probe for the details of the molecular environment. Using this technique Bertie and Whalley (1964a,b) found that in Ices I_h, I_c and V the O—D stretching band near 2400 cm^{-1} is rather broad and featureless, indicating a variety of slightly differing molecular environments and hence suggesting a disordered proton arrangement. In contrast the O—D stretching band in Ice II shows four distinct peaks and that for Ice IX two peaks, which indicates that there are these numbers of distinctly different deuteron environments in these two structures. A somewhat similar situation applies in the libration band near 800 cm^{-1}. In Ice I and V the band is featureless while in Ices II and IX it shows fine structure. The Raman studies (Taylor and Whalley 1964) show similar effects. In their paper, Bertie and Whalley (1964b) believed they were studying Ice III rather than the then unrecognized Ice IX and stated their results accordingly. However, since the specimens were prepared and studied at ordinary atmospheric pressure by Tammann's technique, the temperature was actually about 100 K where we should now expect the form concerned to be Ice IX.

The far infrared spectrum (50–350 cm^{-1}) associated with lattice vibration modes has also been studied for Ices I_h and I_c by Bertie and Whalley (1967) and for Ices II, V, VI and IX by Bertie *et al* (1968a,b). Ices I_h, I_c, V and VI show broadly humped absorption spectra which can be explained on the basis that the protons are disordered so that all translational lattice modes are infrared active in proportion to the square of their frequency (Whalley and Bertie 1967). In Ices II and IX, however, the spectrum shows sharp peaks which are characteristic of crystals with ordered dipoles. From these results, then, we conclude that Ices V and VI have disordered structures like Ice I while Ices II and IX have ordered structures. We shall see that other studies confirm and extend these conclusions.

A macroscopic quantity which is strongly dependent on dipole order is the dielectric constant. If the dipoles are disordered and free to rotate, then the static dielectric constant should be large, of the order of 100 as in ordinary ice, while, if the dipole orientations are fixed, the dielectric constant should be less than 10. The dielectric properties of all the high-pressure ices have been studied by Wilson *et al* (1965) and by Whalley *et al* (1966, 1968) and their measurements are summarized in table 17. From this table and the interpretation given above, it is clear that the protons are statistically arranged in Ices I, III, V, VI and VII, while in Ices II, VIII and IX they are ordered. This is in agreement with the conclusions drawn from infrared data.

Finally let us examine the thermodynamic information contained in table 16. Here the last column lists the entropy change, in units of Nk, associated with transitions between the various ice polymorphs. A simple inspection of this column shows that the entropy of Ices II and VIII is about 0·4 to 0·6Nk lower than the entropy of Ices I, III, V, VI and VII, a fact which seems to have been pointed out first by Kamb (1964). We recall that proton disorder in Ice I_h is associated with a configurational entropy of about 0·4Nk and the inference is therefore strong that

Ices II and VIII are ordered while the remainder have statistical structures. If we look at the phase diagram in figure 16, it is also clear from application of equation (6.2) to the horizontal phase boundaries separating Ices III and IX and Ices VII and VIII that $\Delta V = 0$ for these transitions. We conclude therefore that Ices IX and VIII are simply proton-ordered forms of the statistical phases III and VII.

Table 17. Static dielectric constants of ice polymorphs†

Ice	Pressure (kbar)	Temperature (°C)	Dielectric constant
I	0	−30	99
II	2·3	−30	3·66
III	3	−30	117
V	5	−30	144
VI	8	−30	193
VII	>21	+22	≃150
VIII	>21	0	≃4
IX	2·3	−110	≃4

† From Wilson *et al* (1965) and Whalley *et al* (1966, 1968).

7. Crystal structures of the high-pressure ices

Study of the crystal structures of the high-pressure ice polymorphs has, with the exception of two papers by McFarlan (1936a,b), been concentrated in the last ten years and most of our detailed structural knowledge is due to the work of Kamb and his collaborators at the California Institute of Technology. In this section we shall discuss and illustrate each of the structures in turn but it may be useful to have a compilation for comparison. This is given in table 18. The x ray structural

Table 18. X ray structural data for the ice polymorphs

Polymorph	Density (g cm^{-3}) at −175 °C, 1 bar	Crystal system	Space group	Molecules per cell	Cell dimensions (Å)	Reference
I_h	0·92	Hexagonal	$P6_3/mmc$	4	$a = 4{\cdot}48$ $c = 7{\cdot}31$	
I_c	0·92	Cubic	$Fd3m$	8	$a = 6{\cdot}35$	
II	1·17	Rhombohedral	$R\bar{3}$	12	$a = 7{\cdot}74$ $\alpha = 113{\cdot}1°$	1
III, (IX)	1·14	Tetragonal	$P4_12_12$	12	$a = 6{\cdot}79$ $c = 6{\cdot}79$	2
					$a = 6{\cdot}73$ $c = 6{\cdot}83$	3
IV	1·28					4
V	1·23	Monoclinic	$A2/a$		$a = 9{\cdot}22$ $b = 7{\cdot}54$ $c = 10{\cdot}35$ $\beta = 109{\cdot}2°$	4
VI	1·31	Tetragonal	$P4_2/nmc$	10	$a = 6{\cdot}27$ $c = 5{\cdot}79$	4
VII, (VIII)	1·50	Cubic	$Pn3m$	2	$a = 3{\cdot}41$	5

References: 1, Kamb (1964); 2, Kamb and Datta (1960); 3, Hamilton *et al* (1969); 4, Kamb (1965a); 5, Kamb and Davis (1964).

data were mostly taken on the metastable material at −175 °C and 1 bar, since this represents a simpler experimental procedure than high-pressure diffraction studies. A few of these latter measurements have, however, been made and these confirm the expectation that the increase in density in going from the p, T conditions of table 18 to those characteristic of the normal region of existence of the phase is only about 3% (Kamb *et al* 1967).

Another general comment is appropriate before we proceed to detailed discussion of crystal structures, and that is that the diffraction data show the water molecules in all the high-pressure ices to be intact and roughly tetrahedrally bonded to four neighbouring molecules. This persistence of fourfold coordination is one of the most striking and significant features of all the phases of ice.

7.1. *Ice II*

The first reported x ray diffraction study of Ice II is that of McFarlan (1936a,b). Later workers, however, while agreeing among themselves, do not find patterns like his, so that it seems that he must have produced a mixed specimen. Bertie *et al* (1963), in an x ray powder study of several ice polymorphs under metastable conditions at atmospheric pressure, produced the first positive identification of the symmetry and lattice parameters of Ice II as shown in table 19. The primitive cell

Table 19. Lattice parameter determinations for Ice II at atmospheric pressure

Temperature	Rhombohedral cell		Hexagonal cell		Reference
(K)	a (Å)	α	a_H (Å)	c_H (Å)	
~90	7·74	113·1°	12·92	6·23	Bertie *et al* (1963)
~80	7·78 ± 0·01	113·1 ± 0·2°	12·97 ± 0·02	6·25 ± 0·01	Kamb (1964)
~80	7·743 ± 0·002	113·09 ± 0·03°	12·920 ± 0·003	6·234 ± 0·002	Finch *et al* (1968)

is rhombohedral but for many purposes it is simpler to use a triply-primitive hexagonal cell of the dimensions shown. The space group was not determined.

Kamb (1964) found that his particular method for the preparation of Ice II led to single crystals of large enough size for detailed x ray study and he was able, therefore, to find not only the cell dimensions shown in table 19 but also the space group and crystal structure. His conclusion was that Ice II belongs to the space group $R\bar{3}$ (or C_{3i}^2 in the Schönflies notation), though the actual diffraction symmetry was disguised somewhat by twinning of the specimen. This space group is closely related to $R\bar{3}c$ (or D_{3d}^6) but there is a distortion of this pseudostructure, ultimately caused by proton ordering, which results in some violation of the c glide extinction conditions and leads to $R\bar{3}$ symmetry. With the inclusion of hydrogens, to which the x ray diffraction pattern is not sensitive, the structure refines to $R = 0{\cdot}08$ on the basis of 152 observed reflections.

The Ice II structure deduced by Kamb is shown in plate 1(c) and in figure 17, which is a projection on the hexagonal basal plane. The hexagonal ring, which we saw in §3.5 to be particularly stable, is a prime constituent of the structure and there are two nonequivalent rings in the unit cell as shown, one being twisted through about 15° relative to the other. These rings are rather flatter than the equivalent rings in the Ice I structures so that the bond angles are rather distorted.

Each water molecule is, however, tetrahedrally coordinated, with bond lengths in the range 2·75 to 2·84 Å. The O—O—O bond angles range from 85 to 129°. These distortions, together with a different bonding pattern, allow a significantly closer packing than in Ice I, giving a density of 1·17 g cm^{-3}.

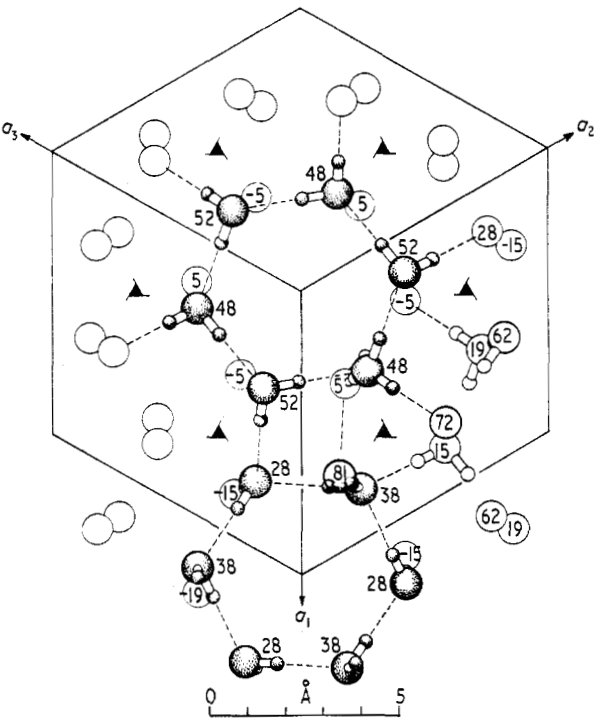

Figure 17. The structure of Ice II viewed in projection along the hexagonal *c* axis. The rhombohedral unit cell is outlined and threefold screw axes are indicated. Figures give the height of each atom above the projection plane in hundredths of the *c* axis length (Kamb 1964).

The spectroscopic and dielectric measurements discussed in § 6 now indicate unambiguously that the protons in Ice II are fully ordered. In the absence of these data Kamb observed the considerable range of bond angles present in the structure and, on the basis of the entropy data, conjectured that the protons are probably located so that the H—O—H angles of individual molecules are as close as possible to the 104·5° characteristic of the free molecule and so that the O—H···O bonds are as nearly collinear as possible. This leads to the configuration shown in figure 17, the H—O—H angles deviating by at most 8° from the free molecule value if collinear bonds are assumed.

More recently Finch *et al* (1968) have performed neutron diffraction studies on powdered D_2O Ice II to locate the protons (deuterons) and have confirmed Kamb's structure. Their lattice parameter determinations are also given in table 19. They found that O—D···O bonds are not, in fact, strictly collinear and that all the D—O—D angles lie in the range $106 \pm 3°$. The O—D distances vary slightly from one bond to another and range from $0{\cdot}96 \pm 0{\cdot}04$ Å to $1{\cdot}04 \pm 0{\cdot}04$ Å. A single-crystal neutron diffraction study by Hamilton *et al* (1969), published in preliminary form, confirms these conclusions, achieving an *R* value of 0·08 for 167 reflections.

7.2. *Ice III and Ice IX*

McFarlan was again the first to report an x ray study of Ice III though, because of his uncertainty about the exact phases involved, he actually reported it as Ice II (McFarlan 1936b). A diffraction study was then carried out by Kamb and Datta (1960), using both powder and single-crystal techniques, and a much more detailed investigation was published recently by Kamb and Prakash (1968). Bertie *et al* (1963) also reported powder diffraction data, and neutron diffraction studies have been made by Rabideau *et al* (1968), Hamilton *et al* (1969) and Rabideau and Finch (1969). All these studies agree that Ice III (or Ice IX, which is the phase actually studied in the quenched metastable form) is a tetragonal crystal (though dimensionally nearly cubic) belonging to the space group $P4_12_12$ or D_4^4. The unit cell contains twelve molecules and its dimensions are shown in table 20. It may perhaps

Table 20. Lattice parameter determinations for Ice IX or Ice III at atmospheric pressure

Temperature (K)	a (Å)	c (Å)	Reference
80	$6{\cdot}745 \pm 0{\cdot}004$	$6{\cdot}745 \pm 0{\cdot}004$	Rabideau *et al* (1968)
83	6·80	6·80	Kamb and Datta (1960)
90	6·75	6·79	Bertie *et al* (1963)
98	$6{\cdot}73 \pm 0{\cdot}01$	$6{\cdot}83 \pm 0{\cdot}01$	Kamb and Prakash (1968)

be significant that the appreciably different c/a ratios found by different workers span the temperature range in which the III, IX transition takes place under pressure. Thus the measurement by Rabideau *et al* (1968) at 80 K almost certainly refers to the completely ordered Ice IX phase, while that of Kamb and Prakash (1968) at 98 K may be at least partly into the disordered Ice III region. A decisive measurement at a higher temperature is difficult because of the slow conversion to Ice I_c at atmospheric pressure, and a diffraction study at high pressure will be needed to clarify the point. The x ray study by Kamb and Prakash (1968) gave almost equally good results for an ordered or a statistical proton distribution ($R = 0{\cdot}057$ and $R = 0{\cdot}051$ respectively) but of course x ray results are rather insensitive to hydrogen positions.

The crystal structure of the Ice IX, as determined by Kamb and Datta (1960), with proton positions determined from neutron diffraction study of D_2O ice (Hamilton *et al* 1968, Rabideau *et al* 1968), is shown in figure 18 and plate 1(*c*). Ice III is exactly similar except that the protons are disordered. The topology of the structure is the same as that of the silica polymorph keatite. As can be seen from plate 1(*c*), the coordination is still fourfold but the hexagonal rings which were a feature of the Ice I_h, I_c and II structures do not occur. In fact the predominant ring is the five-membered ring, which we saw in § 3·5 to be almost as stable, in isolation, as the six-membered ring.

In figure 18 the structure is viewed in projection on the basal plane. Water molecules of type 1 form helical chains about the fourfold screw axes 4_1 parallel to the c axis. These helices are linked together laterally by other water molecules of type 2. Each O(1) molecule is a member of two five-membered rings and each O(2) of four five-membered rings.

The O—O bond lengths in Ice III range from about 2·75 to 2·80 Å, which actually represents a longer average bond distance than the 2·76 Å characteristic of Ice I. The packing is, however, much denser at the second-neighbour level, the

characteristic distance in Ice III being about 3·6 Å instead of the 4·5 Å in Ice I. The O—O—O angles in the structure are distorted appreciably from the tetrahedral value and range from 89·5° to 143·2°. If this single largest angle is omitted, however, the range is only 89·5° to 128·1° which is significantly smaller than in the Ice II structure. The neutron diffraction data on Ice IX show that the actual proton positions occupied are those giving best fit between the O—O—O angles and an assumed 'natural' H—O—H angle of about 104·5°, as predicted by Whalley *et al* (1968).

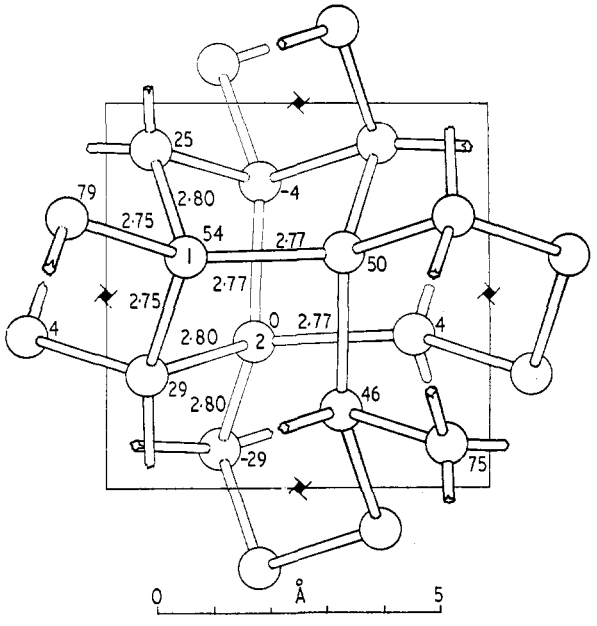

Figure 18. The structure of Ice III or Ice IX. The drawing is projected along the *c* axis and and heights above the projection plane are given in hundredths of the *c* axis length (Kamb and Prakash 1968).

The neutron diffraction studies of Hamilton *et al* (1968) and Rabideau *et al* (1968) differ slightly on the O—D bond lengths and D—O—D bond angles (the O—D···O bonds not being assumed strictly collinear). Hamilton *et al* found O—D distances of 0·97 and 0·98 Å for all molecules and a D—O—D angle of 106° for molecules of type 1 and of 104·5° for molecules of type 2. Rabideau *et al*, however, found bond lengths of $0{\cdot}99 \pm 0{\cdot}06$ and $0{\cdot}93 \pm 0{\cdot}04$ Å with a bond angle of $101 \pm 4°$ for molecules of type 1 and bond lengths of $1{\cdot}00 \pm 0{\cdot}04$ with the surprisingly small bond angle of $90 \pm 4°$ for molecules of type 2. They point out the unlikely nature of this second angle and, granting this, the disagreements are not very significant.

Because of the deviations of O—O—O angles from the tetrahedral value it is not surprising that Ice III becomes an ordered phase, Ice IX, at low temperatures. The extreme angle 143·2° is so large that it is probably avoided by proton pairs even in the Ice III region but, omitting this, the smaller angular spread in Ice III makes it reasonable that it should become ordered at a lower temperature than does Ice II. As Hamilton *et al* (1968) point out, the ordering of protons in the Ice III structure does not cause any change in total crystal symmetry, in distinction from the situation in Ices II and V. The measurements of Whalley *et al* (1968) on

dielectric behaviour of Ices III and IX suggest that ordering begins at about -65 °C and is not complete until -108 °C, so that it is an idealization to simply draw the III–IX phase boundary at -100 °C as in figure 16.

7.3. *Ice IV*

Because of its metastability Ice IV has not been subject to diffraction study so that little is known of its crystal structure. All the evidence suggests that full fourfold bonding is maintained, and the entropy change in the IV–VI transition is only $-0{\cdot}004Nk$ so that the protons in Ice IV are presumably disordered, as they are in Ice VI. The volume change in the IV–VI transition is $-0{\cdot}35$ cm^3 mol^{-1} compared with $-0{\cdot}70$ cm^3 mol^{-1} for the V–VI transition, which suggests an intermediate bonding arrangement. However, as we shall see presently, the bonding in Ice VI is of a dramatically different and more stable type than in Ice V so that it is difficult to guess an interpolated structure.

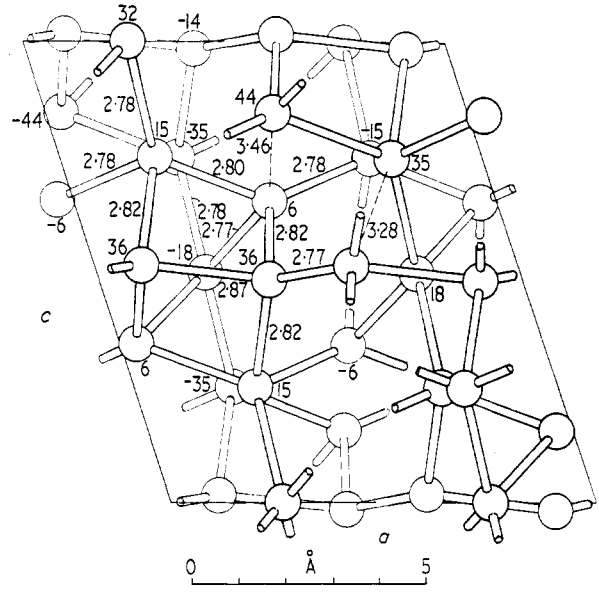

Figure 19. The structure of Ice V projected along the *b* axis. Heights are given in hundredths of the *b* axis length (Kamb *et al* 1967).

7.4. *Ice V*

The first powder diffraction study of Ice V was that of Bertie *et al* (1963) but they did not identify the unit cell. Later Kamb *et al* (1967) confirmed this powder pattern and were able to produce single crystals large enough for study by the precession method, from which the crystal structure was determined. The unit cell is monoclinic with dimensions

$$a = 9{\cdot}22 \text{ Å} \quad b = 7{\cdot}54 \text{ Å} \quad c = 10{\cdot}35 \text{ Å} \quad \beta = 109{\cdot}2^\circ \tag{7.1}$$

and the structure belongs to the space group $A2/a$ (or C_{2h}^6) with twelve molecules in the unit cell. This structure is shown in figure 19 and plate 2(*a*). The O—O bond distances all lie between 2·77 and 2·87 Å, which is still greater than in Ice I,

but distortion of bonding angles allows second neighbours to approach as closely as 3·46 Å. O—O—O bond angles range from 83° to 135° so that, though the thermodynamic, dielectric and infrared evidence indicates a proton-disordered structure under the conditions of study, it is reasonable to expect proton ordering at some lower temperature.

This possibility has been examined by neutron diffraction by Hamilton *et al* (1968). Their measurements indicate significant proton ordering at 100 K but, interestingly, the population factors for the pairs of proton sites, which would be (0·5, 0·5) for a completely disordered and (0, 1) for a completely ordered structure, range fairly evenly from 0·07 to 0·94. This indicates that the structure is only partly ordered at this temperature. It is not yet clear whether this represents the equilibrium situation or whether the relaxation time for the proton configuration at this temperature is so long that the partial order characteristic of a higher temperature is frozen in.

7.5. *Ice VI*

The first reported powder diffraction studies of Ice VI were those of Bertie *et al* (1964) and of Kamb and Davis (1964), while Weir *et al* (1965) actually carried out single crystal diffraction experiments under high-pressure conditions. The unit cell identification of these latter investigators was, however, modified by Kamb (1965a) who carried out a detailed single crystal study of the metastable state at

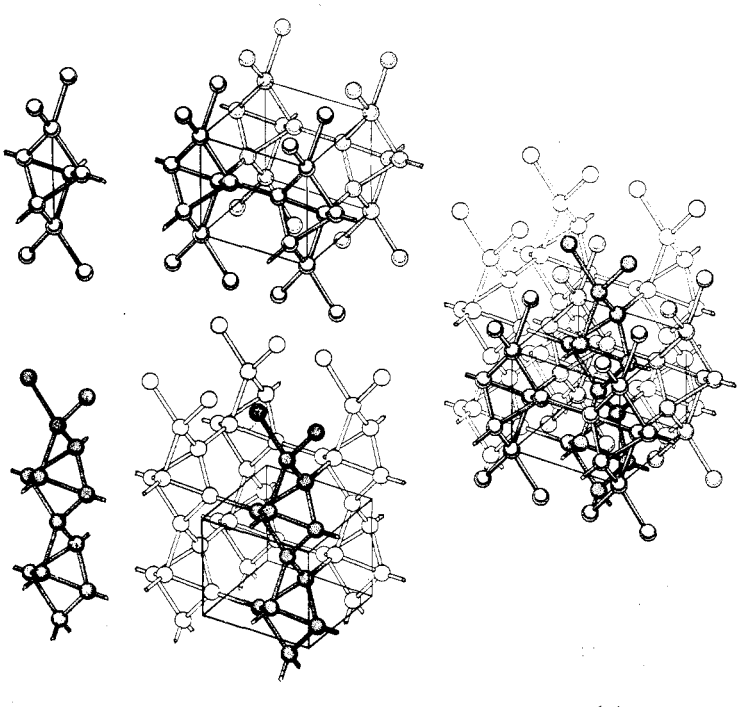

Figure 20. The structure of Ice VI shown by the assembly of its component parts. (*a*) shows the hydrogen-bonded chains of water molecules running parallel to the *c* axis and in (*b*) these chains are linked together sideways to form the two separate molecular frameworks. (*c*) shows these two frameworks combined into a single unit cell to form the interpenetrating Ice VI structure (Kamb 1965a).

98 K and atmospheric pressure. He established the unit cell to be tetragonal with dimensions

$$a = 6{\cdot}27 \text{ Å} \qquad c = 5{\cdot}79 \text{ Å} \tag{7.2}$$

and determined a structure with ten atoms to the unit cell belonging to the space group $P4_2/nmc$ or D_{4h}^{15}.

This structure, which refined to a residual $R = 0{\cdot}07$, is of a particularly interesting new type, shown in figures 20 and 21 and in plate 2(*b*), which can be termed a

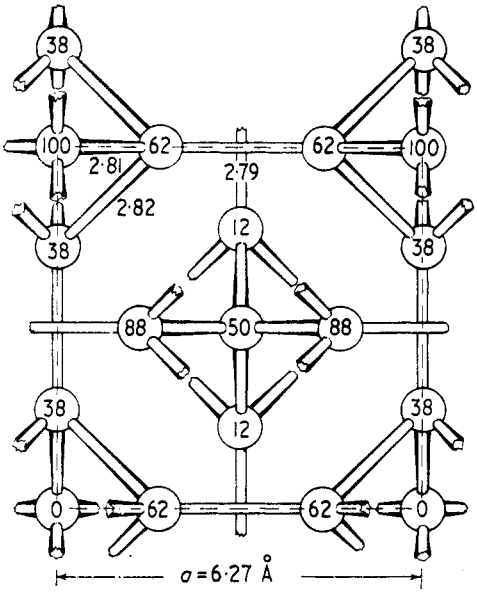

Figure 21. The structure of Ice VI shown projected along the *c* axis. Heights of molecules above the projection plane are given in hundredths of the *c* axis length (Kamb 1965a).

self-clathrate. The molecules in the structure are organized into two entirely separate but equivalent frameworks, each of which consists of chains of molecules, as in figure 20(*a*), running parallel to the *c* axis and bonded together at intervals as in figure 20(*b*). Such a structure has, however, long columnar cavities running parallel to the *c* axis which are precisely able to accommodate the chains of the second framework. This remarkable structure is thus able to preserve fourfold hydrogen bonding within each framework while at the same time achieving a considerable increase in packing density. There is no analogous structure among the silica minerals but chains of similar topology occur in certain of the fibrous zeolites (Kamb 1965a).

In the Ice VI structure each water molecule has four bonded neighbours, all at a distance of 2·81 Å, while the distance to the eight next-nearest neighbours of the other framework is the considerably greater distance 3·51 Å. The O—O—O bond angles in each framework range from 76° to 128° so that, though the infrared and dielectric measurements show the protons to be disordered, we should expect ordering at low enough temperatures if sufficient time is given for equilibrium to be reached. Whalley (1969) describes some evidence for a slow reversible transition in the dielectric properties near 123 K but the time necessary for its completion is several months and further details have not yet been published.

7.6. *Ice VII and Ice VIII*

Diffraction data on Ice VII, held metastably at atmospheric pressure and −190 °C, were first reported by Bertie *et al* (1964). Our present knowledge suggests that the phase involved was actually Ice VIII, which differs from Ice VII only through its proton ordering. Soon after this Kamb and Davis (1964) made a powder diffraction study under high pressure, though still in the stability region of Ice VIII, and Weir *et al* (1965) achieved the difficult feat of performing a single crystal diffraction study at a pressure of 25 kbar, in the stability region of Ice VII.

Table 21. Lattice parameter determinations for Ices VII and VIII

Phase	Pressure (kbar)	Temperature (°C)	*a* (Å)	Reference
VIII*	0	−190	3·41	Bertie *et al* (1964)
VIII	25	−50	3·30 ± 0·01	Kamb and Davis (1964)
VII	25	+25	3·40 ± 0·05	Weir *et al* (1965)

With the reservation that the low-pressure data of Bertie *et al* show extra lines apparently associated with some form of superlattice structure, the studies are in good agreement and show a body centred cubic cell with the dimensions shown in table 21. The space group for the body centred cell, assuming proton disorder, is $Pn3m$ or O_h^4.

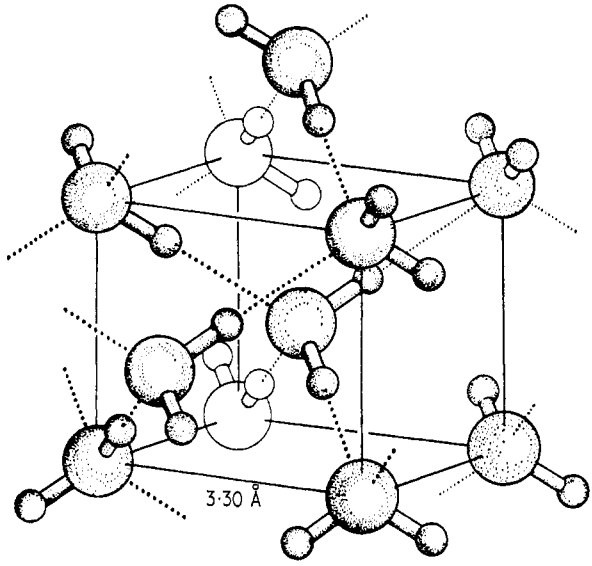

Figure 22. The structure of Ice VII. The unit cell is cubic and oxygen atoms have a BCC arrangement. They are, however, linked together to form two independent hydrogen-bonded frameworks as shown. An arbitrary proton arrangement is shown and hydrogen bonds are indicated by dotted lines (Kamb 1965b).

The body centred cubic structure at first sight represents a significant departure from all the other ice structures, since the coordination number is 8 instead of 4. Kamb and Davis (1964), however, proposed the novel self-clathrate structure shown in figure 22 and plate 2(*c*) in which the body centred structure is actually composed of two identical, interpenetrating but separately bonded diamond cubic (Ice I_c) structures. The similarity in principle between this and the self-clathrate structure which Kamb proposed in 1965 for Ice VI is obvious.

Such a structure is uniquely suitable to provide a high packing density, nearly twice that of Ice I, while maintaining the tetrahedral bonding framework, in this case quite undistorted. The O—O bond length in Ice VIII at 25 kbar is 2·86 Å according to Kamb and Davis and 2·94 Å from the data of Weir *et al*, which is longer than the 2·76 Å characteristic of Ice I, but the distance to the independently bonded molecules of the other framework is also 2·86 Å (or 2·94 Å). All the O—O—O bond angles have the ideal tetrahedral value 109·5°.

In the face of this regularity it is, perhaps, a little surprising that the protons in Ice VII become ordered to give the Ice VIII structure at the comparatively high temperature of 0 °C. The form of the ordering has not yet been elucidated but it seems likely that it is a cooperative effect involving antiparallel orientation of dipoles on the two lattices rather than the gradual concentration of protons on preferred sites which we found, for example, in the III → IX transition. The latter extends, as we saw in § 7.2, over a range of some 40 K, while the measurements of Whalley *et al* (1966) show the VII → VIII transition to occupy less than 2 K, though there seems to be a slight hysteresis effect depending upon the direction of the temperature change.

We have already seen that the experimental evidence of the phase diagram suggests that there are no further phases of ice up to pressures of at least 200 kbar. Kamb (1965b) has discussed in some detail the relative stability of the Ice VII structure and a hypothetical close packed arrangement formed by distorting this, without changing the bonding, to a face centred cubic arrangement. He concludes that the Ice VII structure is the stable one up to at least 200 kbar in agreement with experiment.

The possibility of a more subtle change in which the O—O bonds are all so compressed that the protons take up symmetrical positions has also been examined by Yean and Riter (1971). On the basis of compressibility measurements on both H_2O and D_2O in the Ice VII phase, out to 165 and 220 kbar respectively, by Holzapfel and Drickamer (1968), they concluded that no such symmetrization occurs at least out to these pressures. The O—O distance is 2·55 Å and the O—D distance 0·94 Å at 220 kbar. Such *ab initio* calculations as have been made (eg Weissmann and Cohan 1965) confirm this conclusion.

7.7. *Conclusions*

From the work which has been reported on all the crystalline phases of ice, several important features emerge which it is worthwhile to repeat. This is so, not only because of the importance of these crystalline phases but also because of the bearing which these conclusions have upon structural problems in the liquid state.

The tendency of the water molecule to be bonded to four neighbours is remarkably strong and persists out to the highest attainable pressures. This is a feature of all the ice structures—the bonds may stretch or bend but they do not break. This allows a remarkable sequence of distorted structures and, in addition, the even more remarkable and beautiful self-clathrate structures of Ices VI, VII and VIII.

With bond bending and bond stretching such predominant features of the ice structures, it is useful to have some numerical idea of the magnitudes involved. The stable ice structures have O—H···O bond lengths ranging from 2·75 to as much as 2·94 Å at atmospheric pressure and as short as 2·55 Å at very high pressures. The bond angles range from 76° to 143°, with the more extreme angles being

tolerated by the proton acceptor rather than the proton donor molecule. The bonds themselves are more or less collinear but the proton may be a few tenths of an ångström off the O—O line. Even in the case of the shortest bonds the intramolecular O—H distance is little changed from the free molecule value and the bonds remain asymmetric. The distance of closest approach between nonbonded molecules is usually constrained by the bond configuration but in the self-clathrate structures, where this is not the case, such molecules may approach to within about 2·9 Å of each other.

8. The structure of liquid water

The physical properties of liquid water, both in the pure state and in its interaction with various solutes, have been reviewed in detail by Eisenberg and Kauzmann (1969) and Kavanau (1964), while Samoilov (1957) gives a view in a somewhat different perspective and monographs on electrolyte solutions are plentiful. We shall not attempt to review these properties here but simply refer, when appropriate, to those which are particularly illuminating in the study of water structure. Any thoroughly satisfactory description of liquid water must, of course, explain all the experimental observations and this puts quite strong constraints upon the admissible models.

8.1. *Description of liquid structure*

The instantaneous structure of a liquid like water can be expressed in quite a general case by a symbol such as $\{\boldsymbol{r}_i; \boldsymbol{\theta}_i; \boldsymbol{\xi}_i\}$ where the vectors $\boldsymbol{r}_i$ give the position of the centre of mass of the ith molecule, the angles $\boldsymbol{\theta}_i$ specify its orientation, and the further coordinates $\boldsymbol{\xi}_i$ detail its internal configuration. Since i must range up to about 10^{22} for a macroscopic quantity of liquid, such a specification is clearly unrealistic.

The internal coordinates $\boldsymbol{\xi}_i$ execute oscillations at infrared frequencies ($\sim 10^{14}\ s^{-1}$), so that for time spans longer than this they are irrelevant. The behaviour of the $\boldsymbol{r}_i$ and $\boldsymbol{\theta}_i$ coordinates is somewhat different since, in addition to undergoing small-amplitude interactions at low infrared frequencies ($\sim 10^{13}\ s^{-1}$), they also suffer very much larger changes in times of order 10^{-10} s which can be called structural diffusion. This time can be identified, in the case of water, from diffusion studies, from dielectric relaxation measurements and from neutron inelastic scattering. When we speak of the 'structure' of water, we generally mean the configuration which would be observed as essentially static in a time of order 10^{-11} to 10^{-12} s.

Direct structural observations or measurements cannot reasonably be made in a time as short as this so that the liquid structure can only be inferred indirectly, for example by postulating a particular structure on reasonable physical grounds and then showing that it accounts more or less well for the actual observations. Such a model, to be satisfactory, must account for the observed thermodynamic properties of the liquid and for its optical (especially infrared) and dielectric properties. Most importantly it must agree with the radial distribution function, which is the most detailed structural information available from diffraction studies.

8.2. *The radial distribution function*

From a statistical point of view, the structure of a liquid is defined by a set of correlation functions $g_n(\boldsymbol{r}_1; \boldsymbol{r}_2, \boldsymbol{r}_3, \ldots, \boldsymbol{r}_n)$ which specify the probability that an atom

be found at the position $\boldsymbol{r}_1$, given that there are atoms at positions $\boldsymbol{r}_2, \boldsymbol{r}_3, \ldots, \boldsymbol{r}_n$. For a molecular liquid like water these correlation functions should be generalized to the form $g_n(\boldsymbol{r}_1\boldsymbol{\theta}_1; \boldsymbol{r}_2\boldsymbol{\theta}_2, \boldsymbol{r}_3\boldsymbol{\theta}_3, \ldots, \boldsymbol{r}_n\boldsymbol{\theta}_n)$ where the angles $\boldsymbol{\theta}_i$ now specify molecular orientations. In practice it is only with the three-body correlation function $g_3(\boldsymbol{r}_1\boldsymbol{\theta}_1; \boldsymbol{r}_2\boldsymbol{\theta}_2, \boldsymbol{r}_3\boldsymbol{\theta}_3)$ and the two-body correlation function $g_2(\boldsymbol{r}_1\boldsymbol{\theta}_1; \boldsymbol{r}_2\boldsymbol{\theta}_2)$ that we are concerned, and the only information which diffraction experiments yield is the spherical average of g_2. If we set $\boldsymbol{r}_2 = 0$ so that there is a molecule at the origin and ignore the coordinates $\boldsymbol{\theta}_1, \boldsymbol{\theta}_2$, then the radial distribution function $g(r)$ is defined by

$$g(r) = \frac{1}{4\pi n_L} \int g_2(\boldsymbol{r}; 0)\, d\Omega \tag{8.1}$$

where Ω signifies the angular part of $\boldsymbol{r}$ and n_L is the number density of molecules in the bulk liquid. The probability of finding a molecule at a distance between r and $r + dr$ from another molecule is

$$n(r)\, dr = 4\pi r^2 n_L g(r)\, dr. \tag{8.2}$$

The first x ray diffraction studies of liquid water were made by Meyer (1930), Stewart (1930, 1931) and Amaldi (1931) and the radial distribution function was first calculated by Katzoff (1934) but the classical work on the subject is that of Morgan and Warren (1938) who determined $g(r)$ at five temperatures between

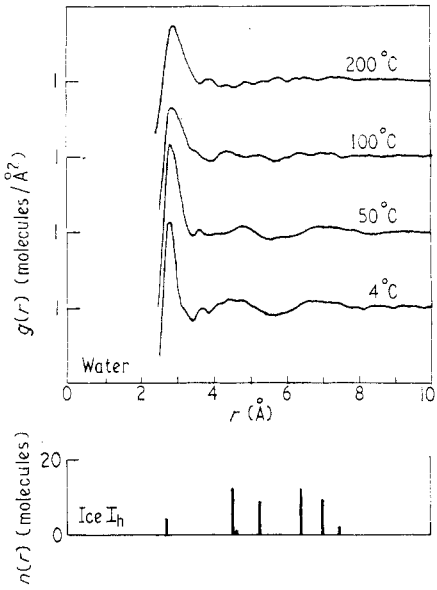

Figure 23. The radial distribution function $g(r)$ for water determined at a range of temperatures by Narten *et al* (1967). The molecular distribution in Ice I_h is shown below for reference.

1·5 and 83 °C. Several other more recent determinations have been made which have not added significantly to the results of Morgan and Warren until the latest published study by Narten *et al* (1967) which extends the measurements on H_2O to 200 °C and includes a measurement on D_2O at 4 °C. The radial distribution functions deduced by Narten *et al* are shown in figure 23. In the region of overlap the results are in good agreement with those of Morgan and Warren, though the more recent techniques have improved resolution.

An examination of figure 23 shows the sharp cut-off at small radius, the nearest-neighbour peak and the less pronounced ripples of further correlation shells typical of all liquids. The cut-off radius of closest approach is about 2·5 Å which is somewhat less than the shortest bond distance found in the ice polymorphs at atmospheric pressure (2·75 Å) or the shortest nonbonded distance in Ice VII (2·9 Å). It is, in fact, similar to the bond length (2·55 Å) in Ice VII at 220 kbar. The nearest-neighbour peak in the $n(r) = 4\pi r^2 g(r)$ distribution shifts from 2·82 Å to 2·94 Å as the temperature is increased from 4 to 200 °C, both these distances being significantly greater than the 2·76 Å bond distance in Ice I at 0 °C.

At first sight this makes it difficult to understand why water should be about 9% denser than ice. The explanation, as with the high-pressure ice polymorphs, lies in the distribution of more distant neighbours and the actual population of the first coordination shell. In Ice I this shell contains just four molecules and the more distant neighbours are distributed as shown at the foot of figure 23. In liquid water Morgan and Warren estimated the coordination in the first shell to range from 4·4 at 1·5 °C to 4·9 at 83 °C while Narten *et al* found a constant coordination of 4·4 at all temperatures from 4 to 200 °C. The ambiguity is largely one of interpretation. It is clear that the coordination number is significantly greater than that of Ice I and very significantly less than the value of ten characteristic of simple liquids.

The more distant neighbour shells, shown by maxima in the $g(r)$ curve, are in general agreement with the arrangement of molecular distances in Ice I but there is also a significant hump in $g(r)$ at about 3·7 Å which has no counterpart in ice. We shall see that this feature plays an important part in many of the structural models for water.

It is possible to fit the $n(r)$ curve by a set of gaussian distributions of molecular distances but this is not a useful procedure until one has a particular structural model in mind. For the present we simply observe that structural effects, as evidenced by oscillations in $g(r)$, persist out to about 8 Å near 0 °C and to about 5 or 6 Å at 200 °C. This observation, too, is of significance when considering water structure models.

8.3. *Hydrogen bonding in water*

Before proceeding to examine any particular structural models for water, we need to determine what part the hydrogen-bonding scheme, which we saw to be so important for the crystalline phases, plays in the liquid state. We recall from § 7.7 that, in the high-pressure polymorphs, fourfold hydrogen bonding is always maintained and identifiable, though the bond length may range from 2·55 to 2·94 Å and the bond angle from 76 to 143°.

One of the difficulties in settling this question is to agree on a definition for the stage at which a hydrogen bond is 'broken'. Clearly the fluid properties of liquid water require the rapid fluctuation of any sort of bonding pattern, but even a velocity shear of 100 cm s^{-1} over a distance of 1 mm requires bond rearrangement at a rate of only 10^4 s^{-1} which is trivially slow compared with the rate of 10^{10} s^{-1} required by dielectric relaxation.

Falk and Ford (1966) have compiled a table of estimates of the percentage of 'broken hydrogen bonds' in water between 0 and 25 °C made by various authors. These range fairly continuously from 0·1%, as estimated from far ultraviolet absorption, and Pauling's well known estimate of 15% on the basis of a comparison

of latent heats of melting and vaporization, through values in the range 30 to 50% based upon infrared and Raman spectral data to an extreme of 71·5% from ultrasonic absorption measurements. Clearly evidence could be adduced from these data to support almost any model.

Perhaps the most direct and at the same time the most controversial evidence is that derived from infrared spectral studies. As we have already mentioned, a free H_2O molecule has two coupled O—H stretching frequencies at 3652 and 3756 cm^{-1} while in ice these appear as a band in the range 3150–3380 cm^{-1}, the broadening being due to multiple coupling and the shift to lower frequency to the effects of hydrogen bond formation. If, instead, a small concentration of HDO in D_2O is used (or alternatively HDO in H_2O) and a double-beam arrangement with pure D_2O (or H_2O) in the reference cell, then the characteristic absorption lines of HDO (at roughly 3400, 2500 and 1400 cm^{-1}) can be observed (Falk and Ford 1966). If the bonding is uniform, then one would expect to see a simple gaussian contour for each of these lines, while if broken bonds are present each line should be split, or at least show a pronounced shoulder.

Infrared and Raman studies of this type, with or without the HDO technique, have been reported by many workers (Cross *et al* 1937, Buijs and Choppin 1963, Thomas and Scheraga 1965, Wall and Hornig 1965, Falk and Ford 1966, Walrafen 1966, 1968, Schiffer and Hornig 1968, Senior and Verral 1969). The experimental evidence itself is by no means entirely clear. Falk and Ford (1966) found simple gaussian profiles in infrared absorption and Wall and Hornig (1965) a similar result for Raman scattering, while Walrafen (1968) reported a shoulder on the Raman band and Senior and Verral (1969) a shoulder on the infrared absorption under similar conditions. Walrafen (1968) also found that the Raman curves shifted with increasing temperature in such a way as to exhibit an isosbestic point (ie all curves passing through a single point on the shoulder of one of them) and interpreted this as a shift in equilibrium between two different components (bonded and unbonded) in the liquid. This interpretation has, however, been the subject of some dispute (Schiffer 1969, Walrafen 1969, Falk and Wyss 1969) and the matter is not yet settled.

An interesting new feature has been added to this discussion recently by a consideration of the likely characteristic frequencies of a water molecule which is not hydrogen bonded but is nevertheless in close association with several other molecules. Franck and Roth (1967) examined the infrared spectrum of water at temperatures up to 400 °C and pressures up to 3·9 kbar, which is well above the critical point so that there should be no hydrogen bonds in the ordinary sense. At this highest temperature they examined vapours with densities ranging from 0·0165 g cm^{-3} to 0·9 g cm^{-3}, again using the HDO in H_2O technique. For densities greater than 0·1 g cm^{-3} the absorption was a simple gaussian curve shifted to lower frequencies than the vapour value, the OD stretching frequency for density 0·9 g cm^{-3} being 2600 cm^{-1} compared with the vapour-state frequency 2824 cm^{-1}. Franck and Roth point out that their data represent a simple continuation of those of Falk and Ford for liquid water at lower temperatures and therefore support a liquid model in which there is a continuum of hydrogen bond strengths rather than a distinction between unbroken and broken bonds. Further consideration of this point, however, by Schiffer and Hornig (1968) and by Frank (1970) suggests rather that the correct interpretation may simply be that infrared methods are not as sensitive to the nature of the bonding as had been previously believed.

We can only sum up this section by saying that, as far as the direct experimental evidence is concerned, the question of the extent of hydrogen bonding in liquid water is still an open one. To some extent the problem is the semantic one of defining what is meant by a broken bond but this is not all, since topological considerations can resolve the question for particular explicit models. We can only reasonably say that the evidence suggests the existence of a substantial hydrogen bonded framework in liquid water (with the necessary small fraction of broken bonds to give fluidity and allow dielectric relaxation—a fraction which need not on this account exceed 1%) while at the same time it does not exclude the possibility of a much greater fraction of broken bonds and an appreciable content of unbonded molecules closely imprisoned by, but not hydrogen bonded to, their neighbouring water molecules.

8.4. *Ab initio approach to water structure*

From many points of view it would be satisfying if we could proceed directly to a discussion of the structure of liquid water beginning from the properties of the water molecule which are now, as we saw in § 2, quite well established and understood. Such a procedure would be relatively straightforward for water vapour but its application to the liquid state has been very recent and, as yet, rather preliminary.

The first such attempt was that of Barker and Watts (1969) who used the Monte Carlo 'computer experiment' type of technique to examine many sets of 64 water-like molecules in a cube with periodic boundary conditions and of such a size as to give the correct liquid density at 25 °C. Whilst the dipole, quadrupole and even octopole moments of the water molecule are now known with reasonable certainty, we have remarked before that such a multipole expansion is not very satisfactory for treating the interactions of molecules in close proximity. For this reason, as well as for mathematical simplicity, Barker and Watts used a four-charge model like that of Rowlinson (1951) for the water molecule. The four-charge potential was supplemented by a Lennard-Jones (6, 12) interaction and a hard-sphere cut-off at small distances. With these choices the second virial coefficient of water vapour and the cohesive energy of ice could be reasonably approximated so that the model was not too unrealistic, although all polarization and cooperative effects were neglected.

With this procedure Barker and Watts computed some 230 000 configurations for their system and evaluated the energy relative to that of separated molecules ($-3{\cdot}50 \times 10^4$ J mol^{-1} compared with the experimental value of $-3{\cdot}40 \times 10^4$ J mol^{-1}) and the molar heat capacity (86 J K^{-1} mol^{-1} compared with the experimental value of 75 J K^{-1} mol^{-1}). The radial distribution function was also computed but showed rather poorer agreement with experiment, the peak being at 2·6 instead of 2·8 Å, the number of calculated neighbours being rather too large and the pronounced hump at about 4·5 Å (the second-neighbour shell) being missing. For an *ab initio* model with no adjustable parameters this agreement is, however, very good. The lack of the second-neighbour peak, which arises essentially through the three-body correlation function $g_3(\boldsymbol{r}_1\boldsymbol{\theta}_1; \boldsymbol{r}_2\boldsymbol{\theta}_2, \boldsymbol{r}_3\boldsymbol{\theta}_3)$, may be associated with the computational method used, with the potential or with the small cell size.

The other attempt which has been made at an *ab initio* treatment is that of Ben-Naim (1970). The molecular potential used was similar to that of Barker and Watts but based this time on the four-charge model of Bjerrum (1951) supplemented by a Lennard-Jones potential. The computation was so arranged that the

angle-dependent Bjerrum part of the potential could be omitted in order to simulate a simple neon-like liquid for comparison.

The computational method of Ben-Naim involved solution of an approximate Perkus–Yevick equation for the system by numerical methods. The main output from the calculation was the radial distribution function $g(r)$, which was in good qualitative agreement with experiment. In particular, it was found that inclusion of the angle-dependent part of the potential moved the second-neighbour hump from 5·8 Å, characteristic of the neon-like interaction, to 4·8 Å in quite good agreement with the value 4·5 Å observed for water. It is clear, then, that the Perkus–Yevick approach is able adequately to include the three-body correlation effects g_3. The calculation still severely overestimated the population of the nearest-neighbour shell but this may be a fault in the original potential. Ben-Naim (1971) has recently undertaken a more detailed examination by this method of a two-dimensional water-like system to examine some aspects of the packing geometry.

8.5. *Models for liquid water*

To proceed further, as in crystallography, we now need to postulate a particular model for the water structure and to investigate its properties. Many such models have been proposed from time to time but for convenience they can be divided into two classes—uniform models and mixture models. The uniform models, as their name implies, regard water as a nearly fully bonded network with a wide continuum of hydrogen bond lengths and angles, while the mixture models identify certain characteristic bonding patterns in small clusters dispersed in a background of one or more other bonding types. In both cases we must remember that we are thinking about a structure which is maintained only for a time of order 10^{-11} s and that during any time significantly longer than this the bonding pattern will be completely rearranged to another configuration (which will be either uniform or a mixture of clusters depending upon one's point of view). The mixture theories are often called 'significant structure theories' or 'flickering cluster theories', these terms having been coined by Eyring *et al* (1958) and Frank (1958) respectively. The uniform theories are closely connected with the work of Bernal in a field which he has termed 'statistical geometry' (Bernal 1964).

We shall now turn to consider a representative selection of these structural models, beginning with the uniform structures (though some of the earliest models were of the mixture variety). It should be emphasized at the beginning that none of these models should be taken too seriously in its finer details—many of the elements of a model have arisen simply because it was necessary to postulate a definite structure for purposes of calculation and these features have then tended to harden into dogma in the minds of the supporters of a particular model. Despite their differences we shall find at the end that most of the structures have a lot in common.

8.6. *Uniform models*

In their classic paper on water and ice, Bernal and Fowler (1933) pointed out the close analogy between the structure of Ice I_h and the silica mineral tridymite and conjectured that one of the high-pressure ice polymorphs might have a structure analogous to that of quartz (a conjecture which turned out to be incorrect, although some other silica mineral structures are represented among the high-pressure ices, as we have seen). Observing that tridymite-ice has a density of 0·92 g cm^{-3} they

remarked that quartz-ice would have a density of 1·08 g cm^{-3} while a close packed arrangement would have a density of 2·0 g cm^{-3}. They therefore proposed a structure in which the bonding contained some of the features of a tridymite structure (at low temperatures), a large element of quartz-like structure at ordinary temperatures and, at high temperatures approaching the critical point, a component of close packed ammonia-like structure. They made it plain that they did not envisage molecular clusters with these kinds of bonding but a homogeneous structure approximating more or less closely to one or other of these ideals.

This model was in reasonable agreement with the limited diffraction data available at the time and the conversion of tridymite structure to quartz structure, followed by a uniform expansion of the whole network, gave a natural explanation of the density maximum observed at 4 °C. Bernal and Fowler did not discuss in any detail the bond distortions inherent in their model so that many of its predictions remained undeveloped.

In his later work Bernal (1964) has emphasized the importance of the pentagonal ring in liquid structure, and its stability, on which we commented in § 3.5, makes it a natural component of liquid water structure. It has the further advantage that it cannot serve as a nucleus for the growth of Ice I_h, so that a structure containing many five-membered rings should be able to be supercooled. Bernal (1964) observed that the silica mineral keatite, when used as a model for an ice structure, would give a density of 1·01 g cm^{-3} and suggested it as a substitute for the quartz-like bonding originally proposed. We shall see later that Jhon *et al* (1966) have made such a model the basis of a significant structure theory.

Pople (1951) was the first to produce a reasonably quantitative treatment of a uniform model for liquid water based on a completely hydrogen-bonded system with allowance made for bending and stretching of bonds. The force constants for these distortions were not then known and he used a simple electrostatic model to estimate for the angular coefficient $f'_{\theta\theta}$ the value $10kT$, which is about 0·01 au if θ is in radians. This is quite close to the coefficient derived in equations (4.9) and (4.10) which is appropriate here. On this basis and assuming a Boltzmann distribution of bond angles, the average bond bending, defined by $\cos^{-1}\overline{(\cos\theta)}$, was 26° at 0 °C and 30° at 100 °C. The stretching force constant f_{RR} was not estimated but a gaussian distribution of bond lengths was assumed to give best fit with the first peak of the radial distribution curve. The halfwidth of this peak was 0·258 Å at 1·5 °C, which could only represent a thermal average if f_{RR} had the unreasonably small value 0·001 au. We presume, therefore, that this bond stretching is due to other constraints associated with the topology of the bond scheme.

With these assumptions, Pople was able to get very good agreement between his calculated radial distribution function and the experimental one at 83 °C and fairly good agreement at 1·5 °C, except that the small hump near 3·6 Å was not reproduced. The theory also leads to a liquid with greater density than ice, as required, but the behaviour is not sufficiently precisely specified to determine this accurately or to seek the density minimum required at 4 °C. The density increase is essentially due to the angular disarray which allows outer-shell molecules to approach the origin more closely than in ice. Pople's model also gives satisfactory predictions for dielectric behaviour but its thermodynamic consequences have not been studied.

An important feature of the model is the quantity which we might term the 'coherence length' for bonding. This is the distance after which all relation

between the orientation of a molecule and that of the molecule at the origin is lost. Since the total angle between two bonds is about 109°, coherence is lost when the uncertainty exceeds about 60°. With an uncertainty of 30° at each bond, this requires an average of four bond steps and so implies a coherence length of about 10 Å. We shall return to this later.

8.7. *Mixture models*

One of the earliest mixture models, based upon quasichemical ideas which had had long currency, was that of Eucken (1946) who supposed water to consist of polymers $(H_2O)_2$, $(H_2O)_4$ and $(H_2O)_8$ mixed with monomer. To fit various thermodynamic data it was required that water at 0 °C consists of roughly equal parts of the 2, 4 and 8 polymers with very little monomer, while at 80 °C its constitution was about half dimer, one quarter each of monomer and tetramer and almost no octomer. These ideas, which have no structural basis, are not now regarded seriously.

Némethy and Scheraga (1962) were among the first to apply in a quantitative manner the suggestion of Frank and Wen (1957) that, since hydrogen bonding is to some extent a cooperative phenomenon, hydrogen-bonded molecules in liquid water should occur as compact clusters rather than as chains or as isolated dimers and trimers. The more recent calculations which we discussed in § 3 show that such cooperative effects occur in reality and that their magnitude is appreciable, though this observation of itself does not necessarily imply a cluster type of structure, since it equally supports a uniform, fully bonded model like that of Pople.

In their model Némethy and Scheraga postulated the existence of compact clusters of molecules with an Ice I-like bonding structure, dispersed in a sea of monomer material—an 'iceberg model' in short. They pointed out that the cluster bonding is not necessarily exactly that of Ice I_h, but this was adopted for calculation purposes since its partition function could be reasonably evaluated. Apart from requiring compact cluster geometry, they made no specific allowance for cooperative effects and assigned each molecule to one of five equally spaced energy levels depending upon the number of bonds (from 0 to 4) in which it participated. With cluster size and monomer fraction as independent variables, the fraction of molecules in each bonding category was evaluated and a total partition function constructed from a knowledge of the partition functions of water molecules in ice and in the vapour.

This model gives quite good agreement with many experimental quantities. It shows the predicted density maximum near 4 °C, due to cluster breakdown, and a heat capacity of the right order, though varying from 20% too high at 0 °C to 25% too low at 100 °C. The radial distribution function is reasonably well reproduced, the cluster molecules providing the first and second coordination shell peaks near 2·8 Å and 4·5 Å respectively and the nonbonded monomer plausibly contributing both to the hump near 3·8 Å and at larger distances.

The cluster size derived from minimizing the free energy of the model ranged from 90 molecules at 0 °C to 21 molecules at 100 °C. This implies a cluster radius varying between 10 Å and 7 Å which is very similar to the coherence distance derived from Pople's uniform model. The monomer fraction ranged from 24% at 0 °C to 44% at 100 °C and the fraction of broken hydrogen bonds from 0·47 to 0·77. In its idealized form, in which bonds are either made or broken, the picture therefore differs very considerably from a uniform model.

A somewhat intermediate view has been taken by Vand and Senior (1965) who modified the Némethy–Scheraga approach by considering only a three-level energy scheme (unbonded, one proton bonded, both protons bonded) and allowing each species to have a gaussian energy distribution. This model gives agreement with various thermodynamic quantities to within about 1%, but this is at the expense of additional parameters. The radial distribution function was not calculated and the description of the structure in terms of clusters is no longer very explicitly apparent. A further development along these lines has been made by Orentlicher and Vogelhut (1966).

A rather different starting point for a mixture model has been adopted by Jhon *et al* (1966). Their model consists of compact clusters of Ice I-like molecules dispersed in an Ice III-like structure with a small admixture of nonbonded monomers. This essentially follows the model of Bernal and Fowler (1933), as revised by Bernal (1964) to replace the quartz-like component by one with keatite (or Ice III) structure. The distinction is, however, that Bernal and Fowler envisaged a uniform bonding arrangement while the model of Jhon *et al* involves clusters. The treatment leads again to quite close agreement with experiment and a cluster size of 46 molecules, implying a coherence length near 8 Å in reasonably close accord with the other theories.

Two other mixture models which we shall not consider in any detail are that of Marchi and Eyring (1964), who used as significant structures tetrahedrally bonded ice-like clusters and freely rotating monomers, and that of Davis and Litovitz (1965), who based their model on the puckered hexagonal rings of the ice structure. In this latter case the two structural components were an ice-like stacking of rings giving maximum bonding and a rather close packed structure in which the upper ring was parallel to the lower so that they fitted together like stacked chairs.

8.8. *Interstitial models*

Among the remaining mixture models we can distinguish one particular type which is characterized by an extensive hydrogen-bonded network into which are inserted unbonded interstitial monomer molecules. One of the prime arguments in favour of this sort of model is the small peak near 3·8 Å in the radial distribution function of water, this distance corresponding roughly to the distance from a framework molecule to the centre of one of the large cavities in an ice-like or a clathrate structure.

Pauling (1959) proposed a water structure based upon the clathrate cages which we discussed in § 3.5, the chlorine molecules in the chlorine hydrate structure being replaced by water molecules. Such a structure receives support from the more recently discovered fact which we discussed in § 7 that Ices VI and VII have self-clathrate structures. It is also an advantage, from the point of view of understanding supercooling phenomena, to have a bond framework rich in pentagonal rings, since they cannot be easily converted to the puckered hexagons characteristic of the ice structure. If interpreted literally the model is, of course, rather too rigid and well defined for a true liquid structure but such an interpretation is not really intended.

Frank and Quist (1961) have analysed the predictions of the Pauling model in some detail and shown that, with reasonable assumptions, it can account fairly satisfactorily for the properties of water between about 0 and 30 °C, the fraction of

interstitial molecules being about 20%. They point out, however, that a third species of molecule of less rigid binding than the clathrate cages appears necessary to provide an adequate model at temperatures above 30 °C.

Another interstitial model was proposed by Narten *et al* (1967) to account for the radial distribution functions which they measured. For this model they took the framework to be of Ice I_h structure but anisotropically expanded to decrease the c/a ratio by about 10% from the ideal value (this is in the direction of the deviation found in Ice I_h itself but is much more extreme). Interstitial molecules were allowed to occupy the large cavities in the framework and, in addition, unoccupied lattice sites were allowed, while the whole framework underwent a gaussian smearing.

In refining their model, Narten *et al* were guided by the radial distribution function and the observed density of water rather than by statistical thermodynamic considerations. They found all network sites to be occupied up to 100 °C but about 25% of network vacancies at 200 °C. The total fraction of molecules in interstitial sites rose from about 20% at 0 °C to 25% at 200 °C. A first-order treatment of thermal behaviour, along the lines followed by Frank and Quist (1961) for the Pauling model, yielded a specific heat which was only half the observed value but, in view of the approximations involved in the derivation, this disagreement was not considered to be of great seriousness.

8.9. *Conclusions*

The description of rival models for the structure of liquid water which we have given above is far from complete but it does go far enough to indicate the essential nature of the problem and the types of structure which might reasonably be proposed to explain it. While it is very likely that the true structure of liquid water contains most if not all of the elements which have been suggested, it seems that all of the models have a tendency to omit, by oversimplification, the really essential topological differences between a crystalline solid and a liquid. Illuminating discussions of this point have been given by Bernal (1964) and Kamb (1970).

Most of the models are based, for obvious reasons, upon clusters or frameworks very closely related to one or other of the ice structures. It is clear, however, from considerations based on the possibility of supercooling water at various pressures, that the liquid does not contain any significantly large fraction of clusters with structure identical with that of one of the ices (Fletcher 1970 pp85–97) and Brillouin scattering studies make large-scale fluctuations in bonding pattern seem unlikely. We conclude, therefore, that it may be the random combination of five-, six- and even seven-membered rings in the liquid, making its structure topologically incompatible with any of the ices, which is an essential feature of any really correct model.

Despite these reservations, the structural models which have been put forward and substantiated all bear some relation to the real water structure and we can draw useful structural conclusions from them. It is likely that water contains a very substantial fraction of fourfold coordinated molecules linked together in such a way that the two-body and three-body correlations are quite similar to those in the ice polymorphs. The disorder in this structure is such, however, that bonding coherence is maintained for a distance which is only of the order of 10 Å at 0 °C, 7 Å at 100 °C and perhaps 5 Å at 200 °C. In addition to these framework molecules there is almost certainly also a fraction of unbonded or partially bonded interstitial molecules which may be constrained by their near-neighbour interactions so that they cannot

rotate and their infrared spectrum is closer to that of a bonded rather than a free molecule. The structure of vitreous ice, to which we referred in § 5.3, forms a natural extension of these ideas with, at −150 °C, almost all the molecules concentrated in the framework and a correlation distance as large as perhaps 15 Å.

9. 'Polywater'

No discussion of structural aspects of the ice–water system would be complete without reference to the experimental and theoretical work which has been done in the past few years on the 'anomalous water' phase first reported by Deryagin and his co-workers in the USSR (Deryagin and Fedyakin 1962). In the course of experiments designed to examine the properties of the boundary layers of liquids in contact with solid surfaces, they found effects which extended surprisingly far into the bulk liquid. In extreme cases these effects persisted to a depth as great as 20 μm, which far exceeds the range of any possible direct surface forces.

The experiment which led to most of the later work was one in which fine silica capillaries (1 to 30 μm in diameter) suspended in a closed chamber containing unsaturated water vapour were sometimes found after a time to contain a liquid condensate. Capillary effects were insufficient to explain this condensation phenomenon and the obvious step was to attribute its formation to hygroscopic impurities in the capillaries. Careful cleaning and purification procedures, however, failed to eliminate the condensation phenomenon and Deryagin was led to the conclusion that he had produced a new and apparently more stable form of liquid water which he termed variously 'anomalous water', 'modified water', 'ortho water', or 'water II'.

During the following years Deryagin and his colleagues applied physical methods to the study of the minute columns produced in the capillaries. They concluded that these consisted of a solution of the anomalous component in ordinary water and, after evaporating off the normal liquid, they were able to determine several properties of the anomalous residue. They found it to be a highly viscous material, stable up to about 400 °C, with a density near 1·4 g cm^{-3} and a refractive index of 1·48 to 1·50. (For summaries of this work see Deryagin (1966, 1970); additional references are given by Mansfield (1970), Allen and Kollman (1970) and in other papers cited below.) Other workers were able to reproduce Deryagin's results fairly reliably, though the generation of an anomalous water condensate in a bundle of capillaries appeared to be a statistical event whose occurrence was related, to some extent, to the prior history of the capillaries.

Progress in understanding came with the application of spectroscopic techniques by Lippincott *et al* (1969). The infrared spectrum which they found was unique, reproducible and quite different from that of water. Instead of the O—H stretching absorption peaks in the 3100–3300 cm^{-1} region and the H—O—H bending peak near 1600 cm^{-1}, anomalous water showed three strong absorption peaks in the range 1360–1600 cm^{-1} and weaker peaks near 1120 and 1050 cm^{-1}. If it was assumed that the anomalous component is pure H_2O, then one might associate the former peaks with a drastically shifted O—H stretching vibration. An extrapolation from analogous hydrogen-bonded systems then suggested that the water molecules are very strongly bonded together with the protons lying nearly symmetrically upon the O—H···O bonds. The hypothesis was therefore put forward that

anomalous water is a polymeric form of H_2O with a novel bonding pattern characterized by nearly symmetric hydrogen bonds. The name 'polywater' was coined for this structure.

The conceptual fascination of this proposal led theorists to investigate possible molecular models in considerable detail, though generally in a speculative and only semiquantitative manner. Since it is virtually obvious that polywater cannot be more stable than normal water, since condensation onto silicaceous surfaces is such a common geophysical phenomenon that water cannot realistically be considered to be only metastable with respect to polywater, the theoretical models have sought to find a metastable water structure of high density separated from the normal water structure by a high free energy barrier. Short, symmetrical hydrogen bonds can be invoked to give the high density and many different specific polymeric structures have been proposed (see eg Allen and Kollman 1970). A critical discussion of these models has been given by Kamb (1971) and references to the original work can be found here.

The conclusion which Kamb draws, supported by detailed argument, is that neither the hypothesis of a symmetrical hydrogen bond nor the required metastability of any of the proposed structures can be accepted. We have already seen that hydrogen bonds maintain their normal asymmetric form under extreme conditions of temperature and pressure and that even the clathrate Ices VI and VII are metastable with respect to ordinary ice only at liquid nitrogen temperatures.

One cannot, of course, rule out the existence of polywater by showing that any number of specific models are untenable, though Kamb has also argued that the plausible catalysis mechanism, by which many people have suggested that the silica surface might promote polywater formation, is fallacious if normal water is really the stable form.

What appears to be the final blow to the polywater hypothesis, however, has been dealt by a number of workers using sensitive modern techniques such as electron spectroscopy to show that the polywater samples which they studied were in fact composed largely of impurities with very little water (see Rousseau and Porto 1970, Mansfield 1970 and Davis *et al* 1971 for references). Other reports (eg Rousseau 1971) show that the infrared spectrum of polywater can be simulated extremely well by common contaminants like the sodium lactate in human perspiration.

The weight of experimental evidence and theoretical argument thus leads quite clearly to the conclusion that 'polywater' is an artifact which need not concern us further here. To return to its original source, however, we must not go so far as to say that the structure of water or ice near a surface or interface has no peculiarities. It is to this question that we devote the final section of this paper.

10. Surfaces and interfaces

It will not be our purpose here to give an exhaustive treatment of the structure of surfaces and interfaces (for which standard sources such as Ono and Kondo (1960) and Adamson (1967) should be consulted) but rather to discuss briefly those structural features which are more or less unique to the water–ice system. The level of sophistication of the treatment is necessarily much less than that for the bulk phases because our understanding of surface structures is in a much more primitive state.

10.1. *The surface of water*

To a first approximation a water surface in equilibrium with water vapour can be described simply as a plane dividing a bulk liquid phase from a bulk vapour phase and this model can be used to derive estimates for numerical values of quantities such as surface energy and surface tension (which, for a liquid, is numerically equal to the surface free energy). The interest from our present viewpoint lies in the deviations from this simple picture. We shall confine our attention to the liquid side of the interface, since any effects on the vapour side are insignificant.

First we have the effects which are common to all liquids. The density of the surface layers of the liquid should be different from that of bulk liquid because of the different degree of coordination for surface molecules: this should lead to a decrease in surface density in the case of water because of the cooperative nature of hydrogen bonding in the liquid. Secondly the vibrational spectrum for surface molecules should be different from that of bulk molecules, both because of the different bonding and because the surface cooperative vibrational modes have a different frequency distribution from the lattice modes: this effect, together with a configurational term, leads to a surface entropy which is nonzero. Thirdly, since the dielectric constant of a liquid is always greater than that of its vapour, there should be a tendency for the self-ions, present in the liquid in equilibrium, to avoid the surface layers.

The most significant deviations of water from this simple behaviour arise from the fact that water molecules are not spherically symmetrical. There is therefore a tendency, discussed long ago by Frenkel (1946 pp353–6), for surface molecules to be oriented preferentially relative to the plane of the surface. Because of the hydrogen bonding characteristic of the water structure, there is then a further tendency for this orientation to persist to some depth below the geometrical surface. It is these two effects which we now discuss.

Because surface orientation implies a reduction of disorder in the surface, we should expect its presence to be manifest in the surface entropy. The surface entropy is just the negative of the temperature derivative of the surface free energy or surface tension for a liquid, so numerical values are readily accessible and have been compared, for a number of liquids, by Good (1957). He found that, for nonpolar and reasonably spherical molecules, the average liquid surface entropy is $24{\cdot}0\ \mathrm{J\,mol^{-1}\,K^{-1}}$, while for asymmetric polar liquids the value is lower, indicating surface orientation. For water near room temperature the entropy has the very low value $9{\cdot}8\ \mathrm{J\,mol^{-1}\,K^{-1}}$ which is about $14\ \mathrm{J\,mol^{-1}\,K^{-1}}$ or about $1{\cdot}7k$ per molecule lower than the value typical of simple liquids. If the orientation of a single molecule is confined to a solid angle of 2π rather than 4π, the entropy loss is $k\ln 2 \simeq 0{\cdot}7k$ so that the observed entropy deficit may be taken as implying that between two and three layers of molecules at the surface are oriented.

The first reasonably detailed semiquantitative discussion of this orientation effect was given by Fletcher (1962b, 1963a) using a quasi-ice-like model for the water structure near the surface. This model suffered from several defects, however, particularly in its treatment of electrostatic interactions between the oriented molecules, and a further paper (Fletcher 1968) sought to correct these as we shall discuss later.

Meanwhile Jhon *et al* (1967) applied their significant structure theory for water to a consideration of surface tension and were able to reproduce the numerical

values almost exactly over the range 0 to 100 °C using an adjustable 'surface field' parameter X to create the necessary orientation. The interaction of this fictitious field with the molecular dipole μ was given the value

$$\epsilon = \mu X = 1{\cdot}416 \times 10^{-13} \text{ erg} \tag{10.1}$$

and we should bear this in mind as a measure of the energy difference between the two possible dipole orientations normal to the surface. Apart from this the treatment does not give us any useful structural information.

At about the same time Stillinger and Ben-Naim (1967) carried out a detailed analysis of surface orientation in water near the critical temperature. In this region it is a good approximation to treat the water molecules as unbonded and freely rotating so that the analysis is very much simpler than for lower temperatures. The liquid/vapour interface is also so diffuse that it is a reasonable approximation to treat the effective dielectric constant as a smoothly varying function of position normal to the interface. With some additional simplifying assumptions these authors were able to calculate the direction of preferred orientation of water molecules in the interface in terms of the dipole moment μ and the quadrupole tensor component θ_{zz} defined by equation (2.14). They found the preferred orientation to be that in which the surface water molecules tend to bury their protons in the liquid, a conclusion which we note for later reference. They were also able to calculate the potential drop across the interface in terms of the measured dielectric constants of the liquid and vapour and found a value of 1 mV at 370 °C rising to 3·8 mV at 320 °C, with the liquid being positive relative to the vapour. One might hope for a direct experimental check on this conclusion but unfortunately different direct measurements do not even agree on the sign (Parsons 1954). This calculation represents a careful approach to some aspects of the problem but some of its assumptions are open to question, for example the neglect of the possible effects of differential adsorption of H_3O^+ and OH^- ions at the interface.

In his revised treatment of water near room temperature Fletcher (1968) attempted to include not only molecular asymmetry but also the effects of water structure and of differential adsorption of self-ions at the interface. The associated nature of hydrogen bonding in water leads, as we have seen in § 8.9, to a correlation distance of order 10 Å. It is not possible for the bonding pattern as a whole to change greatly over a distance shorter than this, so that any preferential orientation of surface molecules will decay slowly into the liquid with a characteristic length of about 10 Å. This greater depth of oriented layer leads to a very considerable field normal to the interface and this, in turn, causes the buildup of an ionic double layer in such a direction as to reduce the polarization field.

A re-examination of this revised treatment suggests, however, that the symmetrical part $\bar{Q}$ of the quadrupole moment tensor has been wrongly included in the analysis, the more nearly correct treatment being similar to that of Stillinger and Ben-Naim and involving only the tensor component θ_{zz}. Even here there is a problem, however, since the $\theta_{\alpha\beta}$ depend upon the choice of origin, which should really be made so that the octopole moments are as small as possible. The moments given in table 5 are calculated with respect to the molecular centre of mass as origin while those used by Stillinger and Ben-Naim were tabulated by Krishnaji (1966) relative to the oxygen nucleus as origin. The point is important, since it affects the sign of θ_{zz}, and does not seem to have been given any detailed consideration.

If we follow Stillinger and Ben-Naim, then the orientation energy for an abrupt interface is approximately

$$\epsilon \sim \frac{\mu\theta_{zz}}{a^4} \sim 10^{-13} \text{ erg} \tag{10.2}$$

where we have chosen for a, the effective molecular radius, the value 1×10^{-8} cm. It is clear that this estimate is close to that given by equation (10.1).

For water at room temperature the shielding effect of self-ions in the surface double layer will be important and it is probable that the surface potential drop will be not much different from the value, 0·1 V, estimated in the original treatment. If we accept the electrostatic treatment of Stillinger and Ben-Naim then the surface molecules will be oriented with their protons towards the liquid, although the detailed bonding pattern requires further examination.

We have already remarked that experiment gives little help in settling this question but there is one striking observation which appears to be repeatable and conclusive, namely that condensation in cloud chambers is nucleated much more readily by negative than by positive ions (Fletcher 1962a pp48–52, White and Kassner 1971). This implies that the minimum-energy surface of liquid water has its protons directed into the liquid in agreement with our discussion above. The point is not yet, however, conclusively decided.

The surface free energy (surface tension) of water is readily measured and ranges from about 76 erg cm^{-2} at 0 °C to 59 erg cm^{-2} at 100 °C. The extrapolated value at −40 °C is about 80 erg cm^{-2} and it vanishes at the critical point 374 °C. Gittens (1969) gives a detailed and comparative tabulation of various data.

10.2. *The surface of ice*

The surface structure of ice has been of continuing interest since Faraday suggested in 1850 that the peculiar properties of snow might be explained if one assumed that there is a thin liquid-like equilibrium transition layer on ice surfaces at temperatures not too far below the melting point. Tyndall supported Faraday's viewpoint but Thomson and Helmholtz attributed most of the phenomena to pressure melting and indeed the question is not fully settled today. A historical review and description of more recent work supporting Faraday's hypothesis is given by Jellinek (1967). Unfortunately most of the evidence is indirect and subject to a variety of interpretations. We shall comment here only on the most nearly direct studies.

At temperatures well below its melting point there is little argument that the surface of ice is other than simple and crystalline. Microscopic studies, of course, lack ability to detect a transition layer of molecular thickness but physical adsorption of nitrogen and various n alkanes onto ice surfaces (Adamson *et al* 1967, Orem and Adamson 1969) shows these surfaces to be inert and relatively nonpolar like the surface of polypropylene or of polytetrafluoroethylene ('Teflon'). This implies, perhaps, some cross bonding between adjacent molecules to reorganize the surface to a lower energy configuration but otherwise indicates nothing abnormal about it. When the temperature is raised above about −35 °C, however, the character of the adsorption changes considerably and resembles much more nearly that onto liquid water, exhibiting a high energy of adsorption for low surface coverages.

Measurements of the electrical conductivity of ice show a similar anomaly: at low temperatures the behaviour is simple (though different workers have obtained

rather different results) but at temperatures above about -10 °C the measurements are dominated by surface conductivity unless appropriately guarded electrodes are used (Bullemer and Riehl 1966, Jaccard 1967, Maidique *et al* 1971). Maidique *et al* estimate the onset of appreciable surface conductivity to occur about -35 °C.

Finally, a recent measurement of the nuclear magnetic resonance spectrum of powdered ice by Kvilividze *et al* (1970) at a series of carefully controlled uniform temperatures in the range -10 to 0 °C show the existence of a narrow quasiliquid absorption line superposed on the broad line due to ice. The behaviour of the narrow line is consistent with that expected from a liquid-like film whose thickness and molecular mobility increase as the temperature is raised towards the melting point.

All these experiments were carried out under equilibrium conditions and refer, therefore, to the situation in which we are interested. The striking variations in the habits of natural snow flakes observed by Nakaya (1954) over very small temperature ranges and the related sharp changes in the velocity of propagation of growth steps over basal surfaces of ice, studied by Mason and his co-workers (see Fletcher 1970 pp119–29), are strongly suggestive of surface phase changes taking place at different temperatures on different crystal faces. These changes occur, however, under conditions of considerable vapour supersaturation, so that they do not necessarily apply to our present discussion.

A fairly convincing argument that a surface phase change is to be expected for ice below its bulk melting point was originally put forward qualitatively by Weyl (1951) and subsequently developed into a semiquantitative theory by Fletcher (1962b, 1963a, 1968). We have already seen that it is a reasonable presumption that the surface molecules in liquid water are preferentially oriented and that this orientation decays away into the liquid with a characteristic length of a few molecular diameters. The energy gained, over that of a surface with random orientation, by this ordering is more than sufficient to outweigh the free energy increase caused by the loss of surface entropy, and the total surface free energy is therefore lowered.

Now in a perfect ice crystal the dipole orientations are always random and the correlation length, which is established by crystal defects, is of the order of one millimetre. We cannot, therefore, orient the surface molecules without orienting molecules throughout a large volume of crystal with an accompanying prohibitively large entropy loss. Near the melting point, however, the free energies of water and ice are nearly the same so that there is only a small free energy penalty to be paid for the formation of a quasiliquid surface layer in which any surface orientation may decay. If the temperature is close enough to the melting point, the energy gained from surface orientation will more than compensate the free energy needed to create the liquid layer.

Both of the semiquantitative treatments by the present author are now known to contain errors, the first through its neglect of several electrostatic terms and the second through an improper treatment of the dipole–quadrupole interaction. These errors are, however, not sufficient to invalidate completely the results and we are led to the conclusion that a quasiliquid surface may exist down to about -10 °C at least and that it should have a very high electrical conductivity because of the self-ions drawn in to shield the polarization field. This transition layer is very shallow, increasing from a few molecular layers to a few tens of molecular layers as the melting point is approached. The theory requires only that it be amorphous, not that its mechanical properties be identical with those of water.

It is clear that the experimental results which we have discussed can all be adequately accounted for by the existence of a layer of this kind. We should be cautious, however, about making a final decision on the reality of the transition layer and even more wary about invoking it to explain other phenomena to which many other physical mechanisms may contribute.

There has been only one relatively direct measurement of the free energy of an ice surface and that, by Ketcham and Hobbs (1969), we shall discuss in the next section. They found a value 109 ± 3 erg cm^{-2} near 0 °C, at which temperature the liquid film was presumably fully developed. Fletcher (1962b, 1963a, 1968) estimated the free energy lowering due to the transition layer to be about 10 erg cm^{-2} so that this result is in quite good agreement with theoretical estimates lying between 100 and 120 erg cm^{-2} for the crystalline surface (Mason 1952, McDonald 1953, de Reuck 1957). The exact value of the surface free energy depends upon the crystal face exposed and various considerations suggest that the energies of (0001) and $(10\bar{1}0)$ faces are very little different—the extreme habits of vapour-grown ice crystals are caused by surface kinetics rather than by equilibrium effects. Finally we should emphasize that surface free energy and surface tension are entirely different and unrelated quantities for a crystal (Benson and Yun 1967).

10.3. *The ice/water interface*

Most of our knowledge of the ice/water interface is drawn from kinetic experiments in the fields of nucleation and crystal growth and these necessarily yield little information of a structural nature. Jackson (1958, 1966), however, has developed a theory with which to discuss the equilibrium roughness of an interface as follows. If an interface is smooth then it possesses no configurational entropy, while if it consists half of bonded molecules (crystal) and half of detached molecules (liquid) the entropy per molecule is about k. If α is the fraction of bonds which a surface molecule makes with other molecules in the surface layer, then the transition between a smooth and a rough interface involves an energy of about $\frac{1}{2}\alpha L$, where L is the latent heat of fusion per molecule. We therefore expect a rough interface if $\alpha L/kT$ is less than about 2. The effect of this distinction between rough and smooth interfaces is very marked: materials like metals with rough interfaces against their melts often have curved interfaces, while materials with $\alpha L/kT \gg 2$ show sharply defined crystal faces. For ice $\alpha = \frac{3}{4}$ and $\alpha L/kT$ is very close to 2 so that no clear conclusion can be reached. Ice dendrites growing in water usually show crystal planes but other interfaces may not.

Measurements of the behaviour of crystal growth velocity as a function of interface supercooling can be made to yield some information about interface structure, though under kinetic rather than equilibrium conditions (Fletcher 1970 pp111–9). Generally speaking these observations suggest that the ice/water interface is relatively smooth, near equilibrium, with crystal growth taking place by a dislocation mechanism. When the supercooling becomes large, however, and the growth rapid, the indications are that kinetic effects may cause the interface to become rough so that there is a transition to a continuous growth regime (Pruppacher 1967).

The only relatively direct determination of the interfacial free energy $\sigma_{\text{ice/water}}$ has been reported by Ketcham and Hobbs (1969) using the usual metallurgical technique of measuring the angles of intersection between two ice-grain surfaces, separated by a grain boundary, and the other phase, either water or vapour. By this

technique they found, at 0 °C.

$$\left.\begin{aligned}\sigma_{\text{ice/vapour}} &= 109 \pm 3 \text{ erg cm}^{-2}\\ \sigma_{\text{ice/water}} &= 33 \pm 3 \text{ erg cm}^{-2}\\ \sigma_{\text{grain boundary}} &= 65 \pm 3 \text{ erg cm}^{-2}.\end{aligned}\right\} \qquad (10.3)$$

The contact angle of water on ice was measured as 1°. This is smaller than the value of 12° reported by Knight (1966) but in his case the temperature was below 0 °C and the water was slowly freezing. A later experiment by Knight (1971) gave somewhat contradictory results.

Two less direct determinations of $\sigma_{\text{ice/water}}$ near 0 °C were made by Kotler and Tarshis (1968) from a theory describing the growth rate of dendrites, and by Hardy and Coriell (1969) using the Mullins–Sekerka analysis of the morphological stability of a cylindrical interface. The values they found were 20 and 22 erg cm^{-2} in mutual agreement but differing considerably from the Ketcham–Hobbs value.

Finally, experiments on the homogeneous nucleation of freezing give a value for $\sigma_{\text{ice/water}}$ at temperatures between -35 and -40 °C. We have discussed the theory of this phenomenon in § 5.4 and the relevant equations relating the nucleation rate J to $\sigma_{\text{ice/water}}$ are (5.2) and (5.3). From the large number of experiments which have been carried out (Fletcher 1970 pp85–97, Kuhns and Mason 1968, Wood and Walton 1970) it seems clear that $\sigma_{\text{ice/water}}$ in this temperature range is between 20 and 24 erg cm^{-2}, with some indication of an increase with rising temperature. The correct value near 0 °C may therefore be closer to 30 than to 20 erg cm^{-2}.

Acknowledgments

This paper was prepared during the course of a study of the physics of ice and related materials supported by the Australian Research Grants Committee and the Australian Institute of Nuclear Science and Engineering. I am also grateful to those people, particularly Dr B Kamb, who gave permission for the reproduction of figures from their publications, and to Crystal Structures Ltd of Cambridge for the photographs of their ice structure models.

Appendix

Numerical values for atomic units $e=\hbar=m=1$

Quantity	Equivalent of 1 au
Length	$5{\cdot}2917 \times 10^{-9}$ cm = 0·52917 Å
Mass	$9{\cdot}1091 \times 10^{-28}$ g
Charge	$1{\cdot}6021 \times 10^{-19}$ C = $4{\cdot}8030 \times 10^{-10}$ esu
Energy	$4{\cdot}3593 \times 10^{-11}$ erg = 27·2097 eV
Moment of inertia	$2{\cdot}5507 \times 10^{-44}$ g cm^2
Dipole moment	$8{\cdot}4778 \times 10^{-28}$ C cm = $2{\cdot}5415 \times 10^{-18}$ esu cm
Quadrupole moment	$4{\cdot}4862 \times 10^{-36}$ C cm^2 = $1{\cdot}3449 \times 10^{-26}$ esu cm^2
Force constant	$1{\cdot}5568 \times 10^{5}$ dyn cm^{-1}
Angular force constant	$4{\cdot}3593 \times 10^{-11}$ erg rad^{-2}

References

ADAMSON A W 1967 *Physical Chemistry of Surfaces* (New York: Interscience)
ADAMSON A W, DORMANT L M and OREM M 1967 *J. Colloid Interface Sci.* **25** 206–17
ALLEN L C and KOLLMAN P A 1970 *Science* **167** 1443–54
AMALDI E 1931 *Phys. Z.* **32** 914–9

ANDRIESSEN J 1969 *Chem. Phys. Lett.* **3** 257–8
ANGELL C A and SARE E J 1970 *J. Chem. Phys.* **52** 1058–68
ARNOLD G P, FINCH E D, RABIDEAU S W and WENZEL R G 1968 *J. Chem. Phys.* **49** 4365–9
ARRIGHINI G P and GUIDOTTI C 1970 *Chem. Phys. Lett.* **6** 435–7
ARRIGHINI G P, GUIDOTTI C and SALVETTI O 1970 *J. Chem. Phys.* **52** 1037–41
AUNG S, PITZER R M and CHAN S I 1968 *J. Chem. Phys.* **49** 2071–80
BADER R F W 1964 *J. Am. Chem. Soc.* **86** 5070–5
BADER R F W and JONES G A 1963 *Can. J. Chem.* **41** 586–606
BARKER J A and WATTS R O 1969 *Chem. Phys. Lett.* **3** 144–5
BARNES W H 1929 *Proc. R. Soc.* A **125** 670–93
BEAUMONT R H, CHIHARA H and MORRISON J A 1961 *J. Chem. Phys.* **34** 1456–7
BENEDICT W S, GAILAR N and PLYLER E K 1956 *J. Chem. Phys.* **24** 1139–65
BEN-NAIM A 1970 *J. Chem. Phys.* **52** 5531–41
—— 1971 *J. Chem. Phys.* **54** 3682–95
BENSON G C and YUN K S 1967 *The Solid–Gas Interface* Vol 1 ed E A Flood (London: Edward Arnold) pp203–69
BERNAL J D 1964 *Proc. R. Soc.* A **280** 299–322
BERNAL J D and FOWLER R H 1933 *J. Chem. Phys.* **1** 515–48
BERTIE J E, CALVERT L D and WHALLEY E 1963 *J. Chem. Phys.* **38** 840–6
—— 1964 *Can. J. Chem.* **42** 1373–8
BERTIE J E, LABBÉ H J and WHALLEY E 1968a *J. Chem. Phys.* **49** 775–80
—— 1968b *J. Chem. Phys.* **49** 2141–4
BERTIE J E and WHALLEY E 1964a *J. Chem. Phys.* **40** 1637–45
—— 1964b *J. Chem. Phys.* **40** 1646–59
—— 1967 *J. Chem. Phys.* **46** 1271–84
VAN DEN BEUKEL A 1968 *Phys. Stat. Solidi* **28** 565–8
BISHOP P G and GLEN J W 1969 *Physics of Ice, Proc. Int. Symp. Munich 1968* ed N Riehl *et al* (New York: Plenum Press) pp492–501
BISHOP D M and RANDIĆ M 1966 *Molec. Phys.* **10** 517–28
BJERRUM N 1951 *K. Danske Vidensk. Selsk. Math.-fys. Meddr.* **27** (1) 3–56
BLACKMAN M and LISGARTEN N D 1957 *Proc. R. Soc.* A **239** 93–107
—— 1958 *Adv. Phys.* **7** 189–98
BONDOT P 1967 *C. R. Acad. Sci., Paris* **B265** 316–8
—— 1969 *C. R. Acad. Sci., Paris* **B268** 933–6
BRAGG W H 1922 *Proc. Phys. Soc.* **34** 98–102
BRIDGMAN P W 1912 *Proc. Am. Acad. Arts Sci.* **47** 441–558
—— 1935 *J. Chem. Phys.* **3** 597–605
—— 1937 *J. Chem. Phys.* **5** 964–6
BRILL R and TIPPE A 1967 *Acta Crystallogr.* **23** 343–5
BROWN A J and WHALLEY E 1966 *J. Chem. Phys.* **45** 4360–1
BUCKINGHAM A D 1958 *J. Chem. Phys.* **30** 1580–5
BUIJS K and CHOPPIN G R 1963 *J. Chem. Phys.* **39** 2035–41
BULLEMER B and RIEHL N 1966 *Solid St. Commun.* **4** 447–8
BURTON E F and OLIVER W F 1935 *Proc. R. Soc.* A **153** 166–72
BUTKOVICH T R 1955 *J. Glaciol.* **2** 553–9
CAMPBELL E S, GELERNTER G, HEINEN H and MOORTI V R G 1967 *J. Chem. Phys.* **46** 2690–707
CHAMBERLAIN J S 1971 *PhD Thesis*, University of New England
CHAMBERLAIN J S and FLETCHER N H 1971 *Phys. Kondens. Mater.* **12** 193–209
CHAMBERLAIN J S, MOORE F H and FLETCHER N H 1972 *Proc. Int. Symp. Phys. Chem. Ice, Ottawa* to be published
CHIDAMBARAM R 1961 *Acta Crystallogr.* **14** 467–8
COULSON C A 1959 *Hydrogen Bonding* ed D Hadzi (London: Pergamon) pp339–60
—— 1961 *Valence* (Oxford: Clarendon Press)
COULSON C A and DANIELSON L 1954 *Ark. Fys.* **8** 239–44, 245–55
COULSON C A and EISENBERG D 1966a *Proc. R. Soc.* A **291** 445–53
—— 1966b *Proc. R. Soc.* A **291** 454–9
CROSS P C, BURNHAM J and LEIGHTON P A 1937 *J. Am. Chem. Soc.* **59** 1134–47
CUBIOTTI G and GERACITANO R 1967 *Phys. Lett.* **24A** 179–80
DANTL G 1962 *Z. Phys.* **166** 115–8

DANTL G and GREGORA I 1968 *Naturwiss.* **55** 176
DAVIS C M and LITOVITZ T A 1965 *J. Chem. Phys.* **42** 2563–76
DAVIS R E, ROUSSEAU D C and BOARD R D 1971 *Science* **171** 167–71
DEL BENE J and POPLE J A 1970 *J. Chem. Phys.* **52** 4858–66
DENGEL O, ECKENER U, PLITZ H and RIEHL N 1964 *Phys. Lett.* **9** 291–2
DENNISON D M 1921 *Phys. Rev.* **17** 20–2
DERYAGIN B V 1966 *Disc. Faraday Soc.* **42** 109–19
—— 1970 *Scientific American* **223** (5) 52–71
DERYAGIN B V and FEDYAKIN N N 1962 *Dokl. Akad. Nauk SSSR* **147** 403–6
DIERCKSEN G H F 1969 *Chem. Phys. Lett.* **4** 373–5
DIMARZIO E A and STILLINGER F H 1964 *J. Chem. Phys.* **40** 1577–93
DORSEY N E 1940 *Properties of Ordinary Water Substance* (New York: Reinhold)
DOWELL L G and RINFRET A P 1960 *Nature, Lond.* **188** 1144–8
DUNCAN A B F and POPLE J A 1953 *Trans. Faraday Soc.* **49** 217–24
DVORYANKIN V F 1960 *Sov. Phys.–Crystallogr.* **4** 415–34
EISENBERG D and KAUZMANN W 1969 *The Structure and Properties of Water* (Oxford: Clarendon Press)
ELLISON F O and SHULL H 1953 *J. Chem. Phys.* **21** 1420–1
—— 1955 *J. Chem. Phys.* **23** 2348–57
ENGELHARDT H and RIEHL N 1966 *Phys. Kondens. Mater.* **5** 73–82
EUCKEN A 1946 *Nachr. Wiss. Göttingen* **1** 36–48
EVANS L F 1967 *J. Appl. Phys.* **38** 4930–2
EYRING H, REE T and HIRAI N 1958 *Proc. Nat. Acad. Sci. USA* **44** 683–8
FALK M and FORD T A 1966 *Can. J. Chem.* **44** 1699–1707
FALK M and WYSS H R 1969 *J. Chem. Phys.* **51** 5727–8
FINCH E D, RABIDEAU S W, WENZEL R G and NERESON N G 1968 *J. Chem. Phys.* **49** 4361–5
FLETCHER N H 1962a *The Physics of Rainclouds* (Cambridge: Cambridge University Press)
—— 1962b *Phil. Mag.* **7** 255–69
—— 1963a *Phil. Mag.* **8** 1425–6
—— 1963b *J. Chem. Phys.* **38** 237–40
—— 1968 *Phil. Mag.* **18** 1287–1300
—— 1970 *The Chemical Physics of Ice* (Cambridge: Cambridge University Press)
FLUBACHER P, LEADBETTER A J and MORRISON J A 1960 *J. Chem. Phys.* **33** 1751–5
FRANCK E U and ROTH K 1967 *Disc. Faraday Soc.* **43** 108–14
FRANK H S 1958 *Proc. R. Soc.* A **247** 481–92
—— 1970 *Science* **169** 635–41
FRANK H S and QUIST A S 1961 *J. Chem. Phys.* **34** 604–11
FRANK H S and WEN W-Y 1957 *Disc. Faraday Soc.* **24** 133–40
FRENKEL J 1946 *Kinetic Theory of Liquids* (Oxford: Clarendon Press)
GHORMLEY J A 1956 *J. Chem. Phys.* **25** 599
—— 1968 *J. Chem. Phys.* **48** 503–8
GIAUQUE W F and STOUT J W 1936 *J. Am. Chem. Soc.* **58** 1144–50
GIBBS J W 1928 *Collected Works* Vol 1 (New York: Longmans Green) pp94, 252–8, 367–8
GITTENS G J 1969 *J. Colloid Interface Sci.* **30** 406–12
GLOCKMANN H P 1969 *Physics of Ice, Proc. Int. Symp. Munich 1968* ed N Riehl *et al* (New York: Plenum Press) pp502–13
GOOD R J 1957 *J. Phys. Chem.* **61** 810–3
GOUGH S R and DAVIDSON D W 1970 *J. Chem. Phys.* **52** 5442–9
GUBERMAN S L and GODDARD W A 1970 *J. Chem. Phys.* **53** 1803–14
HAMILTON W C, KAMB B, LA PLACA S J and PRAKASH A 1969 *Physics of Ice, Proc. Int. Symp. Munich 1968* ed N Riehl *et al* (New York: Plenum Press) pp44–58
HANKINS D, MOSKOWITZ J W and STILLINGER F H 1970 *J. Chem. Phys.* **53** 4544–54
HARDY S C and CORIELL S R 1969 *J. Cryst. Growth* **5** 329–37
HARRISON J F 1967 *J. Chem. Phys.* **47** 2990–6
HASEGAWA M, DAIYASU K and YOMOSA S 1969 *J. Phys. Soc. Japan* **27** 999–1008
HELMREICH D and BULLEMER B 1969 *Phys. Kondens Mater.* **8** 384–92
HIRTH J P and POUND G M 1963 *Prog. in Materials Sci.* Vol 11 (Oxford: Pergamon) p190
HOLLINS G T 1964 *Proc. Phys. Soc.* **84** 1001–16
HOLZAPFEL W and DRICKAMER H G 1968 *J. Chem. Phys.* **48** 4798–800

HONJO G, KITAMURA N, SHIMAOKA K and MIHAMA K 1956 *J. Phys. Soc. Japan* **11** 527–36
HONJO G and SHIMAOKA K 1957 *Acta Crystallogr.* **10** 710–1
HUGHES D J and SCHWARTZ R B 1958 *Neutron Cross Sections* USAEC Report BNL–325 2nd edn suppl 2 Vol 1
INTERNATIONAL UNION OF CRYSTALLOGRAPHY 1952 *International Tables for X-ray Crystallography* (Birmingham: Kynoch Press) Vol 1
JACCARD C 1967 *Physics of Snow and Ice, Proc. Int. Conf. Sapporo* 1966 Vol 1 ed H Ôura (Sapporo: Hokkaido University) pp173–9
JACKSON K A 1958 *Growth and Perfection of Crystals* ed R H Doremus *et al* (New York: Wiley) pp319–24
—— 1966 *Crystal Growth* ed H S Peiser (Oxford: Pergamon Press) pp17–24
JAKOB M and ERK S 1928 *Z. ges. Kälteind.* **35** 125–30
JEFFREY G A and MCMULLAN R K 1967 *Prog. Inorg. Chem.* **8** 43–108
JELLINEK H H G 1967 *J. Colloid Interface Sci.* **25** 192–205
JHON M S, GROSH J, REE T and EYRING H 1966 *J. Chem. Phys.* **44** 1465–72
JHON M S, VAN ARTSDALEN E R, GROSH J and EYRING H 1967 *J. Chem. Phys.* **47** 2231–4
KAMB B 1964 *Acta Crystallogr.* **17** 1437–49
—— 1965a *Science* **150** 205–9
—— 1965b *J. Chem. Phys.* **43** 3917–24
—— 1970 *Science* **167** 1520–1
—— 1971 *Science* **172** 231–42
KAMB B and DATTA S K 1960 *Nature, Lond.* **187** 140–1
KAMB B and DAVIS B L 1964 *Proc. Nat. Acad. Sci. USA* **52** 1433–9
KAMB B and PRAKASH A 1968 *Acta Crystallogr.* B**24** 1317–27
KAMB B, PRAKASH A and KNOBLER C 1967 *Acta Crystallogr.* **22** 706–15
KATZOFF S 1934 *J. Chem. Phys.* **2** 841–51
KAVANAU J L 1964 *Water and Solute–Water Interactions* (San Francisco: Holden–Day)
KERN C W and MATCHA R L 1968 *J. Chem. Phys.* **49** 2081–91
KETCHAM W M and HOBBS P V 1969 *Phil. Mag.* **19** 1161–73
KLESSINGER M 1965 *J. Chem. Phys.* **43** S117–9
KNIGHT C A 1966 *J. Colloid Interface Sci.* **25** 280–4
—— 1971 *Phil. Mag.* **23** 153–65
KOLLMAN P A and ALLEN L C 1969 *J. Chem. Phys.* **51** 3286–93
KÖNIG H 1944 *Z. Kristallogr.* **105** 279–86
KOTLER G R and TARSHIS L A 1968 *J. Cryst. Growth* **3–4** 603–10
KRISHNAJI V P 1966 *Rev. Mod. Phys.* **38** 690–709
KUCHITSU K and MORINO Y 1965 *Bull. Chem. Soc. Japan* **38** 814–24
KUHNS I E and MASON B J 1968 *Proc. R. Soc.* A **302** 437–52
KVILIVIDZE V I, KISELEV V F and USHAKOVA L A 1970 *Dokl. Akad. Nauk SSSR* **191** 1088–90
LA PLACA S and POST B 1960 *Acta Crystallogr.* **13** 503–5
LIPPINCOTT E R and SCHROEDER R 1955 *J. Chem. Phys.* **23** 1099–106
LIPPINCOTT E R, STROMBERG R R, GRANT W H and CESSAK G L 1969 *Science* **164** 1482–7
LIPSCOMB W N 1954 *J. Chem. Phys.* **22** 344
LISGARTEN N D and BLACKMAN M 1956 *Nature, Lond.* **178** 39–40
LONG E A and KEMP J D 1936 *J. Am. Chem. Soc.* **58** 1829–34
LONSDALE K 1958 *Proc. R. Soc.* A **247** 424–34
MCDONALD J E 1953 *J. Met.* **10** 416–33
MCFARLAN R L 1936a *J. Chem. Phys.* **4** 60–4
—— 1936b *J. Chem. Phys.* **4** 243–9
MCMILLAN J A and LOS S C 1965 *Nature, Lond.* **206** 806–7
MCWEENY R and OHNO K A 1960 *Proc. R. Soc.* A **255** 367–81
MAIDIQUE M A, VON HIPPEL A and WESTPHAL W B 1971 *J. Chem. Phys.* **54** 150–60
MANSFIELD W W 1970 *Search* (*Australia*) **1** 332–5
MARCHI R P and EYRING H 1964 *J. Phys. Chem.* **68** 221–8
MARCKMANN J P and WHALLEY E 1964 *J. Chem. Phys.* **41** 1450–3
MASCARENHAS S 1969 *Physics of Ice, Proc. Int. Symp. Munich 1968* ed N Riehl *et al* (New York: Plenum Press) pp483–91
MASON B J 1952 *Quart. J. R. Met. Soc.* **78** 22–7
MEYER H H 1930 *Ann. Phys., Lpz.* **5** 701–34

MILLER A A 1969 *Science* **163** 1325–6
MILLS I M 1963 *Infrared Spectroscopy and Molecular Structure* ed M Davies (Amsterdam: Elsevier) pp166–98
MOCCIA R 1964 *J. Chem. Phys.* **40** 2186–92
MORGAN J and WARREN B E 1938 *J. Chem. Phys.* **6** 666–73
MOROKUMA K and PEDERSEN L 1968 *J. Chem. Phys.* **48** 3275–82
MOROKUMA K and WINICK J R 1970 *J. Chem. Phys.* **52** 1301–6
MOSKOWITZ J W and HARRISON M C 1965 *J. Chem. Phys.* **43** 3550–5
NAGLE J F 1966 *J. Math. Phys.* **7** 1484–91
NAKAYA U 1954 *Snow Crystals: Natural and Artificial* (Cambridge, Mass.: Harvard University Press)
NARTEN A H, DANFORD M D and LEVY H A 1967 *Disc. Faraday Soc.* **43** 97–107
NELSON R D, LIDE D R and MARYOTT A A 1967 *Natl. Std. Ref. Data Series, Natl. Bur. Std. (US)* Vol 10 (Washington: US Government)
NÉMETHY G and SCHERAGA H A 1962 *J. Chem. Phys.* **36** 3382–400
NEUMANN D and MOSKOWITZ J W 1968 *J. Chem. Phys.* **49** 2056–70
DE NORDWALL H J and STAVELEY L A K 1956 *Trans. Faraday Soc.* **52** 1061–6
OCKMAN N 1958 *Adv. Phys.* **7** 199–220
ONO S and KONDO S 1960 *Handb. Phys.* **10** 134–280 (Berlin: Springer-Verlag)
ONSAGER L and DUPUIS M 1962 *Electrolytes* ed B Pesce (London: Pergamon)
OREM M W and ADAMSON A W 1969 *J. Colloid Interface Sci.* **31** 278–86
ORENTLICHER M and VOGELHUT P O 1966 *J. Chem. Phys.* **45** 4719–24
ÔURA H (ed) 1967 *Physics of Snow and Ice, Proc. Int. Conf. Sapporo 1966* (Sapporo: Hokkaido University)
PARSONS R 1954 *Modern Aspects of Electrochemistry* Vol 1 ed J O'M Bockris and B E Conway (New York: Academic Press) pp123–4
PAULING L 1935 *J. Am. Chem. Soc.* **57** 2680–4
—— 1959 *Hydrogen Bonding* ed D Hadzi (London: Pergamon) pp1–5
—— 1960 *The Nature of the Chemical Bond* (Ithaca: Cornell University Press) Chapter 4
PETERSON S W and LEVY H A 1957 *Acta Crystallogr.* **10** 70–6
PETKE J D and WHITTEN J L 1969 *J. Chem. Phys.* **51** 3166–74
PICK M A 1969 *Physics of Ice, Proc. Int. Symp. Munich 1968* ed N Riehl *et al* (New York: Plenum Press) pp344–7
PISTORIUS C W F T, PISTORIUS M C, BLAKEY J D and ADMIRAAL L J 1963 *J. Chem. Phys.* **38** 600–2
PISTORIUS C W F T, RAPOPORT E and CLARK J B 1968 *J. Chem. Phys.* **48** 5509–14
PITZER R M and MERRIFIELD D P 1970 *J. Chem. Phys.* **52** 4782–7
POPLE J A 1950 *Proc. R. Soc.* A **202** 323–36
—— 1951 *Proc. R. Soc.* A **205** 163–78
POWELL R W 1958 *Adv. Phys.* **7** 276–97
PRUPPACHER H R 1967 *J. Chem. Phys.* **47** 1807–13
PRYDE J A and JONES G O 1952 *Nature, Lond.* **170** 685–8
RABIDEAU S W and FINCH E D 1969 *Physics of Ice, Proc. Int. Symp. Munich 1968* ed N Riehl *et al* (New York: Plenum Press) pp59–80
RABIDEAU S W, FINCH E D, ARNOLD G P and BOWMAN A L 1968 *J. Chem. Phys.* **49** 2514–9
DE REUCK A U S 1957 *Nature, Lond.* **179** 1119–20
RIEHL N, BULLEMER B and ENGELHARDT H (ed) 1969 *Physics of Ice, Proc. Int. Symp. Munich 1968* (New York: Plenum Press)
ROOTHAAN C C J 1951 *Rev. Mod. Phys.* **23** 69–89
ROUSSEAU D L 1971 *Science* **171** 170–2
ROUSSEAU D L and PORTO S P S 1970 *Science* **167** 1715–19
ROWLINSON J S 1951 *Trans. Faraday Soc.* **47** 120–9
RUNDLE R E 1953 *J. Chem. Phys.* **21** 1311
—— 1955 *J. Phys. Chem.* **59** 680–2
SAMOILOV O YA 1957 *Structure of Aqueous Electrolyte Solutions* English trans. 1965 (New York: Consultants Bureau)
SCHIFFER J 1969 *J. Chem. Phys.* **50** 566–7
SCHIFFER J and HORNIG D F 1968 *J. Chem. Phys.* **49** 4150–60
SENIOR W A and VERRAL R E 1969 *J. Phys. Chem.* **73** 4242–9

SHALLCROSS F V and CARPENTER G B 1957 *J. Chem. Phys.* **26** 782–4
SHIMAOKA K 1960 *J. Phys. Soc. Japan* **15** 106–19
SLATER J C 1930 *Phys. Rev.* **36** 57–64
STEWART G W 1930 *Phys. Rev.* **35** 1426–7
—— 1931 *Phys. Rev.* **37** 9–16
STILLINGER F H and BEN-NAIM A 1967 *J. Chem. Phys.* **47** 4431–7
SUGISAKI M, SUGA H and SEKI S 1968 *Bull. Chem. Soc. Japan* **41** 2591–9
TAMMANN G 1900 *Ann. Phys, Lpz.* **2** 1–31
—— 1909 *Z. Anorg. Allgem. Chem.* **63** 285
TAYLOR M J and WHALLEY E 1964 *J. Chem. Phys.* **40** 1660–4
THOMAS M R and SCHERAGA H A 1965 *J. Phys. Chem.* **69** 3722–6
TSUBOMURA H 1954 *Bull. Chem. Soc. Japan* **27** 445–50
VAND V and SENIOR W A 1965 *J. Chem. Phys.* **43** 1869–73, 1873–7, 1878–84
VERHOEVEN J and DYMANUS A 1970 *J. Chem. Phys.* **52** 3222–33
VOLMER M 1939 *Kinetik der Phasenbildung* (Dresden and Leipzig: Steinkopff)
WALL T T and HORNIG D F 1965 *J. Chem. Phys.* **43** 2079–87
WALRAFEN G E 1966 *J. Chem. Phys.* **44** 1546–58
—— 1968 *J. Chem. Phys.* **48** 244–51
—— 1969 *J. Chem. Phys.* **50** 567–9
WEIR C, BLOCK S and PIERMARINI G 1965 *J. Res. Nat. Bur. Stand.* **69**C 275–81
WEISSMANN M, BLUM L and COHAN N V 1967 *Chem. Phys. Lett.* **1** 95–8
WEISSMANN M and COHAN N V 1965 *J. Chem. Phys.* **43** 119–23
WEYL W A 1951 *J. Colloid Sci.* **6** 389–405
WHALLEY E 1957 *Trans. Faraday Soc.* **53** 1578–85
—— 1969 *Physics of Ice, Proc. Int. Symp. Munich 1968* ed N Riehl *et al* (New York: Plenum Press) pp19–43
WHALLEY E and BERTIE J E 1967 *J. Chem. Phys.* **46** 1264–70
WHALLEY E, DAVIDSON D W and HEATH J B R 1966 *J. Chem. Phys.* **45** 3976–82
WHALLEY E, HEATH J B R and DAVIDSON D W 1968 *J. Chem. Phys.* **48** 2362–70
WHITE D R and KASSNER J L 1971 *Aerosol Science* **2** 201–6
WILSON G J, CHAN R K, DAVIDSON D W and WHALLEY E 1965 *J. Chem. Phys.* **43** 2384–91
WOLLAN E O, DAVIDSON W L and SHULL C G 1949 *Phys. Rev.* **75** 1348–52
WOOD G R and WALTON A G 1970 *J. Appl. Phys.* **41** 3027–36
WORKMAN E J and REYNOLDS S E 1950 *Phys. Rev.* **75** 1348–52
YANNAS I 1968 *Science* **160** 298–9
YEAN D H and RITER J R 1971 *J. Chem. Phys.* **54** 294–6

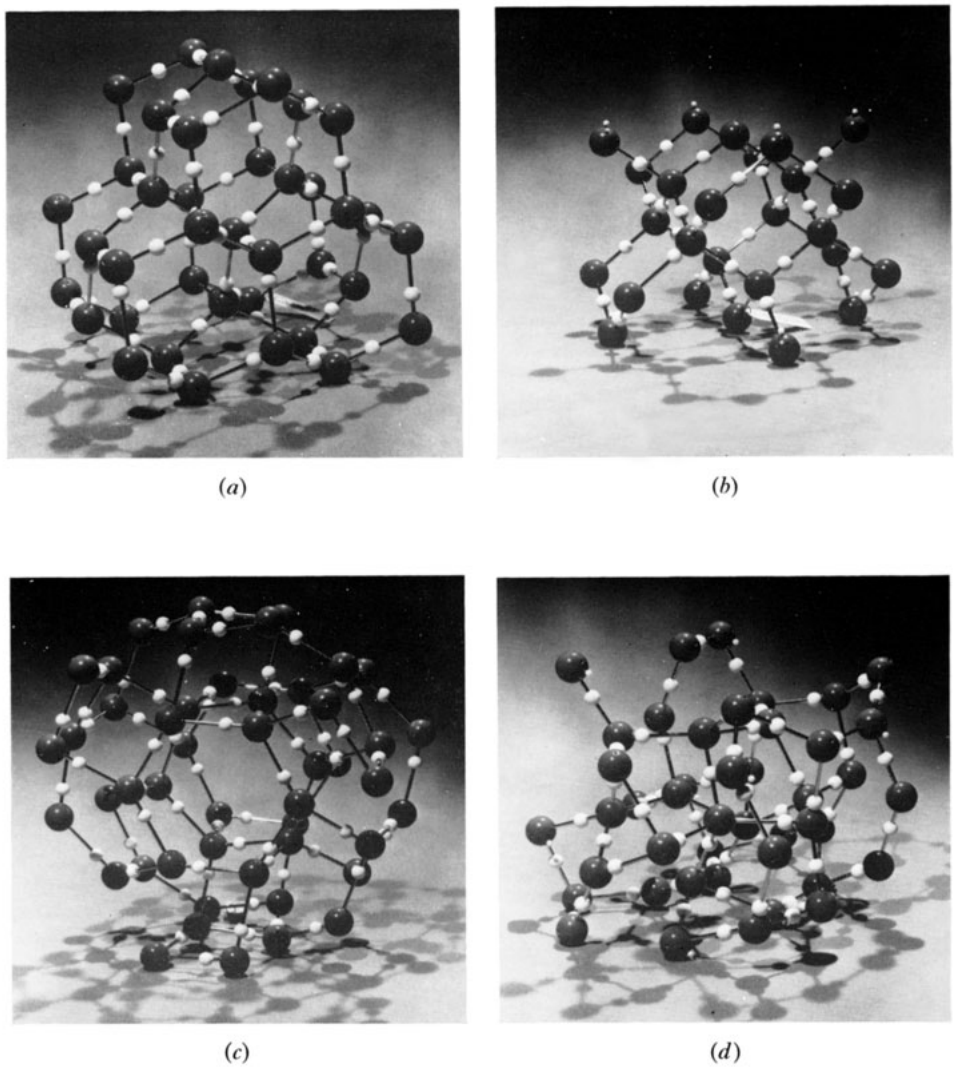

(*a*) (*b*)

(*c*) (*d*)

Plate 1. The structures of (*a*) Ice I_h, (*b*) Ice I_c, (*c*) Ice II and (*d*) Ice III. Note the puckered molecular planes in Ices I_h and I_c, the predominance of six-membered rings in I_h, I_c and II and the change to five-membered rings in Ice III (Crystal Structures Ltd).

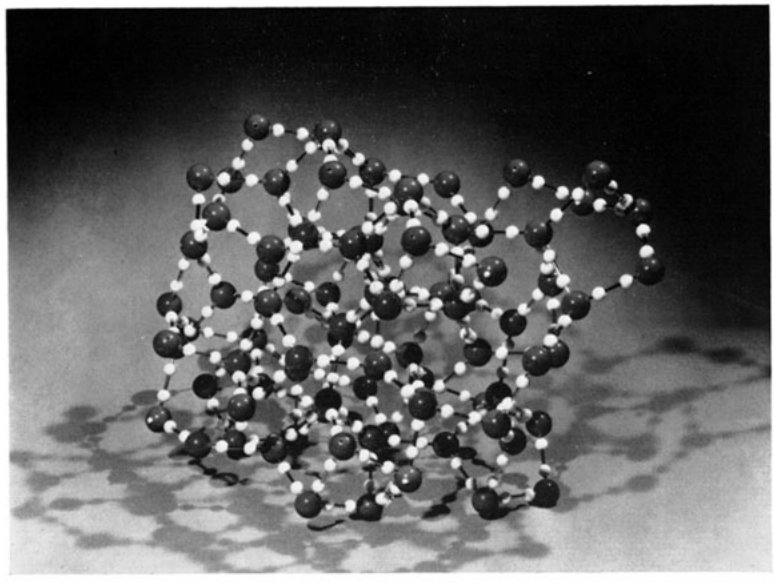

(*a*)

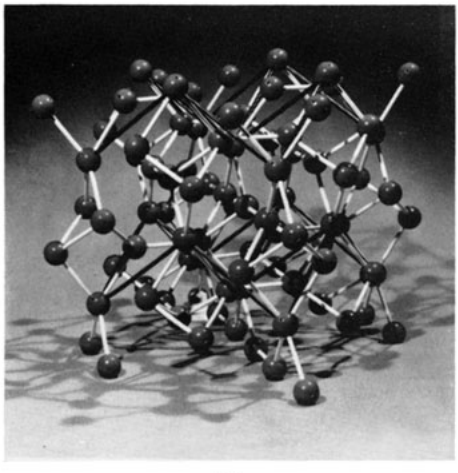

(*b*)

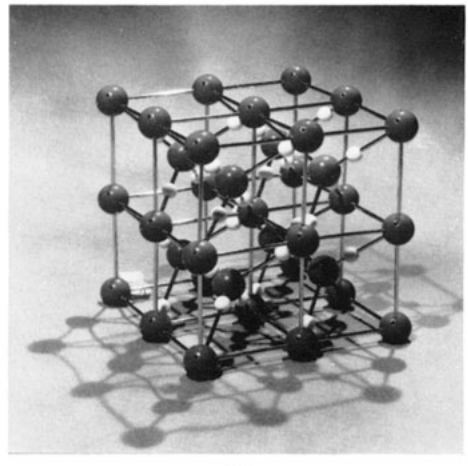

(*c*)

Plate 2. The structures of (*a*) Ice V, (*b*) Ice VI and (*c*) Ice VII. Note the five-membered rings in Ice V (in which two halfprotons are shown on each bond) and the dense packing achieved by the two interpenetrating frameworks in Ices VI and VII (the black rods in VI and the 'cubic' rods in VII are not part of the structure but are simply necessary to make the models rigid) (Crystal Structures Ltd).